January 2012

ZnO Nanostructures: Growth, Characterization and Applications

Mikhail Ladanov
University of South Florida, mladanov@mail.usf.edu

ZnO Nanostructures: Growth, Characterization and Applications

by

Mikhail Ladanov

A dissertation submitted in partial fulfillment
of the requirements for the degree of
Doctor of Philosophy
Department of Electrical Engineering
College of Engineering
University of South Florida

Co-Major Professor: Ashok Kumar, Ph.D.
Co-Major Professor: Jing Wang, Ph.D.
Garrett Matthews, Ph.D.
Manoj K. Ram, Ph.D.
Andrew Hoff, Ph.D.
Sylvia Thomas, Ph.D.
Arash Takshi, Ph.D.
Anna Pyayt, Ph.D.

Date of Approval:
November 7, 2012

Keywords: Nanowires, Hydrothermal, Microcontact, ALD, Microfluidics

Dedication

I dedicate this dissertation to Tamara Ladanova, my mother; Viktoriya Ladanova, my wife; and Dastan Seitmuratov, my friend. This dissertation would not have happened without their help, support and inspiration.

Acknowledgments

Above all, I would like to thank my co-advisors Dr. Ashok Kumar and Dr. Jing Wang for their supervision and help during my research work. I am grateful to Dr. Manoj K. Ram for his constant encouragement and help. Valuable insights and suggestions were provided by Dr. Matthews Garrett. I was constantly testing my ideas and thoughts against his knowledge and experience, and I am very grateful for that. This dissertation would not be completed without support from my fellow researchers: Kranthi Kumar Elineni, Pedro Villalba Amaris and Paula Algarin-Amaris. In addition, I am grateful to Nano Materials Research Laboratory (NMRL) members, and Nanotechnology Research and Education Center (NREC) staff for providing all the possible help in my research work.

This work was partially supported by NSF Grant#0854023 and NREC.

Table of Contents

List of Tables

List of Figures

Abstract

ZnO nanostructures have been investigated for quite a long time. However, only recently they triggered much interest due to advances in materials synthesis and characterization, as well as emerging demand for new nanostructured materials in novel device implementations.

A large part of the work was devoted to exploring new methodology for patterning growth sites and controlling nanowires morphology using the deposition methods that are compatible with integrated circuits (IC) processing. Microcontact printing was used to pattern the seeding layer, and, subsequently, ZnO nanowires through a resistless soft lithography process.

When considering hydrothermal growth of ZnO nanowires in the framework of IC compatible techniques, it is favorable to keep the chemistry of the process constant, while tailoring morphological properties of ZnO nanowires through other means. Therefore, control over morphology of ZnO nanowires was realized by setting the physical properties of seeding layers. Atomic Layer Deposition (ALD)

was used to deposit seeding layer required for hydrothermal growth and the effect of the physical properties of ALD thin films on resultant ZnO nanowires was studied.

Opto-electrochemical properties of ZnO nanowires were studied in various electrolytes and performance of ZnO nanowires as an electrode material for multifunctional applications was investigated. Also, bulk nucleation and growth of novel aster-like nanostructures was investigated. These nanostructures may prove useful for creation of mechanically reinforced biocompatible polymers.

Another key objective of the present work was to create strategies for controlled growth of ZnO nanowires on substrates previously unavailable for conventional hydrothermal growth of ZnO nanowires. The newly developed approach greatly facilitates growth of ZnO nanowires in confined microstructures, which greatly enhances the possibilities for the usage of ZnO nanowires in applications where they act as a porous electrode. These novel techniques open wide possibilities for improving performance of devices such as dye sensitized solar cells or supercapacitors.

Chapter 1: Properties, Synthesis and Application of ZnO Nanostructures

Zinc oxide (ZnO) is a rather remarkable semiconductor material, which belongs to a II-VI semiconductor group and usually exhibits a strong *n*-type conductivity. ZnO has three possible crystal structures: wurtzite, zinc blende and rocksalt. Under normal conditions only the wurtzite structure is a stable one. ZnO with stable zinc blende crystal structure can be grown on cubic substrates while rocksalt structure can be grown at high pressures.

Wurtzite crystal structure is common for binary compounds and has a hexagonal unit cell, belonging to $P6_3mc$ space group. It consists of two interpenetrating hexagonal closed-packed sublattices, each sublattice comprised of one type of atom. This structure lacks inversion symmetry, which is the reason that binary compounds with this crystal structure often exhibit piezoelectric and pyroelectric properties. Wurtzite structures of ZnO is presented in Figure 1(a), while three kinds of crystal facets for ZnO nanostructures are shown in Figure 1(b)

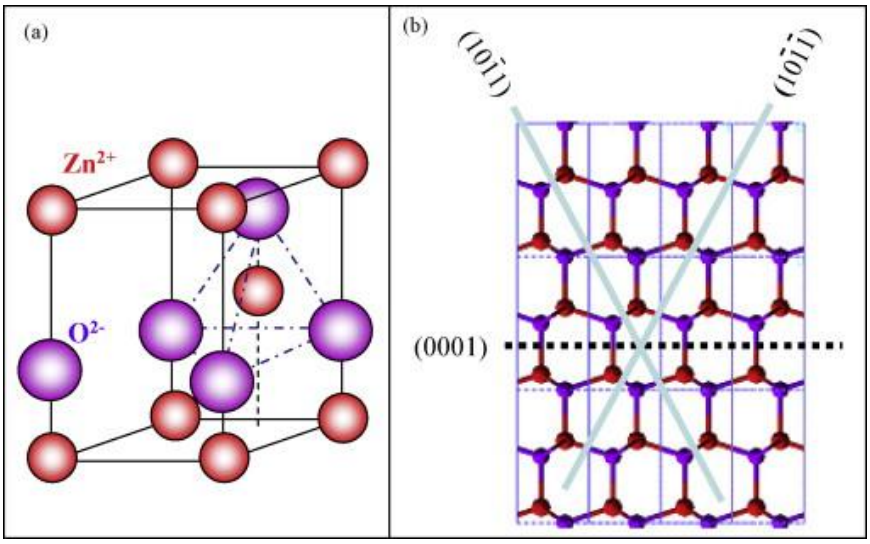

Figure 1. (a) Wurtzite crystal structure of ZnO, (b) Crystal facets of ZnO nanostructures. Reprinted from Materials Science and Engineering: R: Reports, Volume 64, Zhong Lin Wang, ZnO nanowire and nanobelt platform for nanotechnology, 33-71., Copyright (2009), with permission from Elsevier

ZnO exhibiting wurtzite structure has a wide direct band gap of 3.37 eV at 300 K and a large exciton binding energy (60 meV) which makes excitonic emission[1] efficient at room temperature. ZnO nanostructures currently are being studied extensively as a promising functional material. They possess interesting optical[2] and electronic[3] properties and therefore are used in a wide variety of devices such as mechanical transducers,[4, 5, 6] chemical and gas sensors,[7, 8] electrochromic field emission devices,[9, 10] dye sensitized solar cells,[11, 12, 13, 14, 15, 16, 17, 18] light emitting diodes[19] and UV lasers.[20, 21] The summary of applications and properties of ZnO is given in Figure 2.[22]

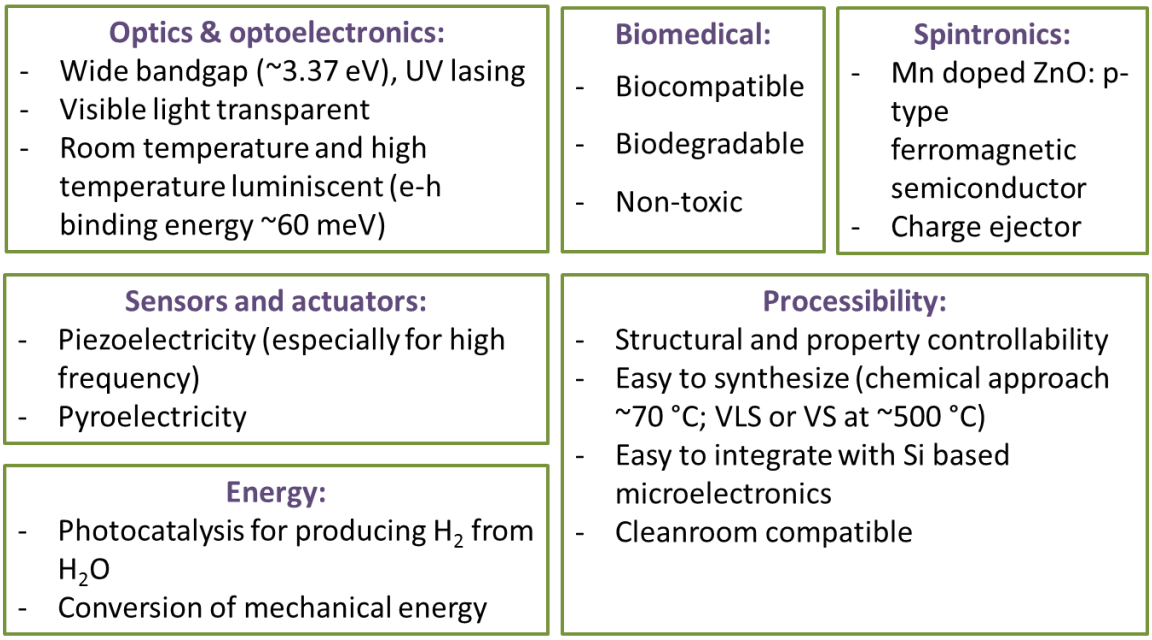

Figure 2. Some of the applications with relevant properties of ZnO. Reprinted from Materials Science and Engineering: R: Reports, Volume 64, Zhong Lin Wang, ZnO nanowire and nanobelt platform for nanotechnology, 33-71, Copyright (2009), with permission from Elsevier.

Meanwhile, ZnO nanostructures have been used as a promising biocompatible material for biological applications[23, 24] and recently were studied as an electrode material for electro- and optoelectrochemical applications.[25]

There is a wide variety of form factors of ZnO nanostructures, such as nanowires, nanorods, nanoparticles, nanobelts, nanoribbons, nanosheets etc. Some of the structures are shown in Figure 3. This wide variety of forms of nanostructures is defined by three families of fast growing planes: <2110>, <0110> and <0001>. Typical morphologies of ZnO nanocrystals are shown in Figure 4.

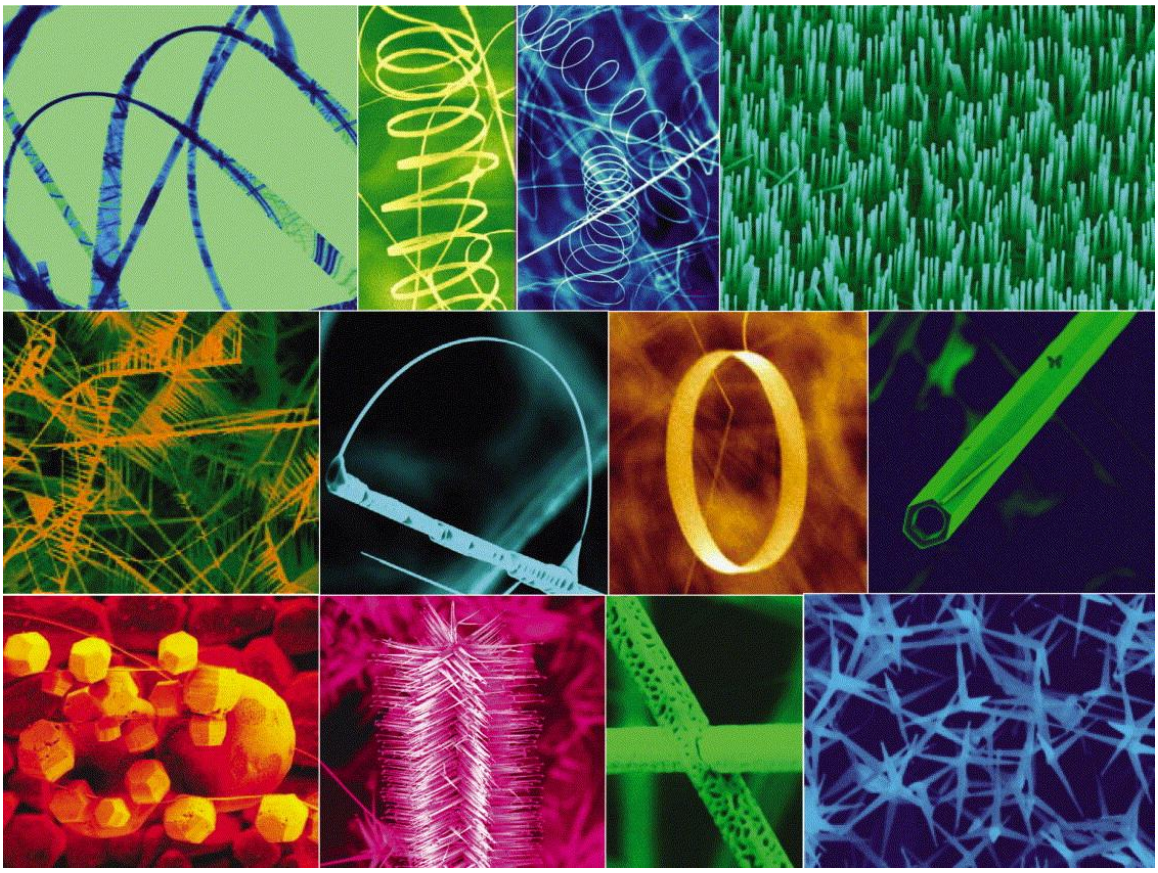

Figure 3. A variety of ZnO nanostructures. Reprinted from Materials Today, Volume 7, Zhong Lin Wang, Nanostructures of zinc oxide, 26-33, Copyright (2004), with permission from Elsevier.

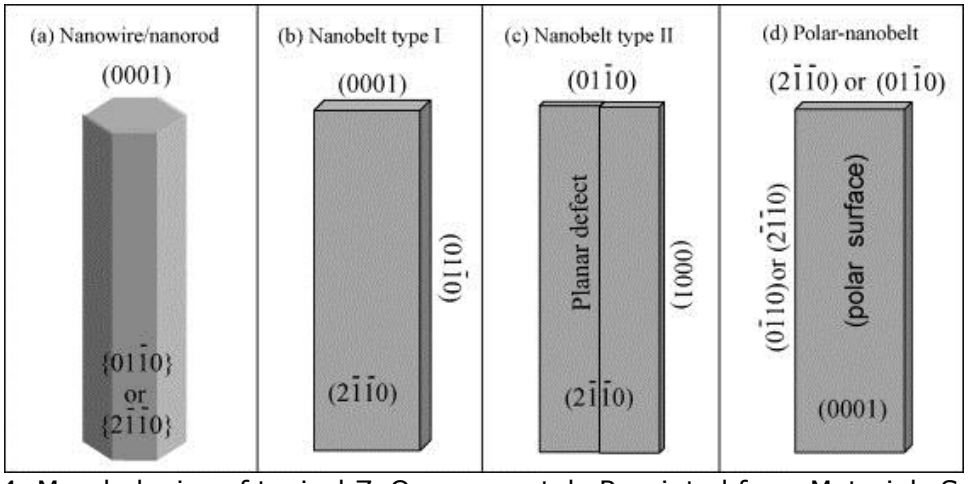

Figure 4. Morphologies of typical ZnO nanocrystals.Reprinted from Materials Science and Engineering: R: Reports, Volume 64, Zhong Lin Wang, ZnO nanowire and nanobelt platform for nanotechnology, 33-71., Copyright (2009), with permission from Elsevier

Synthesis of ZnO Nanowires

Gas Phase Synthesis

This family of methods is based on production of vapor of zinc and oxygen and their transport with the flow of carrier gas onto the substrate, where they react to form ZnO.[7, 26, 27, 28] The combination of vapors of Zn and O can be produced by either melting and evaporation of Zn metal under oxygen flow or thermal decomposition of ZnO powder. The latter is most commonly done in presence of graphite powder which significantly lowers the temperature required for decomposition of ZnO powder.

The growth is usually carried out in a three-zone tube furnace under base pressure of the order of mTorrs and under flow of Argon as carrier gas only or Argon as carrier gas and Oxygen as source of O vapor. The substrate is located down the flow away from the boat with source of Zn vapor. The quality and the type of ZnO nanostructures are determined by pressure, pressure ratio between Ar and O_2 and temperature on the substrate.

There are several growth modes.[29] Some of them require catalyst for nucleation or growth, the others are catalyst free. Figure 5 presents three general growth modes of ZnO nanowires. Vapor-Liquid-Solid (VLS) process mode (Figure 5(a) - top) requires a catalyst such as Au, Fe or Sn for nucleation and growth. At high temperature thin

film of such a metal forms liquid droplets. Zn vapor forms a liquid alloy with the catalyst material, and when the liquid alloy becomes supersaturated in presence of oxygen, ZnO crystallizes at the interface between the substrate and catalyst droplet. This way, the catalyst droplet remains at the tip of the nanowire and is usually observable on SEM or TEM images of the resultant nanowires.

The vapor-solid (VS) mode growth may have catalyst assisted (Figure 5(a) – middle) or catalyst free (Figure 5(a) – bottom) nucleation, but the growth is catalyst free. Figure 5(b-d) illustrates the resultant ZnO nanowires for aforementioned modes.

For the catalyst assisted growth, the size of nanowires can be controlled by the size of catalyst droplets, which, in turn, can be controlled by the thickness of the catalyst film, deposited prior to ZnO nanowires growth.

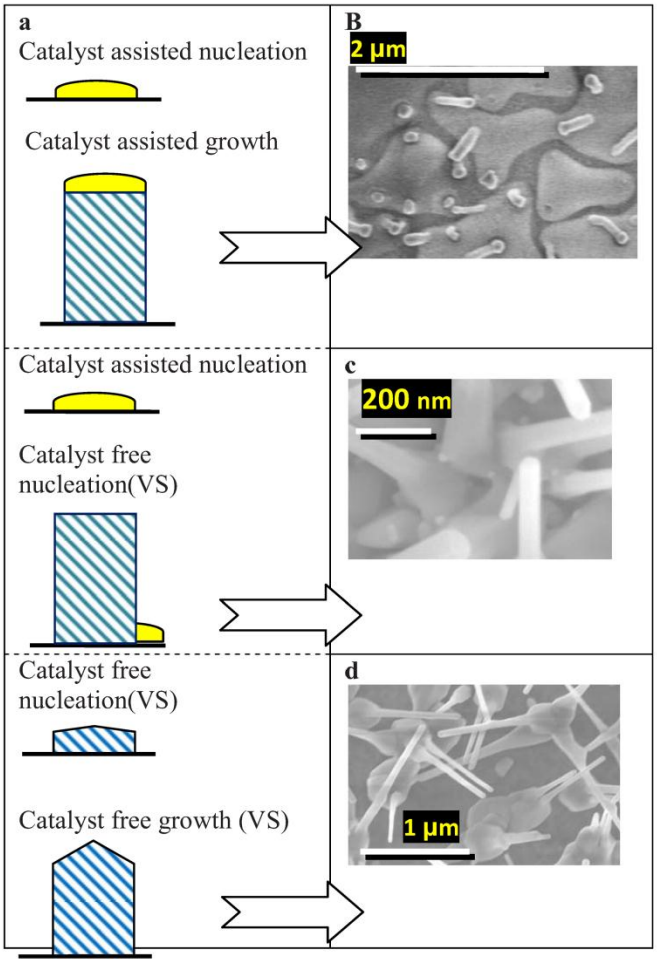

Figure 5. Three growth modes for gas phase deposition of ZnO nanowires.Reprinted with permission from I. Amarilio-Burshtein, S. Tamir, and Y. Lifshitz, Appl. Phys. Lett. **96**, 103104 (2010). Copyright 2010, American Institute of Physics.

Another mode is a vapor-solid-solid mode (VSS)(as shown in Figure 6), where the nanowires undergo comparable nucleation and growth with the only difference that catalyst droplet is in solid phase. In this case Zn, O and ZnO species (for which the catalyst surface is the preferential site for adsorption) diffuse over the semispherical surface of the droplet to the nanowire underneath.

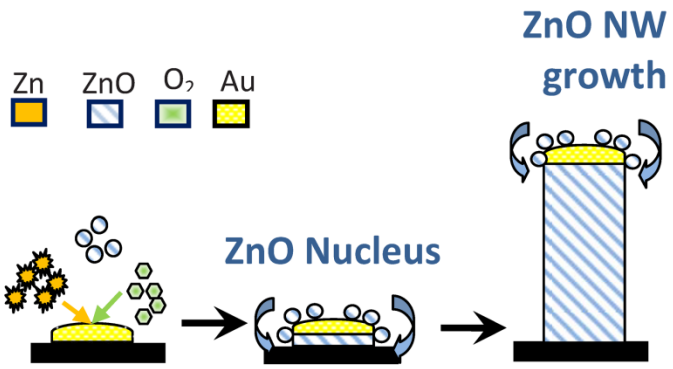

Figure 6. Schematics of Vapor-Solid-Solid growth mode.Reprinted with permission from I. Amarilio-Burshtein, S. Tamir, and Y. Lifshitz, Appl. Phys. Lett. 96, 103104 (2010). Copyright 2010, American Institute of Physics.

Other gas-phase deposition methods for growth of ZnO nanowires include metal-organic chemical vapor deposition (MOCVD),[30, 31, 32] metal-organic vapor-phase epitaxy (MOVPE),[1] molecular beam epitaxy (MBE),[33] pulsed laser deposition (PLD),[29, 34, 35] and sputtering.[36] Among these, the MOVPE growth is of greater interest as it is similar to atomic layer deposition (ALD) technique, used in current work for deposition of highly conformal thin film of ZnO over high aspect ratio structures. Similar to ALD, diethylzinc and oxygen (water vapor) are usually used as reactants in MOVPE growth. Resultant nanowires, unlike those obtained with, for instance, VLS growth mode, do not have catalyst droplets at the end of nanowires. Instead, flat steps or terraces are observed at the end of nanowires, as aresult of alternating deposition by diethylzinc and oxidizer.

Wet Chemistry Synthesis

Gas phase methods mentioned above may provide (along with many other types of nanostructures) high quality monocrystalline ZnO nanowires that have very high aspect ratio and high degree of vertical alignment. With careful control of the growth parameters such as pressure, Ar/O_2 pressure ratio and temperature of the substrate, as well as the crystal properties of substrate and catalyst film thickness, this wide variety of nanostructures with well tailored properties can be reproduced repeatedly. However, the drawbacks of these methods include the need for complex and expensive equipment, strict requirements for crystal properties of the substrate (substrates such as GaN or sapphire are required for close crystal lattice match with ZnO for growth of perfectly aligned ZnO nanowires), relatively high growth temperatures, challenging scalability, incompatibility with IC processes.

An alternative way of synthesizing ZnO nanostructures is through aqueous route.[37, 38, 39] These solution based methods include electrodeposition, sol-gel and hydrothermal method, the latter one being the main synthesizing method for current work.

The hydrothermal process is one of the most simple and cost-effective techniques.[37, 38, 39] The simplicity, scalability of this growth method as well as great compatibility with IC processing make it

highly suitable for commercial applications. This solution phase approach has attracted a great deal of attention due to its ability to facilitate large-scale, low-cost, and controllable growth of one-dimensional ZnO nanocrystals.[37, 38, 40] Due to the unique features the hydrothermal approach has been applied as the main ZnO nanowires synthesis method in this work. The background and the details of the process is explained in more depth further.

Hydrothermal Growth of ZnO Nanowires

The hydrothermal growth requires low temperatures and is easily scalable and compatible with IC processing. However it is quite challenging to control the morphology of the synthesized ZnO nanowires. These challenges are partially addressed by this dissertation work. Also, the patterning techniques are not as well established for hydrothermal growth as compared for to the gas phase growth. An attempt was made in the current work to exploit the necessary groundwork for patterning technique that is repeatable and controllable, yet easy, cost-effective and readily available without special equipment.

The hydrothermal growth of ZnO Nanowires was first demonstrated by Vayssieres et al.[41] The authors have proposed a method of precipitation of divalent Zn^{2+} ions in an aqueous solution resulting in vertically aligned, hexagonally shaped nanorods of ZnO.

The main driving reaction of the synthesis was decomposition of Zn^{2+} amino complex. Chemicals used were zinc nitrate and methenamine with equimolar concentration of 0.1 M. Since then, a wide variety of chemicals, conditions and treatment approaches were explored and used to form ZnO nanowires and other nanostructures on virtually any substrate. The main topics in hydrothermal growth of ZnO nanowires are discussed further, followed by justification for the growth conditions applied in this research.

The process parameters and chemicals involved in the growth can vary greatly, resulting in a broad variety of ZnO nanostructures.[42, 43, 44, 45] A large number of different growth modifiers have been used in hydrothermal growth[15, 46, 47, 48, 49] including: surfactants (such as citrates), polyethylenimine (PEI),[15] polyethylene glycol (PEG),[50, 51] ammonium hydroxide or even other metal ions.[52]

Although a hydrothermal method generally requires a seeding layer, some work was done on seedless approach to hydrothermal method. A group from Georgia Institue of Technology [53] has developed a method that does not require a seeding layer of ZnO, instead, a layer of Au was deposited to facilitate the growth of ZnO nanowires. In this case the density of nanowires was primarily controlled by the precursor concentration. The density of resulting ZnO nanowires is extremely low, with wide separation between the nanowires. Also, the

effects of temperature and growth time on the properties of nanowires were investigated. Although the authors are unclear of the role of hexamine in the reaction, they suggest that it acts as a slowly decomposing weak base, providing OH^- ions for the growth process.

A lot of work was done on studying the effect of seeding layer on the growth of ZnO nanowires. The conventional method for deposition of ZnO seeding layer is a thermal decomposition of zinc acetate, solution of which in different solvents can be deposited by drop casting or spin on process. Teng Ma et al.[54] among many other groups have studied the effect of seeding layer and the parameters of its preparation, including the concentration of Zn in the colloid being spun, annealing temperature and spin coating. Lori Greene et al.[38] have also studied effect of the seeding layer prepared by thermal decomposition of zinc acetate or dispersion of ZnO quantum dots. Ethanol was used as solvent for zinc acetate, while the size of dispersed ZnO quantum dots was 3-4 nm. Hydrothermal growth along with gas phase growth was used in the study. They have performed scanning tunnel microscopy (STM) for characterizing the ZnO platelets formed after thermal decomposition of zinc acetate and established that the platelets are primarily have flat top surface with *c*-axis perpendicular to the substrate. They explain this *c*-axis alignment by intrinsic thermodynamic feature rather than interaction between ZnO

and substrate. They have also performed hydrothermal growth on seedless, Au-coated substrate. Among these three approaches (thermal decomposition of zinc acetate, dispersion of ZnO quantum dots and seedless approach) the highest degree of vertical alignment is associated with the first one for both types of growth.

There are many other parameters influencing the growth of ZnO nanowires in hydrothermal process. For instance, Sweden researchers[55] have reported on influence of substrate pre-treatment, the angle at which the substrate placed in the chemical bath, pH of the growth solution and growth time.

Although the role of hexamine in hydrothermal growth of ZnO nanowires is not fully understood, attempts have been made to explain how it affects the growth of nanowires. Sugunan et al.[56] studied effect of hexamine, where the concentrations of the precursors were not always equimolar and the growth solution was preheated for a long time prior to immersion of the substrate. The hypothesis[53] that one of the important factors in the growth of highly anisotropic ZnO nanowires was slow decomposition of hexamine due to the elevated temperature and therefor slow rise in pH, is not confirmed by the authors. They did not see a significant deviation of morphology of ZnO nanowires in the growth with different preheating times. Instead, they suggest that non-ionic hexamine molecule attaches to non-polar sides

of the growing ZnO nanowire, effectively inhibiting growth on the side of the nanowires.

Willander et al.[57] from the same group in Sweden observed difference in density and shape of the tip of the nanowires due to different pH of the growth solution. Authors also gave extensive explanation of chemical reactions during the growth when pH is being adjusted by addition of aqueous ammonia.

Xu et al.[58] have performed a hydrothermal growth of high aspect ratio ZnO nanowires for application in dye-sensitized solar cells. They have studied effect of the concentration of growth precursors as well as such growth modifiers as polyethyleneimine (PEI) and ammonium hydroxide.

Hydrothermal growth with other growth modifiers was also studied. For instance, Liu et al.[51] from Institute of Metal Research in China carried out hydrothermal growth of ZnO nanorods in bulk solution with addition of polyethylene glycol and studied effect of its concentration on resulting ZnO nanorods.

Greene et al.[37] demonstrated a wafer-scale (4 inch wafer was used) growth of ZnO nanowires, proving it to be extremely easy compared to gas-phase synthesis of ZnO nanowires.

It is essential to develop methods of growing *p*-type ZnO nanowires for application in optoelectronic device. There are still certain obstacles in reproducible p-type doping of ZnO nanowires. A research group from Hong Kong[39] have demonstrated production of stable undoped *p*-type ZnO nanorods through adjusting of the parameters of the seeding layer. Lu et al.[4] have demonstrated growth of phosphorus-doped ZnO nanorods and their application in a prototype energy harvesting device.

One of the critical parameters for performance of such devices as supercapacitor or dye-sensitized solar cell is the specific surface area of the electrode. When ZnO nanowires used in such device, it is beneficial to create nanowires with high porosity. It can be achieved by growing high aspect ratio nanowires, as mentioned before. Other way to dramatically increase the specific surface area and therefore the porosity of the forest of ZnO nanowires is to create hierarchical nanowires. There has been extensive amount of work done in this direction. Generally, hierarchical ZnO nanostructures are formed following numerous chemical deposition baths with steps between then that ensure the growth of hierarchical structures.

For instance, Ko et. al[15] have prepared tree-like branched ZnO nanowires through multi-step growth method. Authors used the grown forest of branched ZnO nanowires as a photo-anode in a DSSC and

observed efficiency increase of up to 5 times compared to the anode comprised of ZnO nanowires with the same length as the backbone of the branched structures. Researchers from North Carolina State University[59] have used ALD technique to deposit ZnO on top of already grown ZnO nanowires to change the surface polarity of the nanowires, thus promoting the hierarchical growth.

Patterning of ZnO Nanowires

There are quite few ways to pattern ZnO nanowires. The pre-growth alignment methods may vary greatly and include many different techniques and combinations of them. Generally, it includes either patterning the seeding layer by any possible technique, or printing the seeding layer. There are few works, where the direct microcontact printing of the solution of zinc acetate on the substrate was implemented. Kang et al.[60] used PDMS stamp to print the seeding layer on Au covered substrate to pattern ZnO nanowires. The same approach was used for patterning the growth of other nanostructures. For instance, Kind et al.[61] have used the microcontact printing for patterning growth of carbon nanotubes. Other way to pattern is to create a self-assembling monolayer through microcontact printing that inhibits the growth of ZnO nanowires ("negative" printing). Hsu et al.[62] have used a self-assembled monolayer of COOH terminated $HSC_{10}H_{20}COOH$ molecules, which acted as an inhibitor for growth of

ZnO nanowires on Ag thin film. The authors have also used sodium citrate as a surfactant agent, and they observed the dependence of morphology of ZnO nanowires on concentration of sodium citrate. However, they have not compared the morphology of the nanowires in the forest grown on uniformly seeded substrate with that of nanowires grown on patterned seeding layer with the same growth conditions. This observation has led us to understanding the effect of local environment in the growth of ZnO nanowires, which is discussed later in this work.

Summary of Prior Art

The summary of discussed literature above is given in Table 1 presenting the main growth process parameters necessary for successful reproduction of the growth.

Table 1. Summary of the growth conditions and applications for the discussed published research.

Authors	**Growth conditions**
Xu et al.[53]	Substrate and seeding layer: Au thin film on Si, polymer substrate Growth Solution: Zinc nitrate and Hexamine, 0.1-100 mM Temperature: 60-95°C Time: 30 min to 48 hours Growth Modifiers: None Application: None
Ma et al.[54]	Substrate and seeding layer: ITO, Zinc acetate colloid 0.1 mM- 1 M, spin-coated, annealed at 300 – 700 °C for 5-60 min. Growth Solution: Zinc Nitrate, Methenamine, 0.1 M Temperature: 95 °C Time: 4 hours Growth Modifiers: None Application: None

Table 1 (continued).

Authors	Growth conditions
Greene et al.[38]	Substrate and seeding layer: ITO, Zinc Acetate, zinc acetylacetonate or zinc nitrate hexahydrate, 5mM annealed at 200-350°C Growth Solution: Zinc Nitrate, Methenamine or Diethylenetriamine, 25 mM Temperature: 90°C Time: 0.5 to 6 hours Growth Modifiers: None Application: None
Yang et al.[55]	Substrate and seeding layer: Si, spin coated Zinc Acetate 5 mM, annealed at 250 °C for 30 min Growth Solution: Zinc Nitrate and Methenamine 0.1 M Temperature: 93 °C Time: 2 hours or 5 hours Growth Modifiers: Ammonia water 2-4 mL to adjust pH Application: None Additional: Angle to horizontal was changed at which substrate was held
Sugunan et al.[56]	Substrate and seeding layer: Glass, Si, Zinc Acetate, 80ml of 1 mM diluted to 920 ml and 80 ml of 20 mM Sodium Hydroxide at 50 °C for 2 hours, spin coated Growth Solution: 1 and 0.5 mM Zinc Nitrate and Hexamine Temperature:60- 95 °C Time: 24, 7 hours Growth Modifiers: None Application: None
Willander et al.[57]	Substrate and seeding layer: Si and other, Zinc Acetate 5mM, spin coated, annealed at 250 °C for 30 min Growth Solution: Zinc Nitrate and Methenamine 0.1 M Temperature: 93 °C Time: 2 or 5 hours Growth Modifiers: 2-4 ml of Ammonia Application: glucose ZnO nanowire extended gate field effect transistors, selective calcium ion sensor, LED
Xu et al.[58]	Substrate and seeding layer: ITO, Zinc Acetate 5 mM annealed at 300 °C for 20 min Growth Solution: Zinc Nitrate 25-50 mM, Hexamine 12.5-25 mM, PEI 5 mM, Ammonium Hydroxide 0.35-0.45 M Temperature: 87-88 °C Time: 2-7 hours Growth Modifiers: PEI, Ammonia Application: DSSC
Liu et al.[51]	Substrate and seeding layer: None, NaOH 0.03 M in Methanol and Zinc Acetate 0.01 M in Ethanol stirred at 60 °C for 2 hours Growth Solution: 0.5 M hexamethylene tetramine, PEG Zinc Nitrate 0.25 M Temperature: 90 °C Time: 2 hours Growth Modifiers: PEG Application: None

Table 1 (continued).

Authors	Growth conditions
Greene et al.[37]	Substrate and seeding layer: Si, NaOH 0.03 M in Methanol and Zinc Acetate 0.01 M in Ethanol stirred at 60 °C for 2 hours Growth Solution: Zinc Nitrate and Hexamine 25 mM Temperature: 90°C Time: 0.5 – 6 hours Growth Modifiers: None Application: None
Hsu et al. [39]	Substrate and seeding layer: Si, ITO, Zinc Acetate annealed at 200 °C or 300 °C Growth Solution: Zinc Nitrate and Hexamine 25 mM Temperature: 90 °C Time: 2.5 hours Growth Modifiers: PEI Application: *p*-type conductivity, LED
Ko et. al[15]	Substrate and seeding layer: FTO, ZnO quantum dots Growth Solution: Zinc Nitrate, Hexamine 25 mM Temperature: 65-95 °C Time: 3-7 hours Growth Modifiers: PEI 5-7 mM Application: DSSC Additional: Annealing ZnO nanowires at 350 °C for 10 min, depositing seeding quantum dots and repeating hydrothermal growth resulted in hierarchical structures
Na et al.[59]	Substrate and seeding layer: Si, ZnO deposited by ALD Growth Solution: Zinc Nitrate and Hexamine, 20 mM Temperature: 80 °C Time: 6 hours Growth Modifiers: None Application: None Additional: ALD on grown ZnO nanowires and repeated hydrothermal growth resulted in hierarchical ZnO structures
Kang et al.[60]	Substrate and seeding layer: Si with metal bottom contact, glass, Polyethylene terephthalate (PET) and polyimide (PI), NaOH 30 mM and zinc acetate 10 mM in ethanol at 60 °C for 2 h Growth Solution: Zinc Nitrate and Hexamine, 25 mM Temperature: 95 °C Time: 1 hour Growth Modifiers: PEI 5-7 mM Application: High Performance Field Emission Device Additional: PDMS microcontact printing
Hsu et al.[62]	Substrate and seeding layer: Ag thin film on Si Growth Solution: Zinc nitrate and Hexamine 20 mM Temperature: 50−60 °C Time: 2-6 hours Growth Modifiers: None Application: None Additional: Microcontact printing of 11-mercaptoundecanoic acid inhibits nucleation of ZnO in printed regions

Table 1 (continued).

Authors	Growth conditions
This work	Substrate and seeding layer: Si, Zinc Acetate 0.1, 0.5, 2, 10 mM annealed at 350 °C for 30-35 min, ALD deposited thin film of ZnO Growth Solution: Zinc Nitrate and Hexamine 25 mM Temperature: 82-90 °C Time: 10 min to 8 hours, 2 hours mostly Growth Modifiers: PEG, PEI, Ammonia Application: ZnO nanowires in deep trenches as an electrode material Additional: PDMS microcontact printing, Growth inside deep trenches

With large number of processing parameters and growth and patterning recipes, hydrothermal growth proves to be quite well studied method of production ZnO nanowires. However, in spite of the numerous successful applications of ZnO nanowires in previous works, there is wide possibility for improving control over such cheap and reliable patterning method as microcontact printing along with exploring new methods of creating seeding layer such as ALD. This can open a new chapter in production of ZnO nanowires in applications not yet explored.

The main contribution of this work is in the field of controllable patterning of ZnO nanowires through microcontact printing along with exploring ZnO nanowires as an electrode material for future application, including novel techniques of production of ZnO nanowires in a way and manner away from conventionally studied approach.

Chapter 2: Methods, Scope and Goals of Dissertation

ZnO nanowires proved to be a very promising novel material for various applications, and last decade there has been a large volume of published research. Large part of it was devoted to synthesis of the nanowires itself: new methods, new chemicals were explored, new growth parameters and techniques applied. The outcome of this research was creating quite significant knowledge base of synthesis of ZnO nanowires with more or less predefined properties. At the same time, ZnO nanowires have been successfully applied in production of various devices, and recently a rare publication does not have some kind of application demonstrated along with the synthesis of ZnO nanowires. However, there is quite a large niche that takes its place in between understanding the nucleation and growth of ZnO nanowires on the level of chemistry and physics of the processes involved and creating the working devices that utilize ZnO nanowires. This niche is taking the stable and optimal growth techniques of lower level and preparing the material (ZnO nanowires or other nanostructures) to be the building block in implementation on the higher device level. This includes such questions as patterning ZnO nanowires, making the

growth compatible with other processes, such as IC fabrication. Another topic is exploring the difference in fabrication of ZnO nanowires merely for studying their properties and fabrication the nanowires as the functional material for the specific application. For instance, in the current work microcontact printing was explored, and it was shown, that when producing spatially distributed patterns of ZnO nanowires, growth modifiers may introduce quite different effect compared to growth of uniform forest of ZnO nanowires. This lead to understanding of the effect of local environment in the hydrothermal growth of ZnO nanowires, that, to the best of our knowledge, has never been pointed out before. This effect introduced quite a difference into the growth of ZnO nanowires using the well-established method for such application as ultra-high porosity electrode for supercapacitor. The latter is another example of the contribution of this work that has been done in this area. Both, hydrothermal growth of ZnO nanowires and means and ways of production of supercapacitors are well documented and well studied, not so much research was done on what would be the best way to utilize such promising material as ZnO nanowires in an applications such as supercapacitor. This work made an attempt to step further from a mere growth or even patterning a forest of ZnO nanowires to creating

a building block for a whole class of applications that require ZnO nanowires to be ultra-high porosity electrode.

It can be seen that areas of application are very diverse, which requires controlled production of ZnO nanowires with very different and well tailored physical properties. It may include morphological properties such as size, density, length as well as electronic and crystallographic properties such as doping, impurities, crystal orientation of ZnO nanowires and so on. In the particular applications targeted by this research, strategic control over their size, shape, length and surface density is of utmost importance.

Techniques employed to synthesize ZnO nanowires are well developed and have demonstrated the efficiency and accurate control over the resultant morphology of ZnO nanostructures. Moreover, they are generally inexpensive. However, for practical reasons, fabrication of devices based on ZnO nanowires should be relatively simple, straightforward, and cost effective.

The main goal of this research is to gain control over morphological properties of hydrothermally grown ZnO nanowires. It is necessary to grow large scale and uniform forests of vertically aligned ZnO nanowires with predetermined density, length and degree of vertical alignment in a repeatable fashion. Additionally, it is highly

desirable that ZnO nanowires remain nearly perfect crystals as the crystalline quality dramatically affects electron mobility and, therefore, overall efficiency of a device utilizing such nanowires.

Unlike CVD growth which is done primarily on a matching substrate such as sapphire or GaN, hydrothermal growth can be performed on virtually any surface. However, it generally leads to highly disoriented forest of ZnO nanowires. Hence, it is crucial to find a means for increasing the degree of vertical alignment of ZnO nanowires during hydrothermal growth.

Control over size and density also affects the performance characteristics of devices based on ZnO nanowires. While size influences mechanical and optical properties, density defines the specific surface density and, therefore, the reaction rate of any process on the surface of ZnO nanowires.

The general aim of the current work is to explore controlled growth and characterization of ZnO nanowires for purposes of tailoring their physical properties, while better understanding the fundamental mechanisms for nucleation and growth of ZnO nanowires. Furthermore, the obtained knowledge on controlled growth of ZnO nanowires with improved and tailored properties is going to be applied

towards applications such as electrode material for supercapacitor, dye sensitized solar cells.

Structure of the Dissertation

This dissertation is organized as a collection of articles based on each of the projects described further in the chapter. In Chapter 1 review of properties, synthesis and application of ZnO nanowires is given. This chapter gives an overview of the whole dissertation. A published article, or manuscript intended for publication does not generally have elaborated description of techniques or methods used in the work. Therefore, this chapter also has the subsection that gives enough details of the experimental techniques and necessary background. Detailed motivation and goals are given subsequently for each of the included articles. This concludes the current chapter. Chapters 3 to 7 are published articles or manuscripts intended for the publication. Chapter 8 is devoted to conclusion to the whole dissertation and suggestions for the future work.

Experimental Setup and Methods

Generally, hydrothermal growth is carried out in a solution of an alkaline reagent and Zn^{2+} salt. Hexamethylenetetramine and $Zn(NO_3)_2$ are often used to form a growth solution. At elevated temperature around 85-90 °C the following chemical reactions are responsible for growth of ZnO nanowires:[25]

Decomposition reaction:

$$(CH_2)_6N_4 + 6H_2O \rightarrow 6HCHO + 4NH_3$$

Hydroxyl supply reaction:

$$NH_3 + H_2O \Leftrightarrow NH_4^+ + OH^-$$

Supersaturation reaction:

$$2OH^- + Zn^{+2} \rightarrow Zn(OH)_2$$

ZnO nanowires growth reaction:

$$Zn(OH)_2 \rightarrow ZnO + H_2O$$

In wurtzite structure, <002> plane is a polar plane. It has been suggested[56], that in hydrothermal growth, hexamine preferentially

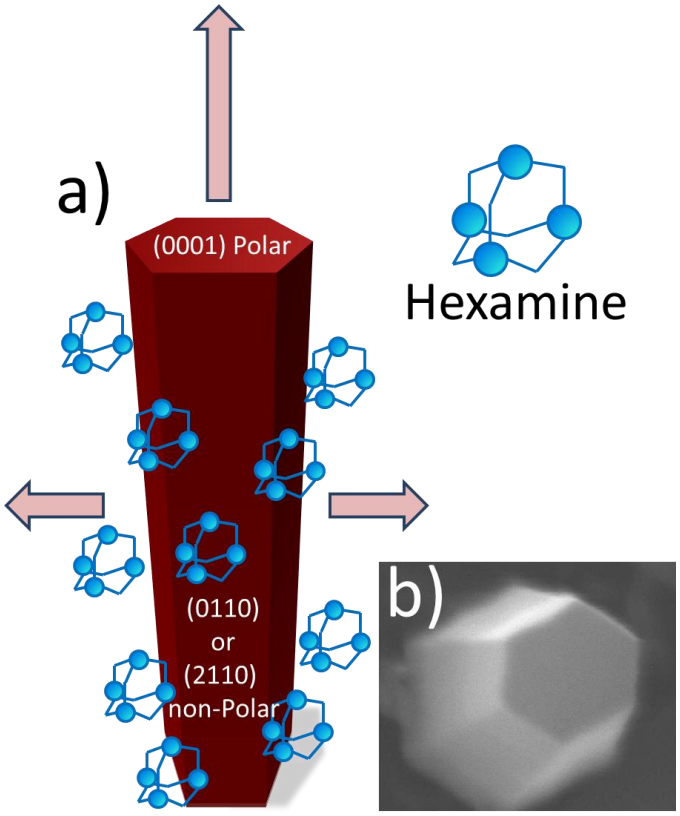

Figure 7. a) Schematics, showing hydrothermal growth of ZnO nanowires, where growth along *c*-axis occurs at higher rate than along other directions and b) SEM image of an actual ZnO nanowire, exhibiting hexagonal shape.

attaches to non-polar side planes of the growing crystal, leaving <002> plane, terminated with positively charged Zn^{+} ions, available for crystal growth. Therefore, the growth rate along the *c*-axis is much higher. The schematics of growing ZnO nanocrystals is shown on Figure 7(a). An example of a typical ZnO crystal exhibiting hexagonal shape is shown on Figure 7(b).

The purpose of current work lies away from tuning the chemistry of the hydrothermal process or studying effect of various parameters of the growth on resultant ZnO nanowires. Rather than that, as part of the work, the controlled growth of ZnO nanowires was explored in terms of both morphology and growth site localization by means of controlling the seeding layer. For this reason a stable, repeatable recipe for growth of ZnO nanowires was created and followed without much of change throughout the whole work.

In this work we have used concentration of 0.25 mM of both zinc nitrate and hexamine, which was chosen as the most widely used and the most efficient in terms of growth rate and morphology of ZnO nanowires. The growth temperature chosen was 82 °C rather than conventional 95 °C due to the limitations of the experimental setup.

The growth was performed in a jacketed beaker that was held at temperature of 82±0.2 °C. The total volume of the growth solution was 250mL. For the purpose of controlling the starting point of the

Figure 8. Illustration showing one of the Teflon substrate holders utilized in hydrothermal growth.

reaction, higher concentration of pre-diluted chemicals was placed in the preheated DI water. Amount of chemicals, necessary for 250 mL of 0.25 mM equimolar solution of zinc nitrate and hexamine were diluted in 40 mL of DI water. 180 mL of DI water were pre-heated to 82 °C in the jacketed beaker. After that, the concentrated growth solution was poured into the heated DI water. Since the dissolution of chemicals was not complete in such a small amount of water, beaker with concentrated solution was washed with additional 10 mL of DI water which were added to the heated growth solution. The final 20 mL were used to introduce growth modifiers, such as PEI, PEG or ammonium hydroxide, or just added to the growth solution as DI water if no modifiers were used. The temperature restores back to 82 °C in a matter of minutes after addition of all the chemicals. Generally, a substrate has to be inside the growth solution being held at any orientation or angle. However, the most often used orientation is face down, as it helps to avoid deposition of large number of bulk grown ZnO nano- and microcrystals. The substrate can float on the solution with face down, can be leaned against the side wall of the beaker, or hold by any other way. In current work, the substrate was placed in the growth solution being held by a Teflon substrate holder at constant distance from the bottom of the beaker. The schematics of the substrate holder is presented on Figure 8. A stirring magnet was used

to mechanically agitate the growth liquid to ensure better refreshment rate of growth chemicals, as it was observed that this dramatically increases overall quality of ZnO nanowires. The beaker then was tightly covered with aluminum foil to minimize water evaporation. Following this recipe, one can achieve repeatable synthesis in terms of dynamics of chemicals dissolution and solution temperature. The growth was usually performed for two hours for the sake of the consistency of such properties of nanowires as their length and thickness.

The method of patterning ZnO nanowires discussed in the next

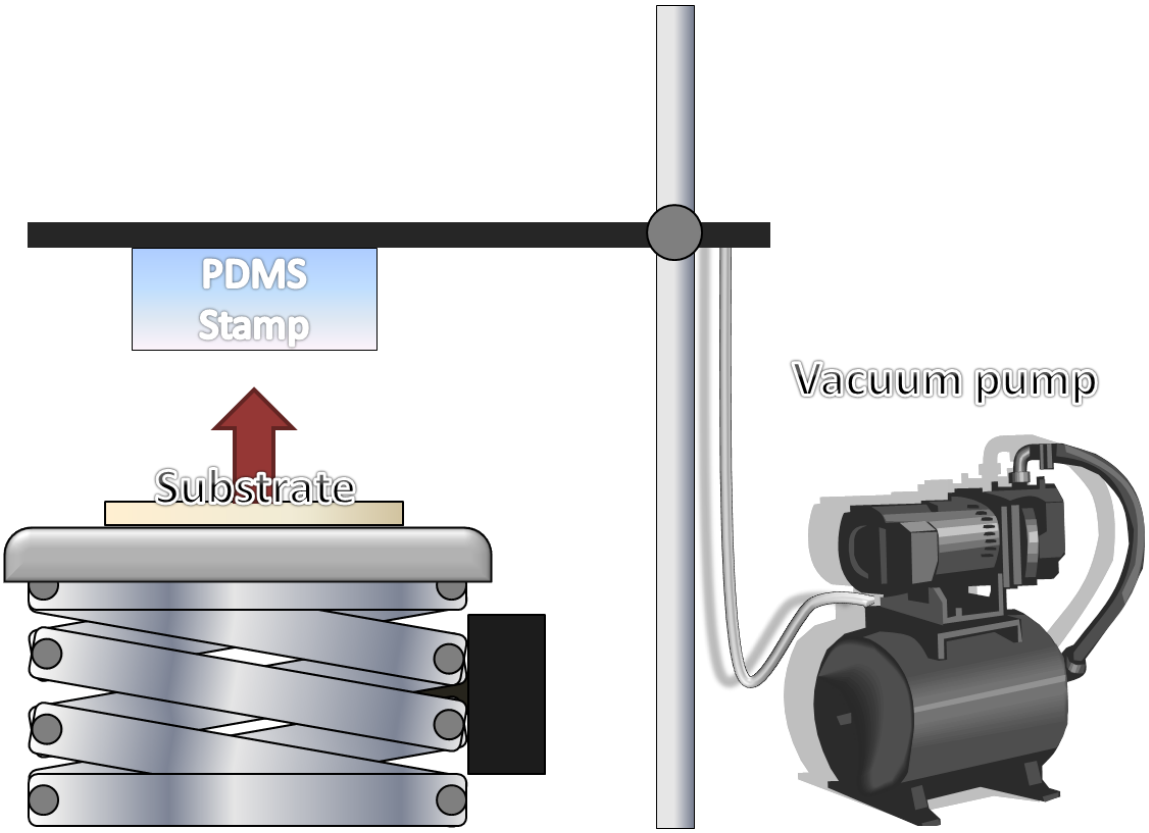

Figure 9. Schematics showing the setup used for the microcontact printing.

chapter is the microcontact printing. It has been used previously, as was discussed before, for patterning ZnO nanowires. However, in this work among other stamps the stamp with low fill factor was used. This allowed to obtain the same patterned features both in presence and absence of surrounding forest of ZnO nanowires, thus giving the opportunity to study the effect of local environment in the growth of ZnO nanowires. More details on the PDMS stamps are given in subsequent chapters. However, the technique used in the stamping needs some clarification. In microcontact printing, especially with the stamps with low fill factor, it is extremely important to perform the contact of the stamp to the surface of the substrate simultaneously for different parts of the stamp, otherwise the collapsing of the roof will occur. For this reason the setup pictured in Figure 9 was used: The PDMS stamp, that was wetted with ink (zinc acetate solution in ethanol) and slightly dried with nitrogen, is hold by vacuum under the horizontal arm. The substrate is brought within less than 1 mm from the stamp by lifting it on the jack. After thorough mutual alignment the vacuum is shut off from the holding arm and the PDMS stamp drops on the substrate from an extremely low height. After it stabilizes on the surface, certain weight that depends on the area of the stamp is placed on the top of the stamp and some time is given for ink to be printed on the surface. After that the stamp is carefully removed from

the surface by lifting it strictly upward. In some experiments an intentionally collapsed roof was needed. For this after placing the weight on the stamp, an additional pressure was applied on the side of the stamp until roof collapses there, then propagating throughout the whole or the part of the stamp.

The rest of this chapter is devoted to an overview of the published or ready to submit works presented in the subsequent chapters.

Patterning of ZnO Nanowires Through Microcontact Printing

Chapter 3 is entirely based upon a published article[63] presented in Appendix A: A Resistless Process for the Production of Patterned, Vertically Aligned ZnO Nanowires, which deals with the microcontact patterning. This is one of the alternative methods to define the areas with ZnO nanowires growth.

In this work, hydrothermal growth of patterned ZnO nanowires has been studied extensively.[64, 65] Patterning of seeding layer is a simple way to produce spatially distributed nanowires for device fabrication. Although the use of microcontact printing[62] has become a widely used technique for the modification of surfaces with monolayer domains, its apllication as a method for patterning the seeding layer for nanowire growth has not been well explored.

This work was devoted to production of vertically aligned and patterned ZnO nanowires on silicon substrates by methods of microcontact printing of the seeding solution. Microcontact printing defines regions where a seeding layer is deposited on a surface which in turn controls the regions where the nucleation of ZnO takes place and the region at which nanowires are grown from the surface.

This project also demonstrated effects of spatial distribution of ZnO nanowires on the size and morphology of ZnO nanowires, which strongly suggests that local concentration of Zn^{2+} ions determined by local geometry affects the morphology of ZnO nanowires.

One of the most important findings was that the growth of ZnO nanowires is dependent not only on conventionally recognized parameters such as temperature, concentration, pH, etc., but also on the local environment in the vicinity of the growth, i.e. at the distances of the order of hundreds of nanometers from the surface of the growing nanowire. Sodium citrate was used as a growth modifier, and it was shown that its effect is more pronounced on the patterned features of small size, such as a line of thickness comparable to the size of nanowires. ZnO nanowires grown on the printed seed layer of large area were subject to much less effect of sodium citrate.

Novel Aster-Like Nanostructures

Chapter 4 is entirely based on a published article[66] which is presented in Appendix B: Novel Aster-like ZnO Nanowire Clusters for Nanocomposites and which deals with bulk growth of aster-like ZnO nanostructures. This work is devoted to the hydrothermal growth of ZnO nanostructures in bulk solution, rather than on a substrate. Morphology that is different from ZnO nanowires grown on substrate is observed. Dependence of the shape and size of nanostructures on growth modifiers is studied.

The nanostructures were grown in bulk with addition of ZnO nanoparticles of various size as a seed for the hydrothermal growth. The bulk-grown nanostructures may be both desired (i.e. for reinforcing polymeric composites etc.) and detrimental (i.e. clogging factor in the growth of ZnO nanowires in deep trenches). Consequently, the formation and growth of the nanostructures in bulk are of certain interest.

Opto-Electrochemical Properties of ZnO Nanowires

Chapter 5 is based upon a published article[25] which is presented in Appendix C: Structure and Opto-electrochemical Properties of ZnO Nanowires Grown on *n*-Si Substrate and which investigates ZnO nanowires as an electrode material for electrochemical reactions. It has been previously established that crystal quality of ZnO nanowires,

their size and morphology play an important role in the electrochemical performance of ZnO nanowires as an anode material.

Previously, it has been proven that controlling the morphologies of transition metal oxides could improve their electrochemical performance including cycling characteristics and rate capability. Therefore detailed studies of the structural, electrochemical and opto-electrochemical properties of ZnO nanowires will improve greatly their applicability in photovoltaic devices. In this work, a conventional hydrothermal method was utilized to synthesize ZnO nanowires on a conducting *n*-type Si surface. Then. the electrochemicals studies were carried out in various electrolytes, showing cycling characteristics and the rate capability. Photoelectrochemical current was observed in electrochemical cell under the UV illumination. Stable, repeatable and optimized electrochemical characteristics may be essential for successful application of ZnO nanowires in photovoltaic devices such as dye sensitized solar cells.

The Effect of Seeding Layer Grown by ALD on the Properties of Hydrothermally Grown ZnO Nanowires

Chapter 6 studies the effects of the seeding layer of ZnO on hydrothermal growth of ZnO nanowires. The dependence of the morphological properties of ZnO nanowires on the seeding layer

deposited by ALD was studied. Optimal conditions aimed at high density, small diameter nanowires was found.

ZnO nanowires are used in a broad variety of applications. Success in these applications will require tight control over their physical properties. Typically, the choice of growth mechanisms and its associated parameters are leveraged to attain such control. In this project, the growth conditions were kept constant deliberately, allowing to specifically address the effects of the seeding layer. The justification for this project is the production of ZnO nanowires as an electrode material for use in applications such as batteries and supercapacitors. In this particular case, the electrode material should provide high specific surface area, which indicates that ZnO nanowires of small size and high density are desired. The project aimed to study how the seeding layer affects the growth of ZnO nanowires. Atomic layer deposition (ALD) was chosen as the growth mechanism for production of the seeding layer, thereby providing: I) production of high quality, stable ZnO thin films; II) a high degree of control over the thickness with ultimate precision; III) compatibility with integrated circuit (IC) processes, IV) high degree of conformity, which allows production of hierarchical structures with ZnO nanowires. With an electrode material for supercapacitor applications in mind, the compatibility with IC processes and conformity of the grown film would

be very favorable for the production of hierarchical three dimensional structures with a high specific surface area of ZnO nanowires. The whole project can be divided into two parts – growth and characterization of ZnO ALD thin films and growth and characterization of ZnO nanowires on top of these films.

Careful characterization of ALD thin films with process temperatures of 150 °C, 200 °C and 250 °C was decided to be necessary as it appears that most often ALD growth of ZnO is performed at lower temperatures of 150-170 °C. Moreover, it was proven that the post-process treatments such as annealing under different atmospheres would affect the ALD thin films and/or the ZnO nanowires grown on them. To this end, oxygen and argon gases were chosen as the obvious first choices for annealing atmospheres at temperatures of 600 °C and 800 °C as it is known from a previous study that annealing within this temperature range gave the best results.

The presented work will be useful for those seeking control over the growth of oxide nanowires using hydrothermal methods in particular and other methods in general. This group includes those working towards implementation of supercapacitors, photovoltaic devices, sensors etc., where large surface areas covered with ZnO nanowires are preferred. In these areas of research, control over the

properties of ZnO nanowires through careful choice of growth parameters of the seeding layer rather than the growth conditions of the nanowires is beneficial because they may have an effect on the production of a particular device.

Microfluidic Hydrothermal Growth of ZnO Nanowires Over High Aspect Ratio Microstructures

Chapter 7 presents a logical extension of the previous research. The main goal of this particular work is to develop an array of aligned and densely packed ZnO nanowires on top of a substrate with complex three dimensional surface. Specifically, this work aims at high specific surface area of an electrode composed of ZnO nanowires.

It was shown that ZnO nanowires are good candidates for electrochemical and photoelectrochemical cells. One of the possible ways to improve performance of such a device would be to increase specific surface area of ZnO nanowires. This can be done by increasing aspect ratio of ZnO nanowires[67] or creating ZnO hierarchical structures,[15, 68] and the work done in this field shows that the efficiency of device that utilizes such an electrode can increase significantly.

Yet another way is to increase effective surface where ZnO can grow per unit area of the substrate, and to the best of our knowledge this approach has not been explored so far. The increase in surface

available for hydrothermal growth of ZnO nanowires with the same die size can be done by forming complex three-dimensional microstructure on the substrate and growing ZnO nanowires over the non-flat surface. The most simple and readily available microstructure would be an array of deep trenches. The effective surface area depends on the aspect ratio, size and spacing of the individual trenches. Provided that ZnO nanowires can be grown on the sidewalls of these trenches, the specific surface area of ZnO nanowires would increase significantly.

It was observed, that the growth of ZnO nanowires is governed not only by previously described parameters such as temperature or concentration of chemicals in bulk, but also by the local environment, specifically, concentration of chemicals in the vicinity of the growth site. This in turn is determined by a combination of depletion of chemicals due to the growth itself and supply of the fresh chemicals through diffusion or mechanical flow (i.e. stirring). Therefore, when the latter is limited, hydrothermal growth slows down or stops. For instance, the growth will be influenced, if there are neighboring nanowires or walls that can affect the diffusion of chemicals toward the growth site. This often happens when the growth site is located in a confined space (e.g., a deep trench or buried channel, etc). In this case, depletion of the chemicals occurs at a faster rate than the fresh chemicals are replenished to the growth site.

Therefore, one obstacle that might prevent an effective growth of ZnO nanowires in deep trenches with width on the order of microns is the effect described in the previously in this work. The ions necessary for hydrothermal growth of ZnO nanowires will not diffuse into such a deep trench fast enough to overcome the consumption rate of these ions in hydrothermal growth.

The main challenge in this work is to find a methodology that would allow ZnO nanowires to effectively grow in a confined space of deep trenches, where refreshing rate of chemicals due to diffusion and\or mechanical stirring of growth solution is less than consumption rate of Zn^{2+} ions during hydrothermal growth of ZnO nanowires. Therefore it is necessary to find a way to forcefully replenish growth chemicals in a confined space. Additional attempts are made to optimize facilitated delivery of fresh chemicals into deep trenches by forced circulation of growth solution.

The approach pursued by this work consists of the hydrothermal growth of ZnO nanowires that is realized through forced circulation of hot growth solution through microfluidic channels in a Si or other substrate fully or partially formed by the microstructures, such as deep trenches and buried channels, on which the hydrothermal growth of nanostructures is highly desired. Obviously, the conventional hydrothermal process is ill-suited for solution-based growth in confined

spaces due to the limitation by the diffusion and depletion of the growth species. This new method results in a hydrothermal growth in confined space by enforced refreshment of chemicals by pumping the growth solution through the microfluidic channels partially formed by etched silicon trenches.

Also required for the hydrothermal growth of ZnO nanowires is a seeding layer, which is a uniform and conformal thin film of polycrystalline ZnO. This seeding layer is needed over the high aspect ratio surfaces where the growth of ZnO nanostructures is desired. The seeding layer can be formed by a conformal deposition method (i.e. ALD). The substrate may be heated to a) provide additional heat to the heated growth solution (as it might have some heat dissipation while being transported to the growth site); b) provide the only heat source to the hydrothermal reaction.

It is worthwhile mentioning that the demonstrated methodology for wet chemistry processes in confined spaces is not limited to growth of ZnO nanowires (used here as a demonstration), but also can be employed for hydrothermal growth of nanostructures comprised of other materials. In other words, this technique is not a standard operating procedure for growth of ZnO nanowires, but rather a generic methodology for synthesis of nanostructured materials in confined, non-flat, high aspect ratio surfaces or buried/sealed channels, where

the traditional bulk reaction growth process could not be used. Instead, any complex texture, buried channels, or high-aspect ratio structures in virtually any substrate can be turned into microfluidic channels with the help of sealant layers such as PDMS, or just used as a microfluidic channels to turn the traditional bulk reaction method into in-situ micro-reactors, where the growth is desired.

ZnO nanowires are successfully used as an electrode material in a number of devices. Apart from their optical, electrical and crystalline properties, the advantage of ZnO nanowires can be attributed to their high specific surface area. It would be of great advantage to grow ZnO nanowires in confined spaces such as buried channels, deep trenches or wells (structures with high aspect ratio). This would greatly increase the specific surface area of ZnO nanowires (area of surface of nanowires per area of the substrate).

Usually, ZnO nanowires are grown on flat or somewhat bent\distorted surface of substrate. Growth of ZnO nanowires in confined spaces (such as inside of deep trenches with width of tens of micrometers and aspect ratio of greater than 5:1) is limited by combination of diffusion of chemicals necessary for growth into the confined space and by high depletion rate (usage of chemicals) inside such space. Means of refreshing growth chemicals in such spaces would mitigate these problems. To the best of our knowledge this

problem was never addressed and ZnO nanowires were never successfully grown inside a deep trench or buried channel or any other confined structure.

In this work, the deep trenches with sizes of 5 μm, 10 μm, 15 μm and 20 μm and comparable depth (depth greater than the width) are a part of the microfluidic setup. This setup was etched using deep reactive ion etching (DRIE) on the silicon wafer to form trenches along with two inlet/outlet ports. The ZnO thin films were deposited using ALD inside these structures to serve as a seeding layer for ZnO hydrothermal growth. After that the microstructure was covered with a thick PDMS spacer, thus sealing the microfluidic structure. Two inlet/outlet ports were connected to the microfluidic pump. Both the growth solution and the substrate were heated to 80-82°C. Special consideration should be taken about the growth solution, as the conventional hydrothermal recipes result in active nucleation in the solution during the reaction. As a result, the pumping of growth solution through the microfluidic structures may clog them. Addition of ammonium hydroxide along with low concentration of low molecular weight PEI to control the pH and nucleation processes may resolve this issue.[69]

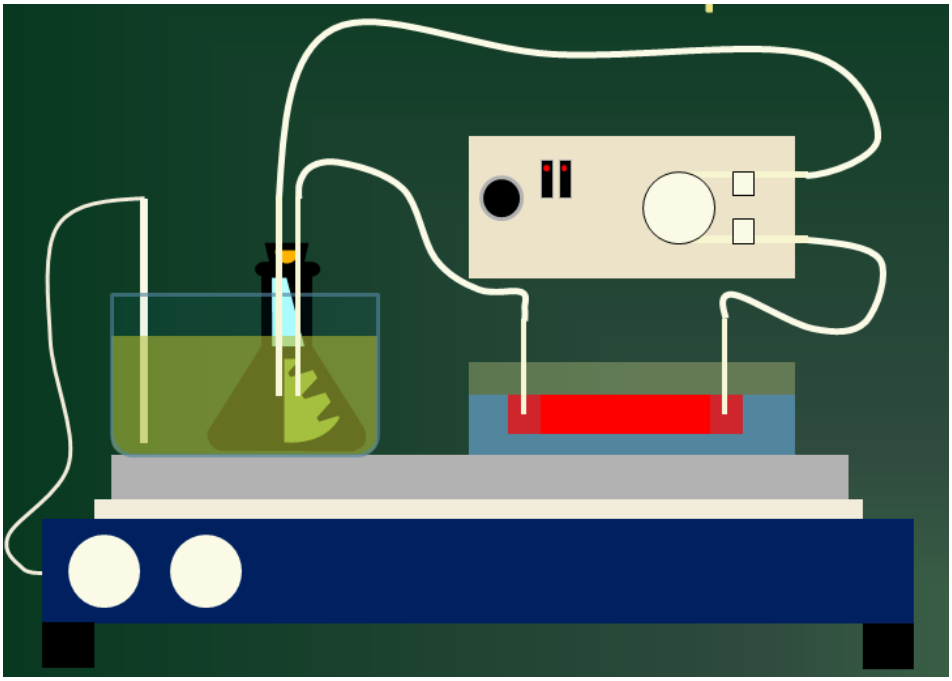

Figure 10. Schematics of proposed experimental set up for microfluidics-assisted hydrothermal growth of ZnO NW. The beaker with heated solution serves as a bulk source for the growth liquid (left). Peristaltic pump (top right) pumps the growth solution through the sample with PDMS cover (bottom right) which is located on the hotplate and then back to the beaker.

A growth solution in air-tight vial is heated up in an oil tank. Temperature of the oil is fed back to the hot plate. The vessel with the oil is placed on a thick polished aluminum plate that serves as a heat buffer and ensures good contact of the substrate with the heater. The reason why the heat buffer is required is that the PID control of the hot plate may cause short time changes in temperature on the surface of the hot plate, which in turn my affect the temperature of growth solution inside trenches on silicon substrate due to small size of the sample. The growth solution was circulated using the peristaltic pump. As the pumping speed is expected to be slow, growth solution may cool down during that time. The aluminum plate serving as heat buffer

is also polished to ensure good thermal contact with silicon substrate. It is expected that the growth solution will be reheated in the trenches. Therefore, the trenches along with the PDMS top cover will effectively form microreactor chambers where the hydrothermal growth of ZnO nanowires occurs. Due to the sustained flow of the growth solution the growth chemicals are replenished and growth does not stop.

Chapter 3: A Resistless Process for the Production of Patterned, Vertically Aligned ZnO Nanowires[1]

Abstract

ZnO nanostructures have attracted a great deal of interest because of their biocompatibility and outstanding optical and piezoelectric properties. Their uses are widely varying, including as the active element in sensors, solar cells, and nanogenerators. One of the major complications in device development is how to grow ZnO nanowires in well aligned and patterned films with predefined geometrical shape and aspect ratio. Controlled growth is required to achieve the optimal density of nanowires and to produce a defined geometric structure for incorporation in the device. In this work, we have presented a method by which vertically aligned ZnO nanowires could be grown in defined patterns on surfaces without the use of resists. We used a hydrothermal method to grow ZnO nanowires on a substrate through growth modifiers that was pre-patterned with a seeding solution by means of microcontact printing. This method

[1]Mikhail Ladanov, Kranthi Kumar Elineni, Manoj Ram, Nathan D. Gallant, Ashok Kumar, Garrett Matthews, A Resistless Process for the Production of Patterned, Vertically Aligned ZnO Nanowires, Mater. Res. Soc. Symp. Proc. Vol. 1302, 2011, reproduced with permission.

produced vertically aligned ZnO nanowires of predefined size and shape with pattern resolution high enough for the production of rows of single nanowires. The nanowires were characterized by using scanning electron microscopy (SEM) and X-ray diffraction spectroscopy (XRD) techniques.

Introduction

Recently, ZnO nanostructures have attracted great attention. ZnO is a II-VI semiconductor with a wide direct band gap of 3.37 eV and large exciton binding energy of 60 meV making it suitable for application in UV lasers,[37] light emitting diodes,[19] sensors,[7] nanogenerators[4, 5, 6] and solar cells.[16]

Many methods have been used to prepare ZnO nanowires, including using chemical vapor deposition,[7, 26] metal–organic chemical deposition,[26, 32] pulsed laser deposition,[70] physical vapor deposition,[31, 71] vapor-liquid-solid methods[6, 27] as well as the hydrothermal method[37, 38, 39] used in this work. The latter is one of the most simple and cost effective methods, making it straightforward to scale up production.[37, 38, 40]

Patterned growth of ZnO nanowires using hydrothermal methods have been studied extensively[64, 65] as it is a simple way to produce spatially distributed nanowires for device fabrication. The use of

microcontact printing (μCP)[62] has become common for the modification of surfaces with monolayer domains, though its use as a method for patterning nanowire growth has not been well explored.

In this paper we have demonstrated vertically aligned and patterned ZnO nanowires on silicon substrates. These structures were produced using μCP to control the regions where a seeding layer is deposited on a surface. In turn, the patterned seeding layer controls the regions where the nanowires are grown from the surface using a hydrothermal growth technique. Additionally, the effects of spatial distribution on the size and morphology of ZnO nanowires are discussed in this paper.

Experimental

Microcontact Printing

For μCP, two types of stamps were made from polydimethylsiloxane (PDMS). Type I was made by molding PDMS on a silicon calibration grating, producing stamps with parallel features of 1500 nm wide platforms having a height of 500 nm. The spacing between the platforms was maintained to be 1500 nm. This stamp would be expected to transfer material onto the surface in a pattern of 1.5 μm wide parallel lines with 1.5 μm wide separation. Type II was made by molding PDMS on wafer template consisting of recessed 10 μm circles or annular rings with a lateral thickness of 1μm obtained by

photolithography using using Shipley 1813 as photoresist. The height of the stamp features was 2 μm and the spacing between features was 75 μm.

The stamping inks were solutions of zinc acetate in ethanol. These solutions were prepared at four different concentrations: 0.1, 0.2, 2, 10 mM/L. For transferring the zinc acetate onto the silicon substrate, the selected stamp was soaked in the zinc acetate solution for 30 to 60 seconds. The 'inked' stamps were then blown dry with a stream of nitrogen, brought in contact with the silicon substrates for 10 seconds, and then quickly separated. Consistent force was applied from sample to sample by ensuring conformal contact due to work of adhesion. After this printing procedure, the samples were baked on a hotplate for 30 min at 350°C. This heat causes the zinc acetate to decompose, reacting with atmospheric oxygen and forming ZnO nanocrystals. These nanocrystals, now patterned on the on Si substrate, acted as a nucleation layer for the growth of nanowires growth.

Hydrothermal Growth

ZnO nanowires were grown using the conventional hydrothermal method. 25 mM L^{-1} of both zinc nitrate and hexamine solutions were prepared in deionized water (DIW) and heated to 80°C. This solution was used as the growth solution. 10 μL of a 10mM L^{-1} stock solution of

sodium citrate were added per 250 mL of growth solution. The Si substrate was placed face down in the growth solution, and held for 2 hours while the solution was stirred vigorously. Afterward, the silicon was removed from the growth solution, and rinsed with DI water and, optionally, sonicated in DIW for 3-5 seconds to remove ZnO debris – ZnO nanowires grown not on the substrate, but rather in the solution and deposited on the substrate afterwards. This debris has been observed in some of the scanning electron microscopy (SEM) images. It typically appears much brighter than nanowires grown on the substrate as they have an open contact with the substrate, therefore experiencing a stronger charging effect. Finally, samples were dried using dry N_2.

Results and Discussion

Figure 11(a) shows an SEM image of ZnO nanowires grown with

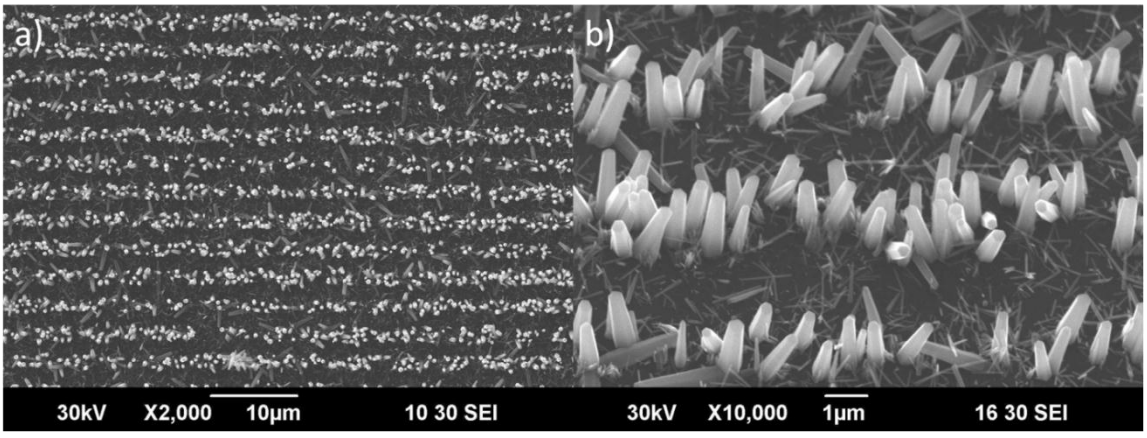

Figure 11. a) SEM image of ZnO nanowires patterned using microcontact printing with type I stamp, b) Zoomed in and tilted 60° SEM image of the same nanowires, revealing their shape and length.

the hydrothermal method on patterned substrates. Patterning was done with the use of microcontact printing with a parallel grating (type I) stamp. The width and spacing of printed lines is approximately 1.5 μm.

As seen in Figure 11(b), the nanowires have a conical shape with a base diameter of approximately 500 nm and an apical diameter of approximately 200-400 nm. These sizes are considerably larger than the sizes observed for nanowires grown under the same conditions on uniformly seeded, rather than patterned, substrates. The reasons for the different sizes observed are unclear. However, a potential explanation may lie in a difference in seeding between the two techniques – even though the same seeding solution was used both for patterned and uniformly seeded samples, the different seeding techniques may introduce a variation in the density of zinc acetate molecules on surface. After baking, different sizes of ZnO nanocrystals would result. Since these nanocrystals serve as growth sites for nanowires, the nanowires produced would have different dimensions. Another potential explanation would be a difference in the growth environment – the patterned nanowires are confined to regions defined by the patterned seeding solution. The patterned surface produces fewer growth sites per area, providing more free space around the wires during the growing stage. This reduced crowding may

lead to more free and rapid access to the zinc ions during the growth. Although a more likely explanation is a combination of these two effects.

Comparable results were observed in work presented below and support the explanations given above. Samples were produced which had relatively large areas patterned with the seeding solution separated by large bare surface. These samples exhibited variations in the size of the nanorods grown within a single sample. Moving from the bare region further into the area of uniform seeding, the nanowires have been found to decrease in size. This decrease is quite dramatic, on the order of a ten-fold change. Also varying is the lateral spacing of the nanowires, with the densest coverage being at the center of the uniformly coated region.

The image in Figure 12 is representative of the ZnO nanowires

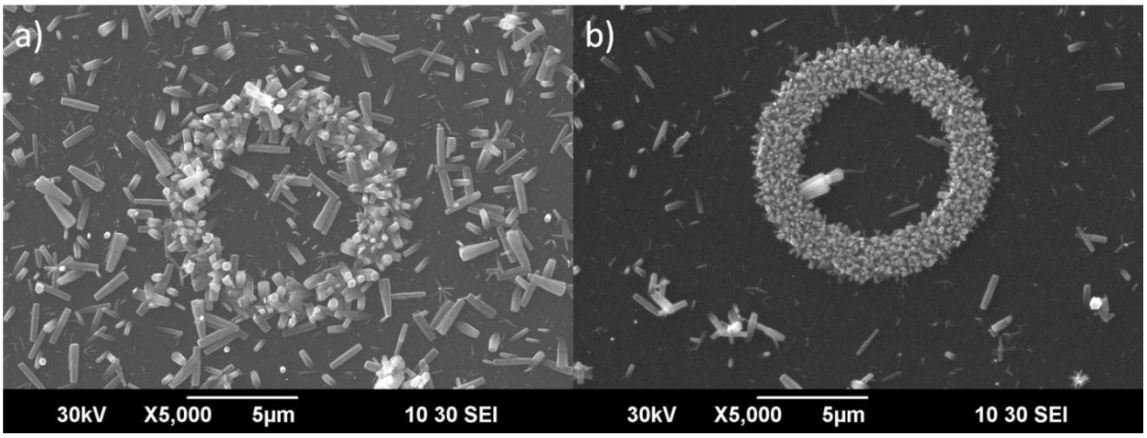

Figure 12. SEM images of ZnO nanowires patterned as annular rings with 10 μm outer diameter and lateral thickness of 1 μm before (a) and after (b) sonication.

as patterned by contact printing the seeding solution with an annular type II stamp. Again, the mean diameter of the resulting nanowires is greater than the mean diameter of the nanowires grown under the same conditions but on surfaces continuously covered by the seeding solution. The nanowires lying around the annular ring are most likely nanowires grown simultaneously in the solution without seeding crystals and deposited on the surface after growth. Alternatively, they may have been grown on the substrate, but they detached and were redeposited. They have a weaker contact with the substrate than the nanowires grown from the seeded ring; therefore, they often have more charging by the SEM and appear much brighter on the SEM images (lower part of the image).

Figure 12(b) is an SEM image of the same patterned ZnO nanowire sample at a different location after light (~3 sec) sonication in DI water. As can be seen, most of the debris is gone. The patterned nanowires predominantly are still attached to the surface, as are some fraction of the nanowires that were grown in the non-seeded areas. The observed in Figure 12(a) and Figure 12(b) difference in the density and size of the nanowires across patterned regions on the same sample may be due to the nature of conformal contact in μCP.

Figure 13(a) is representative of the SEM images of ZnO nanowires patterned with another Type II stamp that had 10 μm solid circles, rather than rings. Interesting to note is that the nanowires on the outside of the circle are of larger diameter than those inside the circle, and the growth is mostly horizontal. Results of this type support the assertion that the larger diameter nanowires has resulted from greater diffusion of the ionic zinc to the growing wires at the edge of the pattern.

Figure 13(b) shows an SEM image of ZnO nanowires grown on the same patterned surface that produced the image shown in Figure 13(a), but in a region where the roof of the stamp was intentionally collapsed. The collapsed part of the stamp printed the seeding solution everywhere except for the region immediately around the feature (residual moat of unsealed area)[72]. Here the restoring forces within the

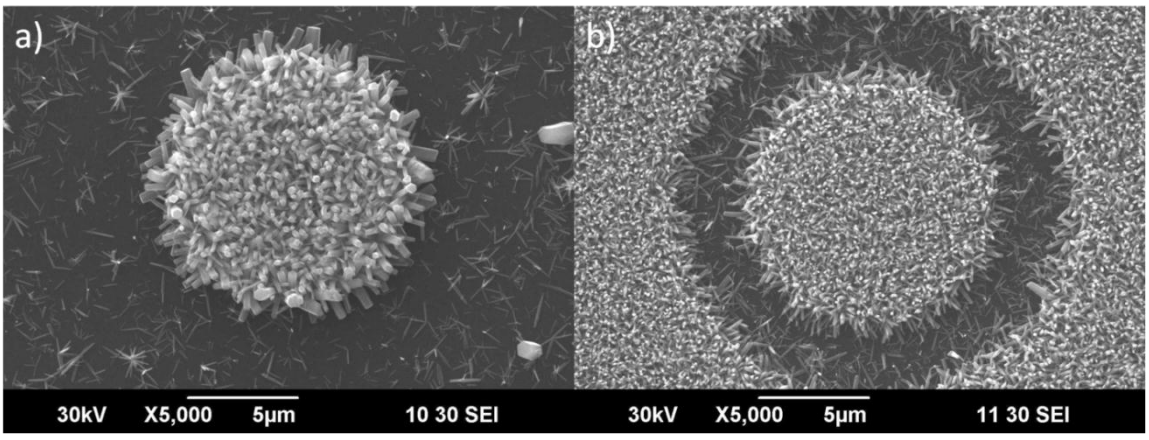

Figure 13. SEM image of ZnO nanowires patterned as circles in areas where microcontact printing was performed (a) normally, (b) with intentionally collapsed roof.

stamp balanced the forces of adhesion between the stamp and the substrate, preventing collapse close to the feature. The variation in nanowire sizes has not occurred in this case. Two reasons likely explain this behavior – 1. the modified distribution of forces in this geometry has changed the deposition density of the seeding solution, resulting in a more uniform distribution of the zinc acetate, and/or 2. the growth of the nanowires around the feature prevented effective refreshing of the chemicals so that the nanowires could not grow at the same conditions as shown in the previous figure. The latter explanation can also be confirmed by the fact that samples with lines printed with stamps of Type I have nanowires of larger sizes as compared with the samples with uniform seeding grown under the same conditions.

Figure 14 shows the typical X-ray diffraction (XRD) patterns of the ZnO nanowire coated substrate. Two peaks are pronounced for the ZnO diffraction pattern: (002) and (101) which appear at 2θ=34.4°, 36.3°, respectively. The ZnO nanowires in the samples under investigation have shown a dominate diffraction peak for (002), which indicates a high degree of orientation with the *c*-axis vertical to the substrate surface. The XRD results suggest that our sample is highly crystallized wurtzite type.

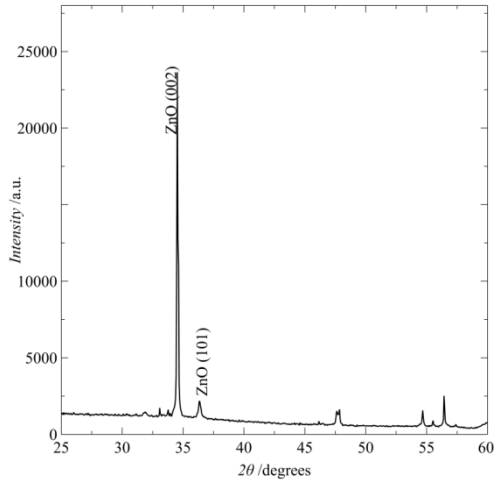

Figure 14. Typical XRD of samples grown with technique described. Pronounced (002) peaks is an indication of predominantly vertically aligned nanowires.

Conclusion

A simple and cost effective technique for the hydrothermal growth of patterned ZnO nanowires is shown in this paper. The microcontact printing technique is employed for growing spatially distributed ZnO nanowires for device applications. Our study has also shown that both the seeding and the local growth environment are critical for the sizes and shapes of the produced nanowires.

Acknowledgments

This research was partially supported by NSF Grant#0854023.

Chapter 4: Novel Aster-like ZnO Nanowire Clusters for Nanocomposites[2]

Abstract

ZnO nanostructures have attracted a great deal of interest because of their biocompatibility and outstanding optical and piezoelectric properties. Their uses are widely varying, including incorporation in sensors, solar cells, and nanogenerators. Biological systems are yet another area of application of ZnO nanowires. Apart from their electrical and optical properties, ZnO nanostructures can be used for the mechanical reinforcement of existing biomimetic scaffolds such as collagen and/or other biodegradable polymers (poly(lactic acid), polyglycolide, poly(alkyene succinate)s or polyhydroxylalkanoates). In this work, we have demonstrated a cheap and comparatively facile hydrothermal growth method for the bulk production of ZnO nanostructures exhibiting an aster-like geometry. The novel nanostructures of ZnO can be used as reinforced material to biopolymers. The aster shape has presented an increased surface

[2] Mikhail Ladanov, Manoj Ram, Ashok Kumar, Garrett Matthews, Novel Aster-like ZnO Nanowire Clusters for Nanocomposites, Mater. Res. Soc. Symp. Proc. Vol. 1312, 2011, reproduced with permission.

area, providing a means for enhancing the stabilization of the gels and\or polymers. With controllable growth of ZnO nanostructures this method allows the geometry which could be tuned for maximal coupling between the two phases of composite and increased mechanical strength.

Introduction

ZnO is a biocompatible piezoelectric II-VI semiconductor with a wide direct band gap of 3.37 eV and large exiton binding energy of 60 meV. Recently, ZnO nanostructures have attracted great attention as a promising functional material due to its suitability for application in UV lasers,[21, 37] light emitting diodes,[19] sensors,[7, 8, 73] nanogenerators[4, 5, 6] and solar cells. Due to biocompatibility,[74, 75] ZnO can be used as a functional material in implantable devices or even as a reinforcing material for different biopolymers. In this case bulk growth of structures with large surface area to volume ratios while keeping the effective volume large enough for successful incorporation into biopolymers is desired.

Many methods have been used to prepare ZnO nanowires, including using chemical vapor deposition,[7, 26] metal–organic chemical deposition,[31, 32] pulsed laser deposition,[70] physical vapor deposition,[31, 71] vapor-liquid-solid methods[6, 27] and hydrothermal methods.[37, 38, 39]

The hydrothermal method is one of the most simple and cost effective methods, making the scaling up of production straightforward.

Growth of ZnO nanostructures using the hydrothermal method has been studied extensively as it is a simple way to produce various shapes and geometries of nanostructures. The use of modifying agents, various substrates, wide spectra of seeding techniques and electric field assistance has become common for the modification of resultant properties, such as shape, size and morphology of ZnO nanostructures. However, mostly these techniques are suitable for the growth of ZnO nanostructures on various substrates.

In this paper, we demonstrate the growth of ZnO nanostructures in a bulk solution, where different sizes of ZnO nanoparticles were used as nucleation sites for the hydrothermal growth. During conventional hydrothermal growth ZnO nanowires grow not only on the surface of the substrate, but in the solution as well. This method often leaves debris on the resultant samples, but has the advantage that adding ZnO nanoparticles as growth sites changes the bulk-grown nanostructures greatly. We demonstrate these nanostructures, and discuss possibilities for large scale repeatable growth of such structures.

Experimental

Chemicals and Reagents

The zinc nitrate hexahydrate ($Zn(NO_3)_2 \cdot 6H_2O$) and hexamethylenetetramine (HMTA), trisodium citrate ($C_6H_5Na_3O_7$), were all ACS grade and purchased from Sigma-Aldrich (USA). Zinc Oxide Nanoparticles with a nominal size of 10-30 nm were purchased from SkySpring Nanomaterials, Inc. and Zinc Oxide Nanopowder of nominal sizes <50 nm and <100 nm were purchased from Sigma Aldrich. All solvents and materials were employed as purchased without any further purification unless specified.

TEM of the nanoparticles was performed. The method followed was: a small amount of nanoparticles as purchased were mixed with ethanol and actively sonicated to separate bundled particles. A TEM copper mesh was dipped in the solution and dried. TEM was performed on this grid.

ZnO Nanostructures Growth

ZnO nanostructures were grown using the conventional hydrothermal method. 25 mM L^{-1} of zinc nitrate and hexamine solutions in deionized water (DIW) at 80°C were used as the growth solution. Different amounts of sodium citrate solution in DIW were added into selected samples, as specified.

ZnO nanoparticles in amount of 20-30 mg were vigorously sonicated in 1 mL of DIW to effectively separate and unclog them and were added to the growth solution. They acted as nucleation sites for nanostructure growth.

The solution was kept at 80°C with vigorous stirring for 4 hours and then washed with DIW and ethanol and finally filtered. Samples obtained were studied using SEM technique.

Results and Discussion

Figure 15(a) shows a TEM image of as purchased ZnO nanoparticles with nominal size <30 nm. The TEM picture reveals less distribution in size than other samples with nanoparticles size of nearly 200 nm in comparison with the nominal 10-30. Figure 15(b) shows a TEM image of as purchased ZnO nanoparticles with nominal size <50 nm. ZnO nanoparticles have a large distribution in size and generally

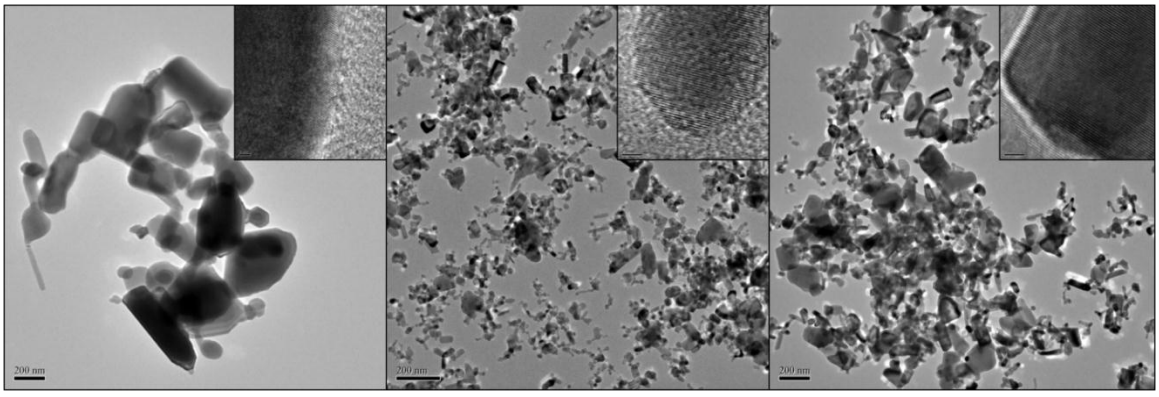

Figure 15. TEM images of as purchased ZnO nanoparticles with nominal sizes of a) 10-30 nm, b) <50 nm, c) <100 nm. Scale bar on the images is 200 nm. Insets: high resolution TEM of atomic planes of the nanoparticles. Scale bar is 2 nm.

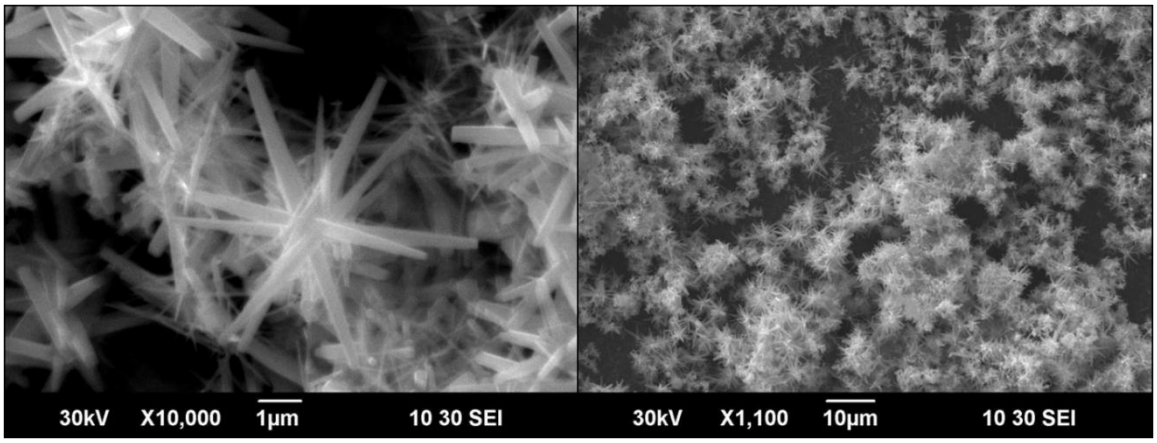

Figure 16. a) SEM image of as grown ZnO aster-like nanostructures with ZnO nanparticles of the nominal size of 10-30 nm acting as nucleation sites, b) Zoomed out SEM image of as grown ZnO aster-like nanostructures with ZnO nanparticles of the nominal size of 10-30 nm acting as nucleation sites. The aster-like structures are the preferable resultant structure with these growth conditions.

are of size much less than 50 nm. Figure 15(c) shows a TEM image of as purchased ZnO nanoparticles with nominal size <100 nm. ZnO nanoparticles have a large distribution in size and generally are of size ~100 nm. Insets in Figure 15 show atomic planes of the corresponding particles; the scale bar is 2 nm.

Figure 16(a) shows a TEM image of ZnO nanostructures grown in bulk solution as described before with addition of 2μL of 0.1 mM/L of sodium citrate. Approximately 24 mg of ZnO nanoparticles with nominal size 10-30 nm were added as nucleation seeds. Aster-like shape of resultant ZnO nanostructure has been observed in the image, showing ZnO nanowires growing out of common nucleation site.

A lower magnification image of the same sample is presented in Figure 16(b) and shows the abundance of aster-like structures in the

samples. This indicates that this growth mode is preferable under the present growth conditions.

An SEM image of ZnO aster-like structures grown with ZnO nanoparticles of nominal size of <50 nm are shown in Figure 17(a). The nanostructures growth was performed following the general recipe with no sodium citrate added. 25 mg of ZnO nanoparticles of nominal size <50 nm were used as nucleation sites. Aster-like nanostructures are not as pronounced as structures with 30 nm ZnO nanoparticles nucleation, but are in abundance as shown in Figure 17(a).

Figure 17(b) shows ZnO nanostructures grown with the same general recipe, with no sodium citrate added. 27 mg ZnO nanoparticles of <100 nm nominal size were added as nucleation sites in this growth. Although aster-like nanostructures have been observed, the

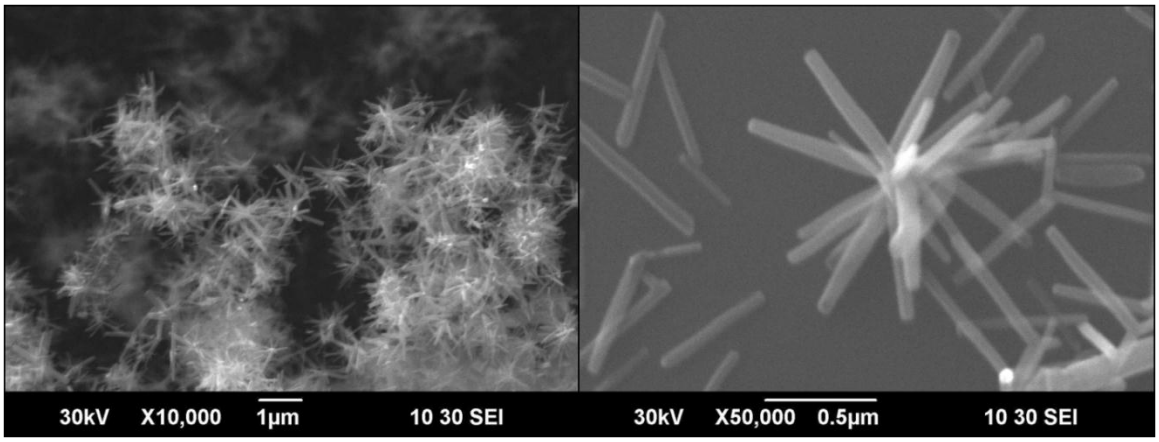

Figure 17. a) SEM image of ZnO aster-like structures grown with ZnO nanoparticles of nominal size of <50 nm, b) SEM image of ZnO aster-like structures grown with ZnO nanoparticles of nominal size of <100 nm.

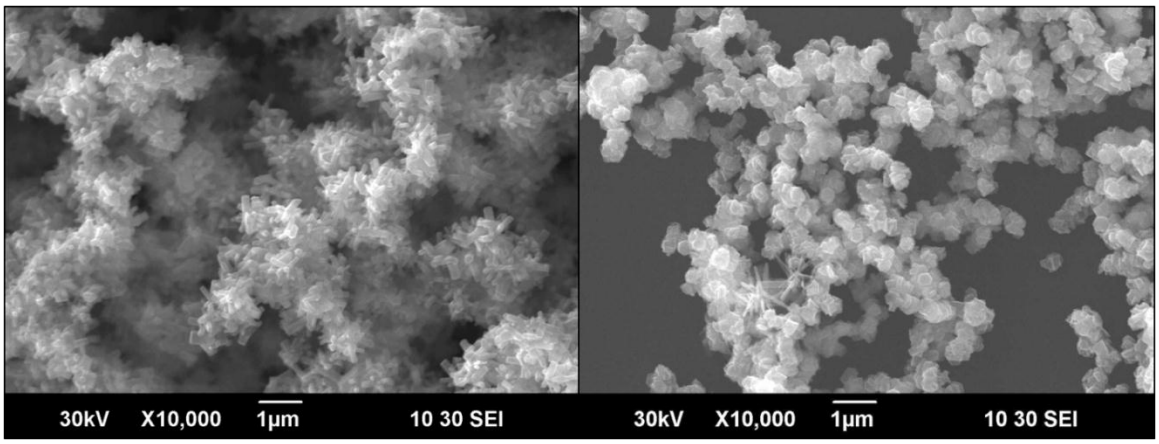

Figure 18. SEM image of ZnO nanostructures grown following general recipe with addition of a) 20 μL of 10 mM/L of sodium citrate per 250 mL of growth solution and b) 2 mL of 10 mM/L of sodium citrate per 250 mL of growth solution.

resultant nanostructures are in mass plain ZnO nanowires.

Also performed was a series of experiments in which higher concentrations of sodium citrate, which acts as surfactant agent, were used. Here aster-like structures were not observed in any sample, as can be seen in Figure 18. Instead, rod-like nanowires of increased size (with addition of 20 μL of 10 mM/L sodium citrate) were obtained. The use of even larger concentrations of the surfactant (addition of 2 mL of 10 mM/L of sodium citrate) somewhat cubic-like structures resulted (Figure 18(b)).

X-ray diffraction (XRD) and Energy-dispersive X-ray spectroscopy (EDS) measurements were also performed to characterize obtained ZnO nanostructures. Figure 19(a) and (b) show typical XRD and EDS spectra, respectively. In XRD measurements obtained peaks at 31.77°, 34.43°, 36.26°, 47.55°, 56.61° and 62.87°

correspond to hexagonal ZnO structure with crystallographic (100), (002), (101), (102), (110) and (103) directions, respectively. EDS measurements reveal that sample generally contains the atomic ratio 35.7% and 53.76% of zinc and oxygen, respectively. Higher atomic percent of oxygen is not uncommon for metal oxides. Meanwhile, EDS measurements support the proper identification of peaks in XRD spectra of ZnO nanostructures.

Conclusion

Conventional hydrothermal growth with addition of ZnO nanoparticles as nucleation sites could be used for growth of aster-like nanostructures. Care should be taken regarding the size and quality of nanoparticles. Uniformly sized seeding particles with lateral dimensions

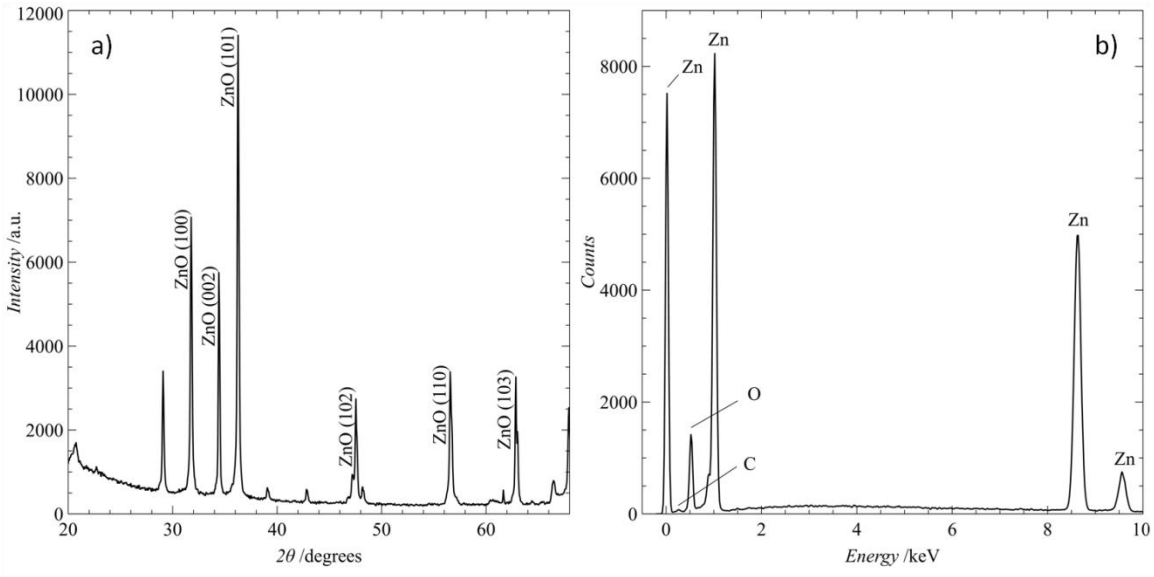

Figure 19. Typical a) XRD spectra and b) EDS spectra of ZnO nanostructures grown following general recipe. Nanostructures were diluted in ethanol, dropcasted on Si substrate and dried for XRD and EDS measurements.

of ~200 nm should be used as nucleation sites. In this study the best results were obtained using nanoparticles with nominal size of 10-30 nm.

Chapter 5: Structure and Opto-Electrochemical Properties of ZnO Nanowires Grown on *n*-Si Substrate[3]

Abstract

Zinc oxide (ZnO) nanostructures have attracted great attention as a promising functional material with unique properties suitable for applications in UV lasers, light emitting diodes, field emission devices, sensors, field effect transistors, and solar cells. In the present work, ZnO nanowires have been synthesized on an *n*-type Si substrate using a hydrothermal method where surfactant acted as a modifying and protecting agent. The surface morphology, electrochemical properties, and opto-electrochemical properties of ZnO nanowires are investigated by using scanning electron microscopy (SEM), energy dispersive X-ray spectroscopy (EDS), cyclic voltammetry, and impedance spectroscopy techniques. The cycling characteristics and rate capability of the ZnO nanowires are explored through electrochemical studies performed under varying electrolytes. The photo response is observed using UV radiation. It is demonstrated that crystallinity, particle size, and

[3] Reprinted (adapted) with permission from M. Ladanov, M. K. Ram, G. Matthews, and A. Kumar, Langmuir, 27, 9012 (2011). Copyright (2011) American Chemical Society.

morphology all play significant roles in the electrochemical performance of the ZnO electrodes.

Introduction

Zinc oxide (ZnO) is an II-VI semiconductor with a wide direct band gap of 3.37 eV at 300 K and large exciton binding energy (60 meV). Its nanostructures have attracted great attention as a promising functional material. The unique properties of nanostructured ZnO make it suitable for applications in UV lasers,[21, 37] light emitting diodes,[19] electrochromic and field emission devices,[9] sensors,[7, 8, 73] field effect transistors,[7, 73, 76] nanogenerators actuated by atomic force microscopy (AFM) tips[4, 6] or driven by ultrasonic waves,[5] and solar cells.[16]

Among the various ZnO nanostructures, well-aligned nanowire arrays are one of the most promising, and consequently they have been extensively studied.[10, 32] Many methods have been used to prepare ZnO nanowire arrays, including using chemical vapor deposition (CVD),[7, 26] metal–organic chemical deposition (MOCVD),[31, 32] pulsed laser deposition (PLD),[70] physical vapor deposition,[31, 71] vapor-liquid-solid (VLS) methods[6, 27] and the hydrothermal method.[37, 38, 39] These techniques are well developed and show the efficiency and accurate control of the processes as well as the resulting morphology of ZnO nanostructures. Moreover, they are generally inexpensive.

However, for practical reasons, fabrication of devices based on ZnO should be relatively simple, straightforward, as well as cost-effective. Therefore, a solution phase approach recently has attracted a great attention due to its simplicity compared to other methods, and due to its ability to produce large-scale, low-cost, and controllable growth of one-dimensional ZnO nanocrystals.[37, 38, 40]

It is known that crystallinity, particle size, and morphology play significant roles in the electrochemical performance of ZnO anode materials. Also, previously it has been proven that controlling the morphologies of transition metal oxides could improve their electrochemical performance, such as cycling characteristics and rate capability. However, detailed studies of the structure, the electrochemical and opto-electrochemical properties of ZnO nanowires will improve greatly their applicability in photocell devices. From this point of view, we utilized a conventional hydrothermal method to synthesize ZnO nanowires directly on a conducting Si surface. We used a surfactant as the modifying and protecting agent in this process. As the seeding of ZnO nanocrystals plays an important role in the resulting morphology of ZnO nanostructures,[39] special attention was paid to developing a repeatable and tunable seeding recipe combined with utilization of surfactant agents. This approach leads to broad control over the morphology of the ZnO nanostructures produced. The

synthesis process did not require high temperature or preformed templates. Thus the advantages of this method for the preparation of ZnO nanowires include its simplicity and mild reaction conditions, as well as its suitability for large-scale preparation of samples with controlled morphologies.

Experimental

Reagents and Materials

The nitrate hexahydrate ($Zn(NO_3)_2 \cdot 6H2O$), hexamethylenetetramine (HMTA), and diethylenetriamine sodium citrate were all ACS grade and purchased from Sigma-Aldrich (U.S.A.). All solvents and materials were employed as purchased without further purification unless specified.

ZnO Nanowire Growth and Characterization

ZnO nanowires were grown using the conventional hydrothermal method. Twenty-five millimolar zinc nitrate and hexamine solutions in deionized water (DIW) at 80 °C were used as the growth solution. Ten microliters of a 10 mM solution of sodium citrate per 250 mL of growth solution were added.

ZnO nanocrystals on Si substrate acted as a nucleation layer for nanowire growth and were created by the following recipe: 2 mL of 0.5 mM of zinc acetate in ethanol were spun on 2 in. Si substrate at 1000-

1200 rpm for 40-50 s. Immediately after ethanol visibly evaporated from the substrate, the substrate was dried by a flow of dry N_2 while spinning to ensure removal of water remnants and achieve uniform seeding. After that, the Si wafer was baked at 350 °C on a hot plate for 30 min.

ZnO nanowires were grown by submerging the seeded n-type Si substrates inverted in the growth solution at 80 °C for 2 h. Temperature was controlled by a water circulation system, and the growth solution was constantly stirred.

The average turnover time to refresh the chemical solution in the reactor was 3 to 5 h in order to enhance the growth rate and aspect ratio of the nanowires for a specific growth time. Finally, substrates were removed from the growth solution, rinsed with DIW, and dried under nitrogen flow.

The basic reaction responsible for the growth of nanowires from solution is described as follows.

Decomposition reaction:

$$(CH_2)_6N_4 + 6H_2O \rightarrow 6HCHO + 4NH_3$$

Hydroxyl supply reaction:

$$NH_3 + H_2O \Leftrightarrow NH_4^+ + OH^-$$

Supersaturation reaction:

$$2OH^- + Zn^{+2} \rightarrow Zn(OH)_2$$

ZnO nanowires growth reaction:

$$Zn(OH)_2 \rightarrow ZnO + H_2O$$

Surface/Structure Characterization

The surface morphology of ZnO nanowires was investigated by scanning electron microscopy (SEM) to determine their size, shape, and density. X-ray diffraction (XRD) of the samples was used to demonstrate the crystallinity of the nanowires and preferred crystal orientation. Energy dispersive X-ray spectroscopy (EDS) was used to determine the chemical composition of the obtained structures.

Electrochemical Measurements/Photo-electrochemical Response Setup

The electrochemical and photochemical measurements were carried out using a Potentiostat/Galvanostat (Voltalab). A standard three electrode configuration was employed, where the n-Si/ ZnO nanowires acted as the working electrode, a platinum wire acted as the counter electrode, and Ag/AgCl acted as the reference electrode. The electrochemical studies were performed in 0.05 mM HCl, 0.01 M NaOH in DIW and 0.1 M LiClO4 in acetonitrile electrolytes. UV light with maximum intensity at 366 nm was used to illuminate the sample from 2 to 3 cm away from the working electrode. The power supplied to the UV light were controlled manually.

Results and Discussion

Structural Studies

The SEM studies indicated that the morphology of the ZnO nanowires produced by this method was not homogeneous across the surface of the silicon substrate. One can clearly distinguish areas with the same seeding as the developed recipe as well as areas with no seeding at all (no ZnO NW observed). Figure 20a shows a top-down

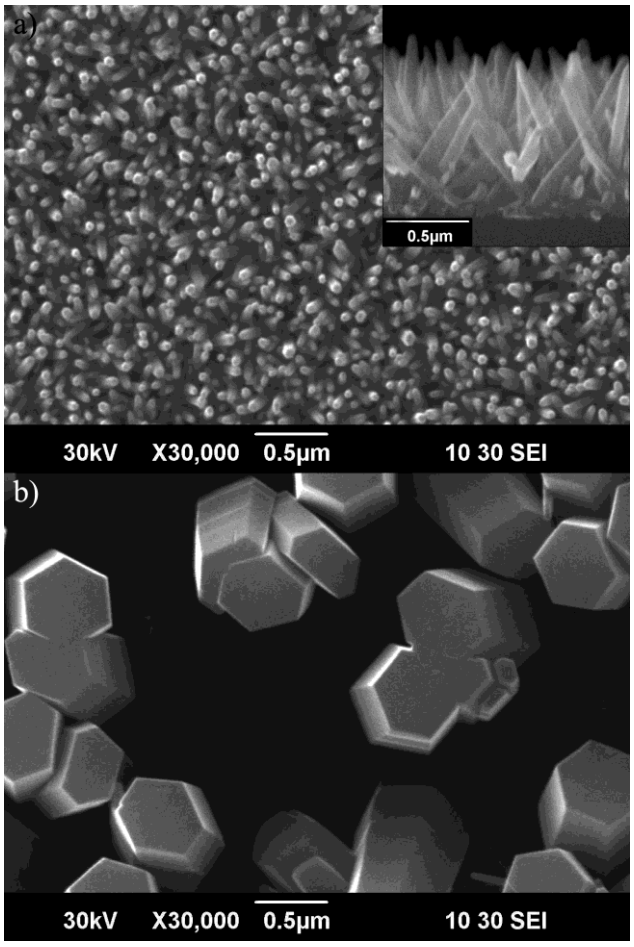

Figure 20. a) SEM image of the as grown nanowires. Inset: cross section of the sample with nanowires. b) SEM image of nanowires on the same sample in the transition area between seeded and non-seeded regions. With the same growth conditions density of ZnO nanocrystals combined with surfactant agent plays significant role in formation of nanowires.

image of the ZnO nanowires grown in a densely seeded region. The diameter of the nanowires in this region was ~50-100 nm, with clear hexagonal structure. Also shown in Figure 20(a) is an SEM image of the cross-section (see inset), revealing that the orientation of the nanowires was predominately vertical. The length of these nanowires was approximately 1 μm for a 2 h growth period, as described in the Experimental Section. In the region transitioning from dense seeding to minimal seeding, the morphology of the nanowires changes. Figure 1b shows an SEM image taken from the same sample, but near the edge of the seeded area. The ZnO nanowires grown in this region had several times larger diameters and again showed clear hexagonal structure. Moreover, the density of the nanowires was much lower. Apparently, the density of ZnO microcrystals that served as the seeding layer was diminished. This change in density resulted in ZnO nanowires being grown under different conditions from those shown in Figure 20(a), even though the growth solution, temperature, and time were identical. It has been shown previously that, even with the same growth conditions, the morphology of nanowires is dependent upon the seeding method.[39] Thus, we have shown that ZnO growth primarily was controlled by the density and the quality (i.e., grain size, thickness of film and\or crystallographic orientation) of seeded ZnO nanocrystals.

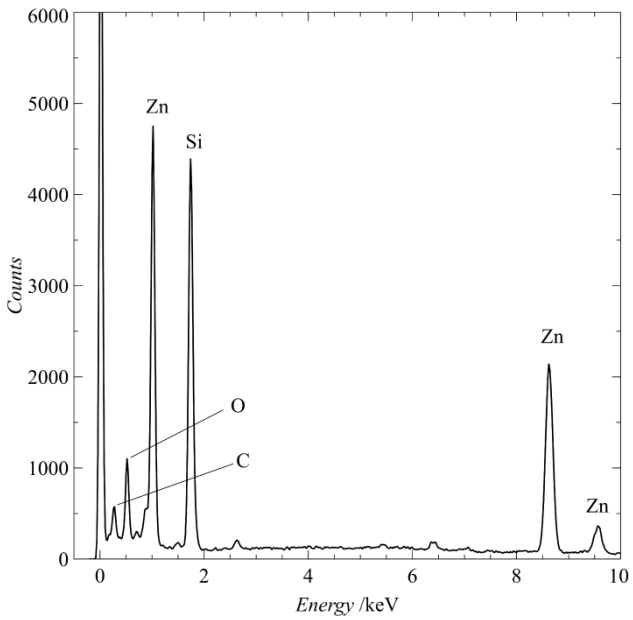

Figure 21. EDS data of as-grown sample with ZnO nanowires. Zn, O, Si and C peaks are present.

EDS of ZnO nanowires grown on *n*-Si was performed, and the resulting spectrographic data is shown in Figure 21. EDS determines the composition of the synthesized ZnO nanostructures, and the results reveal that the nanostructure was composed of Zn, O, C, and Si. Quantitative EDS analysis showed that the element weight ratio of Zn to O was about 1:1. The presence of C can be understood as the residue left from the organic solvent used in preparation of the ZnO nanowires. The presence of the Si peak in the EDS pattern can be assigned to the Si substrate.

Figure 22 shows the XRD patterns of the substrate coated with ZnO nanowires. Four peaks were pronounced for the ZnO diffraction pattern: (100), (002), (001) and (102) appear at 2θ = 31.7°, 34.4°, 36.3° and 47.5°, respectively. As expected, the ZnO nanowires in the sample showed a dominate diffraction peak for (002), indicating a high degree of orientation with the *c*-axis vertical to the substrate surface. The XRD results suggest that our sample was highly crystallized wurtzite type.

Electrochemical Study

In order to explore their possible application, the electrocatalytic performance of the as-prepared ZnO nanowires on doped silicon

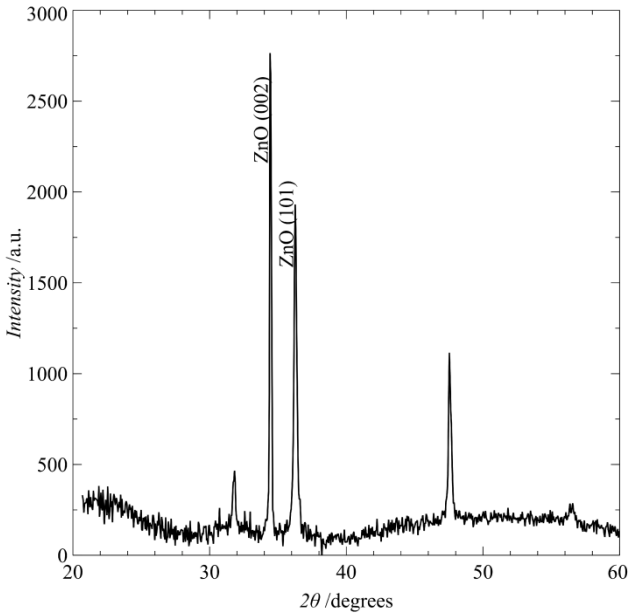

Figure 22. XRD data of the as-grown sample, revealing crystalline structure of ZnO nanowires. Pronounced (002) peak suggests dominating vertical alignment of nanowires.

substrate was characterized. An *n*-Si substrate covered with ZnO nanowires was used as a working electrode, platinum was used as a counter electrode, and Ag/AgCl was used as a reference electrode in the presence of different electrolytic solutions.

Figure 23(a) shows cyclic voltammograms (CVs) of the ZnO array electrode in 0.1 M $LiClO_4$ solution as a function of the scan rate. The CV showed a pair of well-defined redox peaks for ZnO nanowires. The oxidation of the ZnO nanowires was around 0.2 V, whereas the reduction peak was observed at around -0.4 V vs Ag/AgCl. These results imply that the ZnO arrays demonstrate electrocatalytic activity to oxidation in the presence of the $LiClO_4$ electrolyte. The cathodic reduction peak at -0.4 V can be assigned to the reduction of ZnO into Zn. ZnO showed the classical reduction-oxidation behavior of metallic Zinc in ZnO nanorods. There is an increase in the current density due to reduction of Zn^{2+} to Zn, which was accomplished with a hysteresis effect, followed by an anodic peak close to 0.2 V during the reverse scan.

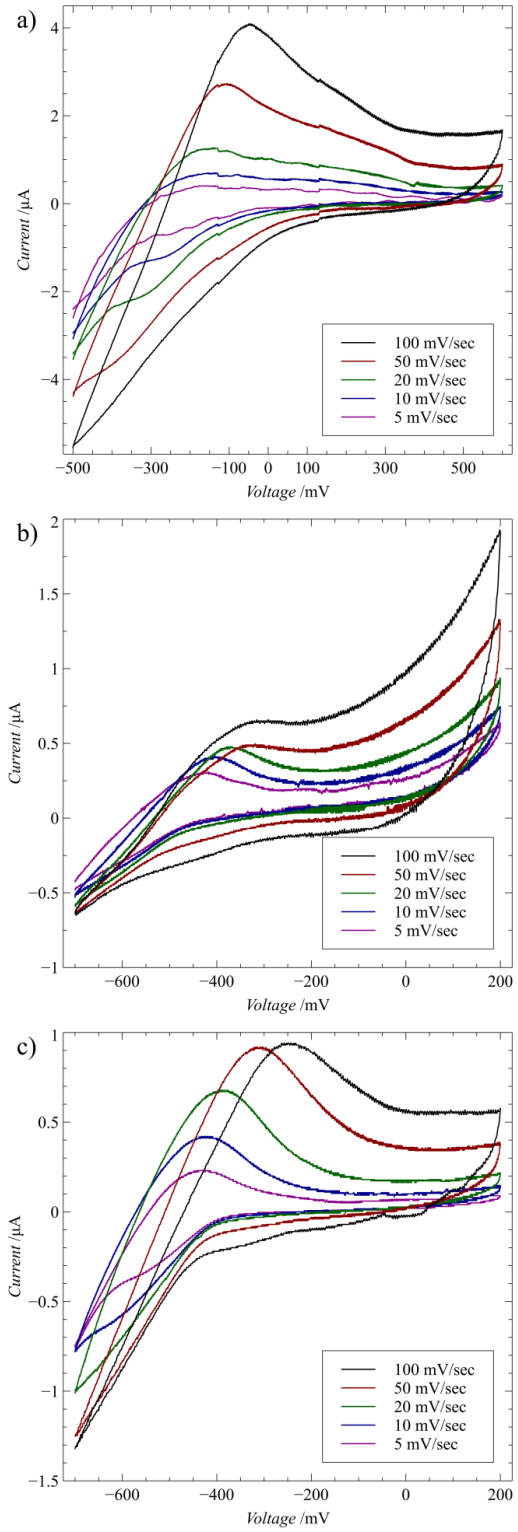

Figure 23. CVs at different scanning speeds for a) LiClO4, b) NaOH and c) HCl electrolytes.

Figure 23(b) shows the CVs of the ZnO array electrode in 0.01 M

NaOH solution as a function of the scan rate. The CVs of ZnO in 0.01 M NaOH generally were used to understand the charge capacity of ZnO. The results revealed interesting CV properties in the oxidation potential at around -0.33 V, and the peak decreased as the scan rate decreased. The reduction potential was not as sharp as was observed for the oxidation potential. Figure 23c shows CVs of the ZnO array electrode in 0.5 mM HCl solution as a function of the scan rate. This figure shows the oxidation peak at around -200mV at 100 mV/s. Interestingly, the oxidation peak was found to shift toward more negative potential as a function of scan rate. The observed shift in redox potential was negative due to the slow kinetics of ZnO reduction. The kinetics of ZnO decreased as a function of scan rate. In the reduction of ZnO electrode, the diffusion coefficient also changed in different solutions. The CVs of ZnO nanowires in different electrolytes show the hysteretic characteristics of electron accumulation and discharge in ZnO nanowires superimposed upon the Faradic current due to the electrolytes. The voltammogram is also completely dependent upon the scan rate. A similar effect was observed for the reduction peak shifting toward more negative potential as a function of scan rate. The reverse scan gives the corresponding cathodic peak, and the anodic peak was well-defined for the repeated scans. The CV measurements shown in Figure 23(a,b,c) are indicative of an

electrochemical diffusion controlled system. Thus, the observed oxidation was totally reversible.

Figure 24 represents chronoamperometric studies, where the potential was varied from -0.2 to 0.5 V vs Ag/AgCl in three different electrolytic systems. The current transient was recorded for the oxidation and reduction potentials. The chronoamperometry study serves as an alternative probe of electron occupancy in ZnO NWs film. The oxidation shows higher current and faster response than the reduction system. A similar effect was observed in Figure 23 for the CV studies. The reduction and oxidation showed a sharp transition as shown in Figure 24. The transient current exhibited a "fast" phase in ZnO NWs, which was complete within 1 s at the applied negative

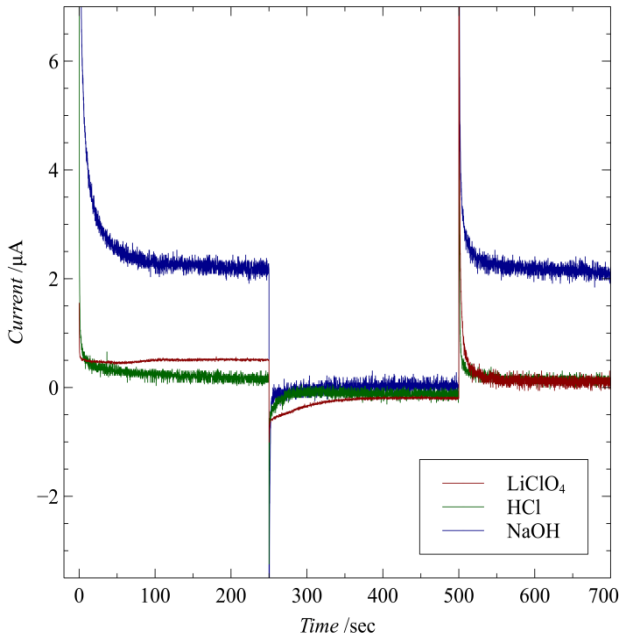

Figure 24. Chronoamperometry for LiClO4, NaOH and HCl electrolytes.

potential.

Electrochemical impedance spectroscopy (EIS), which provides information regarding the resistance and capacitance of the electrode materials, is an effective approach for investigating electron transfer across the electrolyte and the surface of the electrode. Figure 25(a) shows the typical impedance spectra of the ZnO nanowire electrode in 0.1 M LiClO4 solution at an AC frequency varying from 100 kHz to 0.1 Hz. The ZnO electrode displayed semicircles at the high-frequency region and a straight line at the low-frequency region, indicating that the electrochemical reaction at the ZnO electrode was controlled by a mixed process of charge transfer and diffusion limitation. A similar effect was demonstrated in Figure 25(b,c) in 0.01 M NaOH and 0.5 mM HCl electrolytes, respectively.

Photoelectrochemical Current

Figure 26 shows the response of photopotential of the ZnO nanowire electrode under UV irradiation. When the UV-light was switched on, an electron-hole pair was generated showing the photocurrent. The initial charge separation competes with recombination, so both processes have to take place on the same time scale.

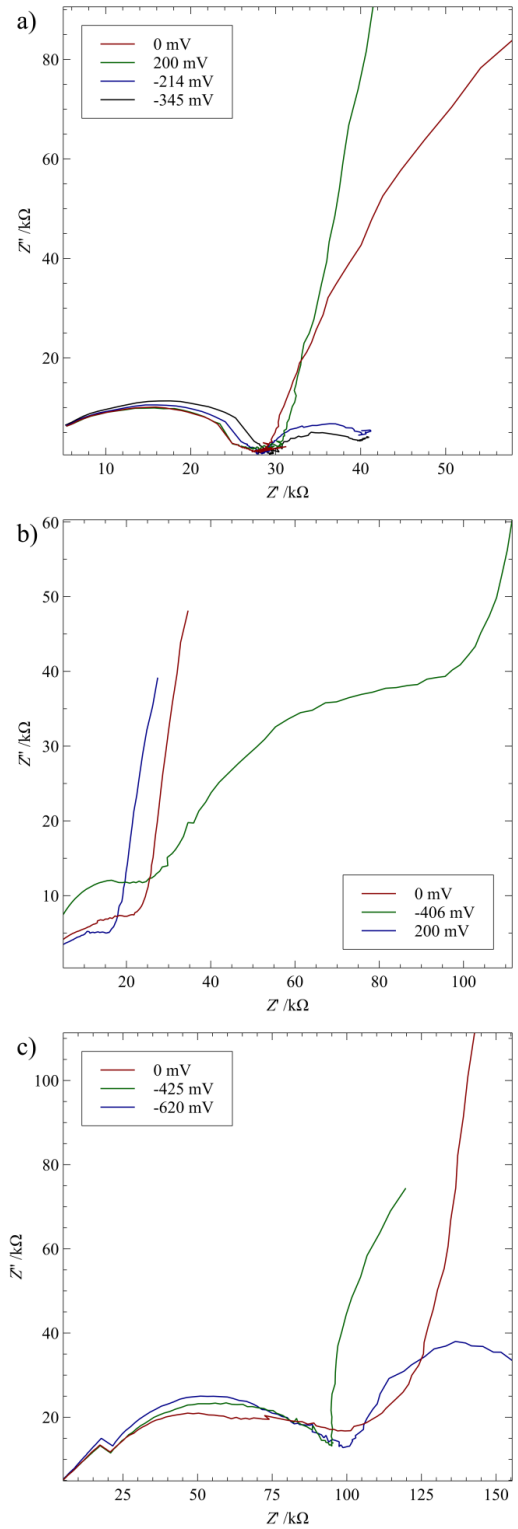

Figure 25. Nyquist plot of samples with ZnO nanowires in a) LiClO4, b) NaOH and c) HCl electrolytes.

The net transport through the electrode was divided into two subsequent processes: one process was charge transport through the nonilluminated part of the ZnO, and the other process was transport through the *n*-Si substrate to the back contact. The UV irradiation changed the current abruptly with little variation, and returns to the initial value after the light is switched off. In addition, it also was noticed that the photopotential sharply reverted when the light was switched off. Although recombination of photogenerated carriers occurred in the ZnO under dark conditions, it was restrained effectively by the internal electrostatic field in the junction region. The separated electrons migrated easily to the external circuit. However, it is well established that liquid electrolytes create Schottky junctions when brought into contact with ZnO. We have tried to understand the

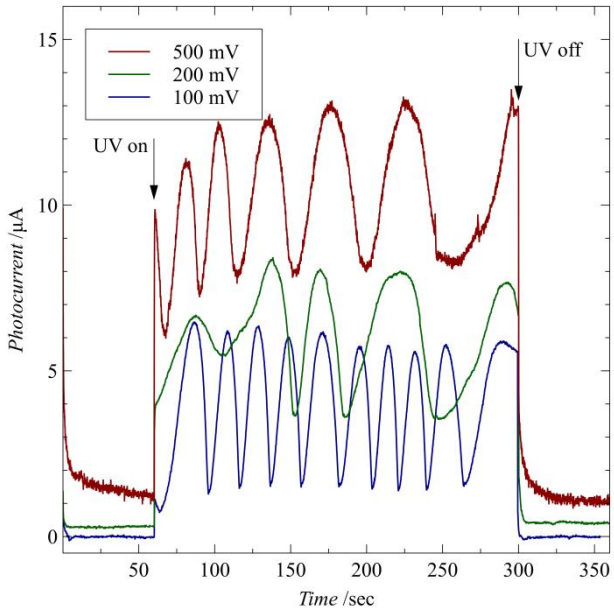

Figure 26. Photocurrent response to UV light at different DC biases.

junction between the liquid electrolyte and ZnO rather than n-silicon and n-type ZnO.

The electron transfer process in the ZnO electrochemical set up is similar to that in a semiconductor-metal composite. The electrons in the valence band of ZnO were excited to its conduction band, giving rise to the formation of an electron-hole pair, as shown in the schematic in Figure 27. The UV irradiation caused a rise in the transient photocurrent followed by an exponential decay after the UV light was switched off.

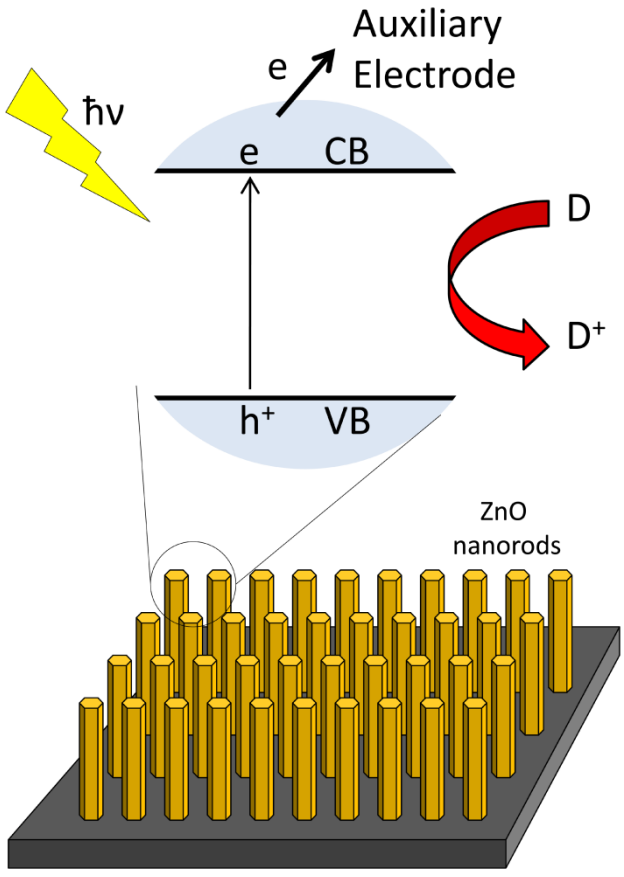

Figure 27. Schematics of electrochemical processes on the surface of the sample.

Conclusion

The growth of ZnO was primarily controlled by the density of seeded ZnO nanocrystals. The electrochemical studies at various electrolytes showed the cycling characteristics and the rate capability of ZnO nanowires. It was established that crystallinity, particle size, and morphology play significant roles in the electrochemical performance of the ZnO nanowire electrode. The electrochemical study also indicated that ZnO nanowires were able to be doped with ions, and the process was reversible. The photoelectrochemical current was observed by illumination with UV-light in an electrochemical cell where ZnO acted as the working electrode in electrolytic media. The detailed structure, electrochemical, and opto-electrochemical studies on ZnO nanowires could provide for their application in photocells and photosensors.

Acknowledgements

This research was partially supported by NSF Grant#0854023.

Chapter 6: Effects of the Physical Properties of Atomic Layer Deposition Grown Seeding Layers on the Preparation of ZnO Nanowires

Abstract

Zinc Oxide (ZnO) nanowires are growing in interest as the number of devices for which they are well suited increases. Success in these applications requires defined and controlled geometric incorporation of the wires into the various platforms. Therefore, establishing the ability to tailor the growth ZnO nanowires to produce specified sizes, surface densities, and orientation will be important. In the reported work, the effects of the seeding layer on these factors were accessed. Atomic later deposition (ALD) was used to produce thin films of ZnO under varying growth and post-processing conditions. These films were fully characterized, including their thickness, surface roughness, and crystalline orientation. Using these well-defined films as the seeding layer, ZnO nanowires were grown and subsequently characterized in terms of morphology and crystalline properties. It was shown that the resulting nanowire properties are dependent upon the nature of the seeding layer, and careful

production of the seeding layer allows for some control over these properties.

Introduction

Zinc oxide (ZnO) nanostructures currently are being studied extensively because of their promising optical and electronic properties and their resulting potential applications in a wide variety of devices. These devices can be divided into several categories, including mechanical transducers,[4, 5, 6] photovoltaic devices,[16, 19] chemical and gas sensors,[7, 8] field emission devices,[9] and lasers.[20] ZnO nanostructures also have been used as a promising biocompatible material for biological applications[23, 24] and recently were studied as an electrode material for electro- and optoelectrochemical applications.[25]

This wide diversity of applications requires controlled production of ZnO nanowires with very different and tailored physical properties. In the particular application of using these nanowires as an electrode material, strategic control over their size, shape and surface density is of high importance.

Many different growth techniques are currently available for production of ZnO nanowires on various substrates,[26, 27, 31, 32, 70, 71] One of the most simple and cost-effective techniques is the hydrothermal process.[37, 38, 39] The simplicity and scalability of this growth method

make it highly suitable for commercial applications. This advantage is especially crucial for usage of ZnO nanowires in high-volume production of electrodes for batteries, as well as for supercapacitor applications.[77]

In the hydrothermal process, growth of ZnO nanowires is facilitated by a suitable substrate with proper surface treatment or coating. For general, non-ideal, substrates, the process requires a seeding layer. The most often used seeding layer is a ZnO thin film. Properties of this thin film such as polycrystallinity, preferred crystal orientation, grain size and roughness all directly influence the morphological properties of the ZnO nanowires grown on its surface.[63] The thin film serving as a seeding layer can be grown by several different techniques. The most frequently used growth processes include thermal decomposition of zinc acetate[38] and sputtering of ZnO.[78] Nevertheless, any other growth technique that results in a polycrystalline ZnO thin film can be used.

In many applications, vertical alignment of the nanowires is desired. It can be seen from previous work[25] that although, densely-packed and vertically-aligned ZnO nanowires are the preferred growth pattern, the resultant orientation of as-grown ZnO nanowires on this type of seeding layer is far from ideal.

A previous study[38] of ZnO seeding layer deposited through thermal decomposition of zinc acetate revealed that the preferred orientation of the seeds in such a thin film is with the *c*-axis perpendicular to the surface. Still, great control over the uniformity of the ZnO thin films deposited by thermal decomposition of zinc acetate is required.[63] Basically, the non-uniformity in the ZnO seed layer produces a large size differential in the resulting ZnO nanowires. It was also reported that the growth morphology depends strongly on the grain size of the seeding layer.[59] Therefore, in order to realize both a favorable vertical orientation and small diameter nanowires, an ultra-thin film, with *c*-axis aligned perpendicular to the substrate and with small grain size, is greatly preferred as a seeding layer.

One of the best coating methods for production of such a seed layer is atomic layer deposition (ALD),[79] which simultaneously offers a high degree of conformity, compatibility with integrated circuit (IC) processing, and precise digital control over the thickness of the deposited layer down to the angstrom range.

Studies on the growth of ZnO nanowires on a seeding layer grown by ALD have been reported recently. In work by J.-S. Na et al.[59] ZnO NW were hydrothermally grown on a seeding layer deposited by ALD at low temperature of 125 °C and no study was done on how the

properties of ALD seeding layer affect the subsequent hydrothermal growth.

In work by S.-Y. Pung et al.[80] ALD was done at temperatures from 60 to 300 °C and crystallinity of the thin films was estimated using XRD. Effects of annealing of ZnO thin films in air at 800 °C were also studied. ZnO nanowires were grown using CVD on these films acting as a seeding layer.

In work by F. Solis-Pomar et al.[81] ZnO thin films of different thicknesses grown by ALD at a constant temperature of 177 °C were used as seeding layers for hydrothermal growth of ZnO nanowires. Crystallinity and roughness of ZnO thin films were measured as a function of film thikness. It was established that the thinner films had higher degree of orientation with *c*-axis perpendicular to the substrate than thicker films leading to hydrothermal growth with higher degree of vertical alignment, while smaller grain size in thinner films lead to smaller mean diameter of ZnO NW.

Based on the later two works it can be established that the thinner (less than ~100nm) films grown at higher temperatures (above 200 °C) will provide high degree of alignment with *c*-axis perpendicular to the substrate.

In the work presented herein, the atomic layer deposition (ALD) technique was used to grow the ZnO seeding layer with tailored properties to explore how the variations in this seeding layer affect the resultant ZnO nanowires. ALD films were grown at temperatures of 150, 200 and 250 °C and used as seeding layers for hydrothermal synthesis of vertically-aligned and densely-packed ZnO nanowires. The thickness of ZnO thin films was in the established earlier regime of less than ~100nm, while temperatures were high enough to ensure dominating orientation of *c*-axis perpendicular to the substrate. These ALD films were used either as grown or rapid thermally annealed in oxygen or argon atmospheres at temperatures of 600 and 800 °C. The temperatures of growth and post-growth rapid thermal annealing were varied to produce samples with seeding layers exhibiting different properties, which in turn affected the morphology of the ZnO nanowires grown atop these layers. Effect of annealing on both crystallinity and roughness of the ZNO thin films and resultant ZnO NW was studied.

The process of hydrothermal growth was standardized to diminish the effects on resultant ZnO nanowires caused by small variations in the growth conditions, thus providing confidence that only the seeding layer causes the observed changes in the properties of the resultant ZnO nanowires.

ALD thin-film seed layers were characterized by means of atomic force microscopy (AFM) and grazing incidence X-ray diffraction (XRD) to determine their roughness, and crystal orientation, while ZnO nanowires were characterized by means of XRD and SEM to estimate their size, shape, density and the degree of vertical alignment.

Materials and Methods

Atomic Layer Deposition

ALD[82] is a variant of chemical vapor deposition (CVD). While

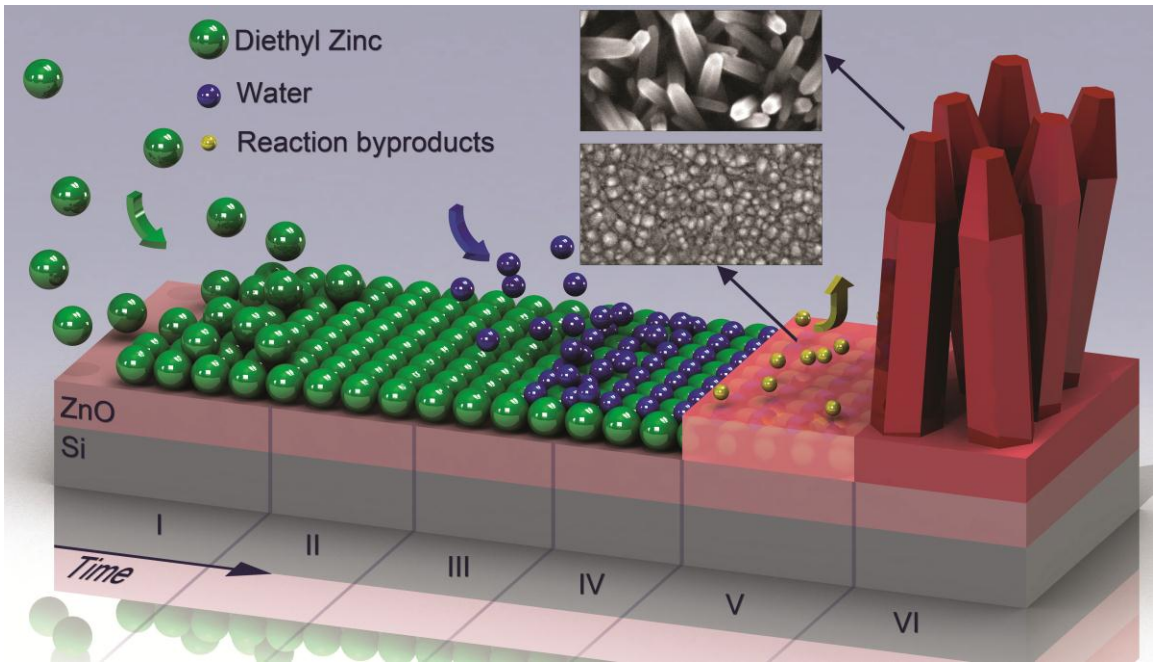

Figure 28. Schematic illustration of the ZnO ALD process. I –Exposure to the first precursor, Diethyl Zinc; II – purge to remove excess of the first precursor, leaving a monolayer of the precursor; III – exposure to the second reactant, water; IV – purge to remove excess water; V – Diethyl Zinc and water react, forming ZnO, byproducts of the reaction are removed. Stages I through V are repeated many times, each cycle resulting in a monolayer of ZnO (a layer of ZnO from previous cycles is shown). VI – resulting layer of ZnO is used for hydrothermal growth of ZnO nanowires. Insets: SEM image of ZnO thin film grown by ALD (bottom), SEM image of ZnO NW grown on ZnO thin film (top), insets show area of 500nm by 250 nm.

conventional CVD results in the deposition of layers whose thickness mainly depends on the deposition duration, ALD uses a self-terminating chemistry, which interrupts the growth process after the surface is covered with a single atomic layer of material. The ALD film growth process takes place in cycles (see Figure 28), one cycle consisting of the following five steps, which are repeated until the desired thickness is obtained: I. A self-terminating reaction of the first reactant (precursor A); II. A purge or evacuation to remove the non-reacted reactants and reaction products; III. A self-terminating reaction of the second reactant (precursor B); IV. A purge or evacuation, and V. After the reaction has terminated and all the byproducts removed, a monolayer of ZnO is formed. When the desired thickness is reached, the ZnO thin film is used as is or after thermal treatment to serve as a seeding layer for growth of ZnO nanowires (step VI of the schematics in Figure 28). It is obvious that the self-termination feature enables extraordinary control over film thickness and quality (pin holes, defects, and clustering are strongly reduced due to the selective interaction at the A/B interface). Another central advantage is the ability to coat 3D features with a conformal layer.

Precursors used for the ZnO ALD process are Diethyl zinc (DEZ) and H_2O, which are the reactant and the oxidant, respectively. The thin film quality depends strongly upon process parameters such as

the substrate temperature and the process time per ALD cycle. An ideal ALD process is based on sufficient feeding of reactants and enough purging of remaining reactants and desorbed by-products. If there is not enough reactant, the resultant thickness of the layer per ALD cycle will be less than that of a monolayer; on the other hand, more than one monolayer is coated over the surface of the substrate through a CVD type of reaction due to insufficient purging time.

Prior to all seeding layer depositions, the polished <100> *n*-type silicon substrates were cleaned using a standard RCA clean method to remove both metallic and organic contaminants. ZnO seeding layers were grown by ALD using Diethyl zinc (DEZ) as the reactant and H_2O as an oxidant. Deposition was performed on a Savannah-100 atomic layer deposition (ALD) tool from Cambridge Nanotechnology Inc. The quality of the thin films produced by the ALD process depends strongly upon process parameters such as the substrate temperature and the process time per ALD cycle. An ideal ALD growth requires sufficient supply of reactants combined with adequate purging of excess reactants and desorbed by-products. If the pulse time for reactants is not sufficient, a non-uniform coating with thickness less than one atomic layer will be deposited during each cycle. Alternatively, if the purging time is too short, both reactant and oxidant will react with each other to induce CVD fashion of deposition. Optimal values for

precursor pulse time and purging time were determined by a series of preliminary experiments performed by the vendor (data not shown). As we show further, values for purging time may not be optimal.

ALD was employed to deposit conformal ZnO seeding layers onto clean substrates. The growth rate of the ZnO thin films was investigated for different substrate process temperatures, under the conditions of reactant feeding and purging times that were provided by the manufacturer and claimed as optimal. The process temperatures, reactant pulse time, and purging times are summarized in Table 2. The growth sequence for each temperature consisted of: 1) a 0.015 sec water exposure; 2) a variable time N_2 purge; 3) a 0.015 sec Diethyl Zinc (Et_2Zn) exposure; and 4) a final variable time N_2 purge. The N_2 purge time should be sufficient and increase exponentially with a decrease of process temperature to circumvent the residual precursor from reacting with the next pulsed precursor. The number of ALD cycles used was 400 with a growth rate of ~1 Å/cycle.

Table 2. Process parameters for ALD growth of ZnO thin films.

	Time (sec)		
Process	250°C	200°C	150°C
H_2O Pulse	0.015	0.015	0.015
N_2 Purge	8	12	30
DEZ Pulse	0.015	0.015	0.015
N_2 Purge	8	12	30

RTP

ZnO thin films produced as above were annealed in either argon or oxygen atmosphere for 60 sec at either 800 °C or 600 °C using rapid thermal process (RTP). Thus, for each of the three growth temperatures, samples were produced consisting of as grown thin films, films annealed in argon at 800 °C, films annealed in argon at 600 °C, films annealed in oxygen at 800 °C, and films annealed in oxygen at 600 °C, resulting in a total of 15 sample types. In addition, one more sample with a seeding layer formed by thermal decomposition of zinc acetate was produced as a control, and the resulting growth of ZnO nanowires was compared with the rest of the 15 ALD samples.

Hydrothermal Growth

ZnO nanowires were grown using the conventional hydrothermal method using nitrate hexahydrate ($Zn(NO_3)_2 \cdot 6H_2O$) and hexamethylenetetramine (HMTA) acquired from Sigma-Aldrich (USA). The growth solution was prepared using the following recipe: a concentrated solution of zinc nitrate and hexamine in deionized water was added to 200 mL of heated deionized water (DIW, 80°C) to form 250 mL of a 25 mM solution of both zinc nitrate and hexamine in DIW. The temperature was controlled by a water circulation system, and the solution was returned to 80°C within several minutes after the addition

of the $Zn(NO_3)_2$ solution. This rapid and careful heating was done to control the initiation of the hydrothermal reaction with greater precision.

ZnO nanowires were grown on Si *n*-type substrates submerged seeding layer down in the growth solution for 2 hrs. A Teflon substrate holder was used to position the substrates in the growth solution. The size of the substrates, their vertical position, and the stirring rate all were kept constant to ensure identical growth parameters for the samples investigated. During the nanowire growth stage, the set point of the water circulation system was set to 80°C while assuring that the actual temperature of the reaction solution did not deviate from the set point by more than 0.2°C.

After the growth was complete, the samples were removed from the growth solution, rinsed with DI water, and then dried under nitrogen flow.

The basic reaction describing the growth of ZnO nanowires in the hydrothermal reaction is as follows:

Decomposition reaction:

$$(CH_2)_6N_4 + 6H_2O \rightarrow 6HCHO + 4NH_3$$

Hydroxyl supply reaction:

$$NH_3 + H_2O \Leftrightarrow NH_4^+ + OH^-$$

Supersaturation reaction:

$$2OH^- + Zn^{+2} \rightarrow Zn(OH)_2$$

ZnO nanowires growth reaction:

$$Zn(OH)_2 \rightarrow ZnO + H_2O$$

Ellipsometry

In our study, thickness measurements were done for each sample at nine different locations using a Rudolph Ellipsometer to extract the mean and standard deviation.

SEM

Scanning Electron Microscopy was performed on a Hitachi SU-70 at an accelerating voltage of 30 kV and working distance of approximately 5.6 mm. SEM images were taken at several positions throughout the sample to ensure uniformity of the grown ZnO nanowires over the entire sample.

Results and Discussion

This work focused on how different seeding layer coating and treatment techniques affected the resultant ZnO nanowires. Consequently, characterization results and the properties of the

seeding layer will be presented and discussed first, followed by more results and discussion of the synthesized nanowires.

ZnO Seeding Layers

SEM was used to study morphology of selected samples with

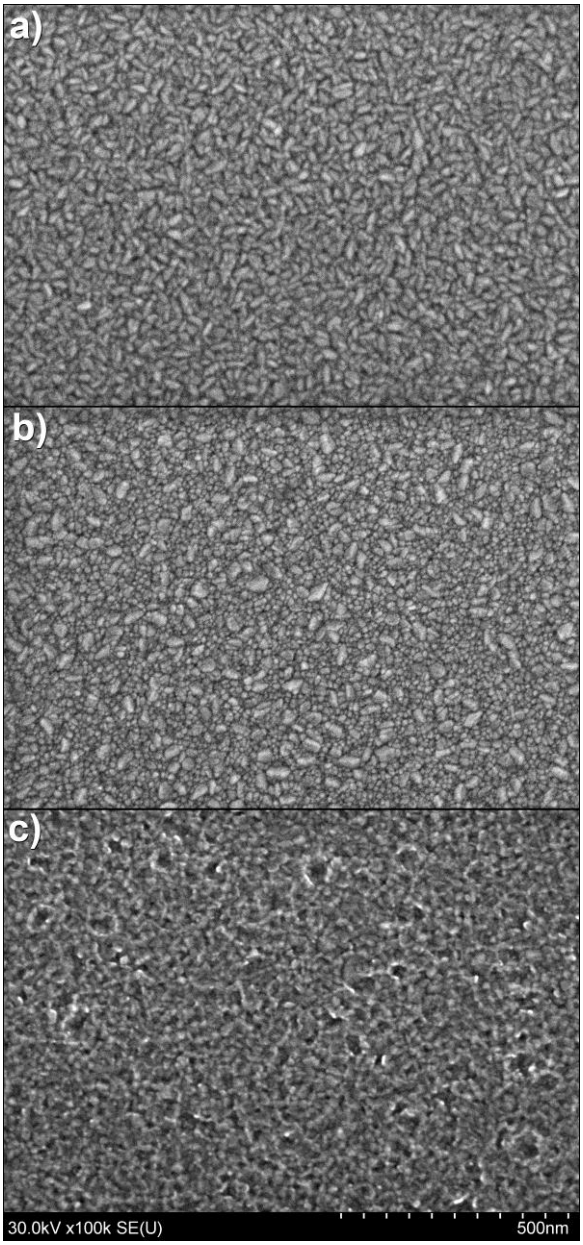

Figure 29. SEM image of ZnO thin films grown at a) 150 °C b) 200 °C and c) 250 °C.

ALD thin film on them. Figure 29 shows SEM images of samples with as-grown thin film of ZnO at three different temperatures, where a), b and c) are images of films grown at 150, 200 and 250 °C, respectively. These films have clearly different morphology. While film grown at 150 °C mostly consists of long nanocrystals that do not exhibit hexagonal features (c-axis is not preferably aligned perpendicular to the substrate), film, grown at 200 °C has nanocrystals that do not have the same elongated morphology. There is inclusion of larger nanocrystals. Film grown at 250 °C is more uniform and has considerably smaller grain size with nanocrystals virtually indistinguishable from each other.

Grazing incidence x-ray diffraction (GI XRD) was used to obtain XRD spectra of ALD ZnO thin films (seeding layers) on Si substrates. This technique allows the measurement of weak signals from samples such as ultra-thin films without interference from the substrate. Figure 30 (a), (b), and (c) shows GI XRD spectra of the samples with ALD layers grown at 150°C, 200°C and 250 °C and annealed in Ar (left) and O_2 (right) atmospheres. Insets show zoomed regions of the spectra adjacent to the <002> peak of ZnO. Vertical lines represent peak positions according to literature values. Spectra of as-grown samples for each growth temperature (shown in red) are the same in the left and right plots in each pair and are duplicated for the ease of

comparison. Prominent peaks corresponding to (100), (002), (101), (102) and (103) planes of wurtzite ZnO were visible. Their relative intensity allowed for the determination of the preferred crystal orientation of the grains in the polycrystalline ZnO film.

From these spectra one can deduce that ALD thin films grown at 150 °C exhibit polycrystalline structure with a random crystal orientation of the grains. Annealing both in Ar and O_2 did not result in substantial changes in the (002) peak intensity, while (100) and (103) peaks became visibly stronger.

Samples with ALD films grown at 200°C and 250 °C exhibited slightly different behavior. The (002) peak was the most intense peak in the corresponding XRD spectra, revealing that a crystallographic orientation of the grains with the *c*-axis perpendicular to the substrate surface was preferred in this case. Nevertheless, rapid thermal annealing in Ar and O_2 resulted in different effects for these samples. While annealing in Ar at 600 °C resulted in the (002) peak being sharpened and increased in its intensity, annealing at the higher temperature of 800 °C resulted in a decreased peak intensity (see insets on the left of Figure 30 (b), (c)). Since this effect was consistent among all the peaks assigned to ZnO, this observation may be the result of reduced during the Ar annealing thickness of the film.

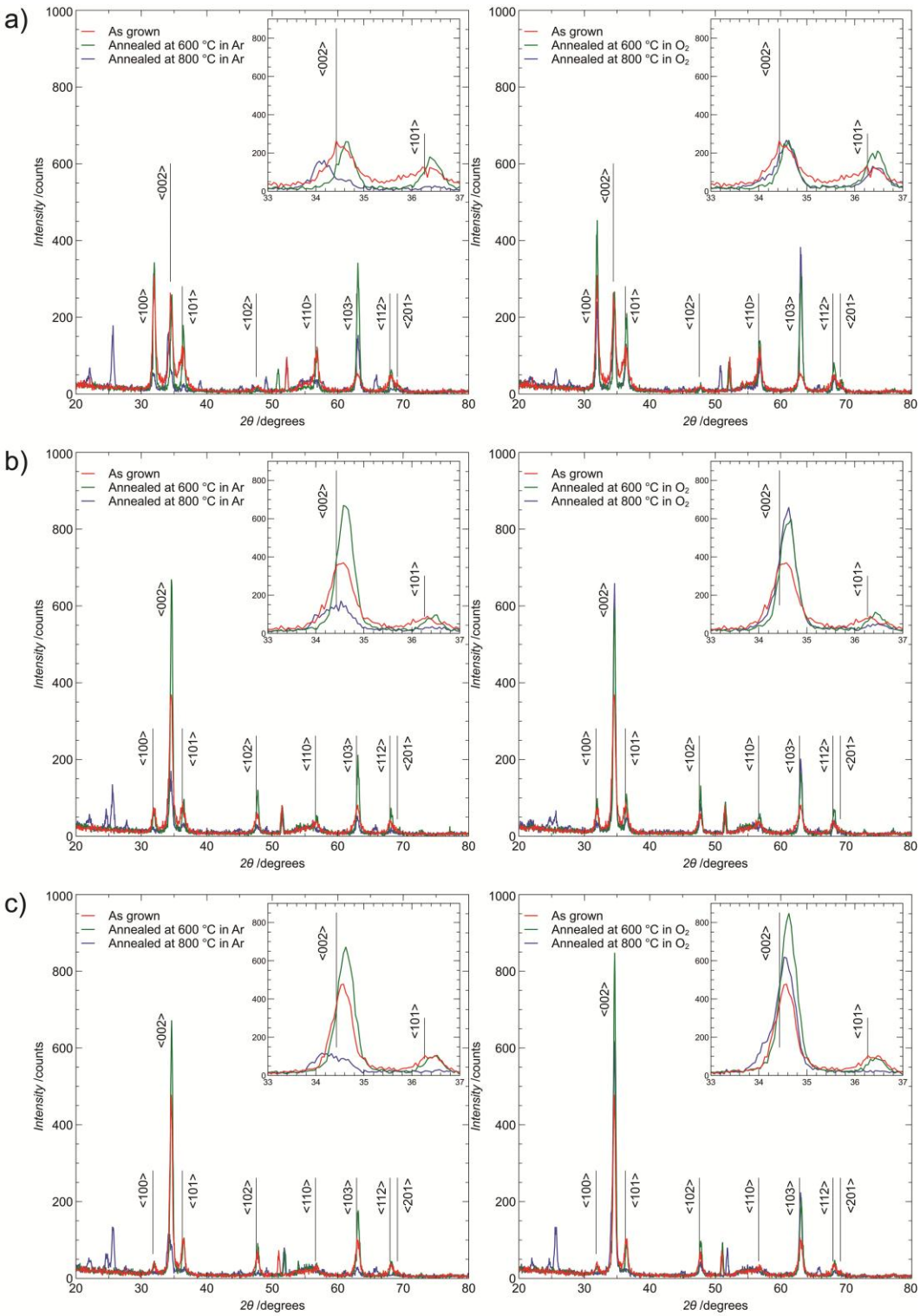

Figure 30. GI XRD of ZnO ALD thin films grown at (a) 150 °C; (b) 200 °C; (c) 250 °C. Insets show relative intensities of <002> peaks of as-grown and O_2/Ar annealed samples.

On the contrary, annealing in O_2 resulted in increased intensity of the (002) peak, as well as all of the other peaks to some degree. The difference in the effect of the two annealing temperatures for samples grown at 200 °C was minimal. However, for the samples grown at 250 °C and annealed at 600 °C in O_2 resulted in the most prominent (002) peak.

Figure 31(a) shows the thickness of the ZnO seeding layers grown by ALD as measured using ellipsometry. The measured mean thickness of as-grown ALD ZnO thin films on Si were 53.7nm, 59.6nm, and 69.5nm for samples grown at 250 °C, 200 °C and 150 °C, respectively. Rapid thermal annealing in Ar and O_2 had opposite effects on the ZnO thin films. Annealing in Ar generally led to a decrease in

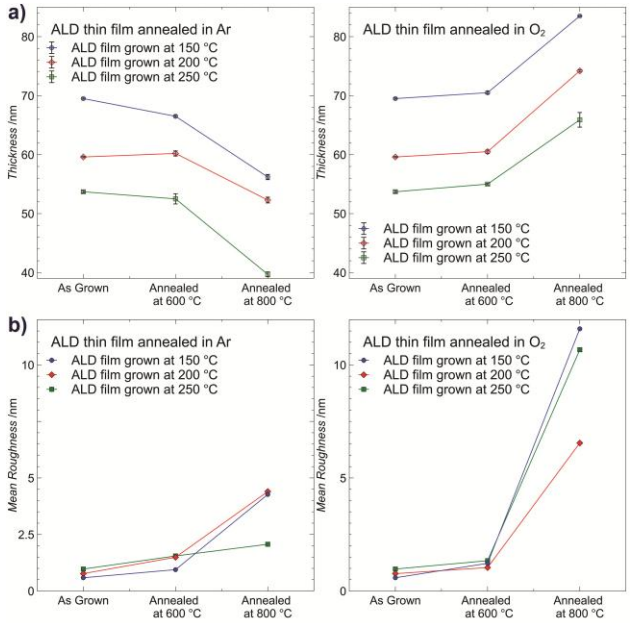

Figure 31. (a) Thickness of ALD ZnO as-grown and annealed thin films measured by ellipsometry, (b) mean roughness of ALD ZnO thin films as measured by AFM.

mean thickness of the thin films of ZnO for all samples.

Quite the opposite, annealing in O_2 increased the thickness of the ZnO thin films. This thickness increase can be ascribed to the growth of an oxide film due to dry oxidation of Zn. For this to occur, one needs a higher prevalence of Zn atoms in the as grown films, which can be accredited to an insufficient purge time for the Diethyl Zinc thus leading to Zn-rich ZnO ALD thin films. This might be an evidence that the recipe provided by the manufacturer of the ALD system is not quite optimized.

Figure 31(b) presents the mean roughness of the ZnO thin films as measured by AFM. Generally, annealing in both Ar and O_2 atmospheres increased the surface roughness, which is more severe for the samples annealed in O_2. This difference can be accredited to active recrystallization and growth of ZnO nanocrystals caused by the reaction of excess Zn atoms in the film and O atoms in the O_2 atmosphere in a dry oxidation process. Notice that, after annealing at 800 °C in O_2, the mean roughness of the ALD film grown at 250 °C was between those of the ALD films grown at 200 °C and 150 °C. One possible explanation is differing amounts of excessive Zn atoms existed in the as grown ALD ZnO films, and, therefore, different growth rates of zinc oxide through the dry oxidation process during O_2 annealing.

The samples with the ALD film that was deposited at 150 °C and 200 °C and then annealed in Ar at 800 °C were distinctive from the other samples. The optical microscopy image shown in Figure 33 reveals that the sample grown at 150 °C has evenly distributed defects which correspond to patterns darker in color. The similar defects were observed on samples grown at 200 °C. The defect formation cannot be assigned to any imperfections or impurities in the film, as the films from the same substrate were used in other samples that were annealed at a different temperature or in a different atmosphere. Moreover, we repeatedly obtained the same structure when annealing this film at the same temperature in Ar. As can be seen in Figure 34(c), there were several unusually large nanowires potentially resulting from the defects in the ALD ZnO seed layer. We suggest that these were the nanowires grown at the locations of the localized defects.

SEM images of ZnO thin film grown at 150 °C and annealed at 800 °C in Ar in Figure 32 show that nanocrystalline grains are of considerably larger size. In the regions that belong to defects (right, dark areas on Figure 33) nanocrystals tend to fuse into clusters with visibly flat top surface and are of slightly different shape compared to the areas in between the defects (left, light areas on Figure 33). Such

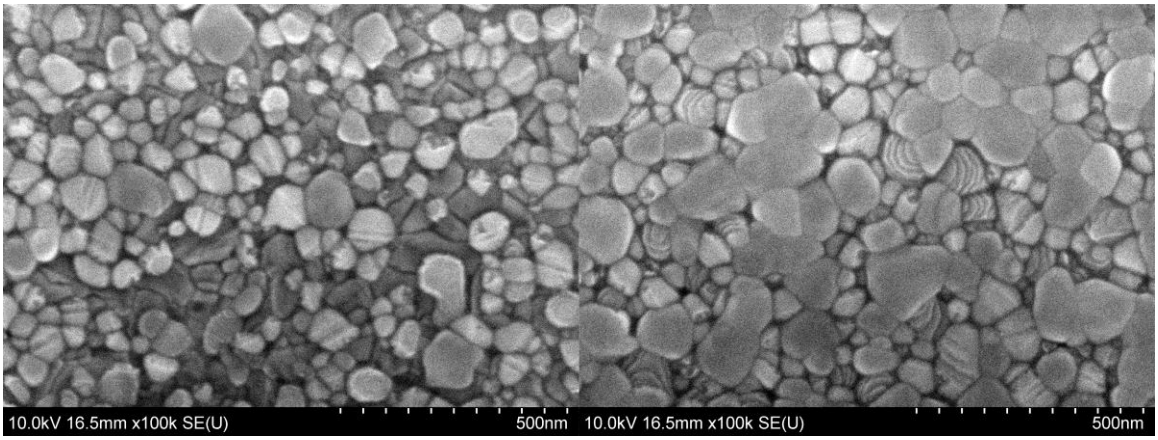

Figure 32. SEM image of ZnO thin film grown at 150 °C and annealed in Ar at 800 °C in the area outside dark defects visible on the previous figure (left) and inside such a defect (right).

clusters may be a suitable nucleation sites for abovementioned unusually large ZnO nanowires.

Similar defects of smaller size also were observed on a sample that was deposited at 200 °C and then annealed in Ar at 800 °C.

ZnO Nanowires

ZnO nanowires synthesized on the as-grown ALD seeding layer

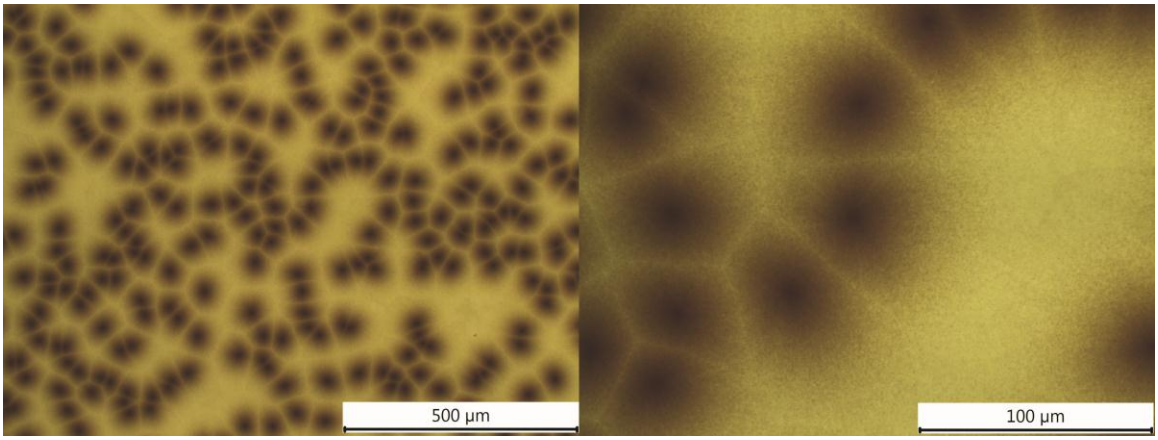

Figure 33. Optical microscopy image of ALD ZnO thin film grown at 150 °C and annealed in Ar at 800 °C.

grown at 150 °C (Figure 34(a)) had base diameters of ~80nm with tapered apical termini. The average surface density of nanowires was ~100 per μm^2. Although vertical alignment of the nanowires was rather preferred, it is fairly challenging to completely fulfill that. When grown on the same ALD thin film that was annealed in Ar at 600 °C (Figure 34(b)), the nanowires exhibited larger average diameters of ~120nm, with a wider size distribution. The tips of the nanowires often had a tapered shape. The density of nanowires was degraded to ~67 per μm^2. When grown on the same ALD thin film that instead was annealed at 800 °C (Figure 34(c)), the nanowires had non-tapered, flat tips with a significantly increased average diameter. The surface density of the nanowires was further reduced to ~57 per μm^2, and their average diameter increased to ~250nm. It also appeared that the nanowires in this case have a much greater degree of vertical alignment. It is worthwhile mentioning that this sample of ZnO nanowires, which was synthesized using a ZnO seeding layer grown by ALD at 150 °C and annealed at 800 °C in Ar, was the only sample that exhibited this flat shape of the nanowire termini.

Figure 34(d), (e) shows ZnO nanowires grown on the same ALD thin films used after being (d) annealed at 600 °C in O_2 and (e) annealed at 800 °C in O_2, respectively. Both samples annealed at 600 °C and 800 °C have the same tendency toward increased average

nanowire size, with the degree of vertical alignment virtually unchanged between the two. The surface density of nanowires was ~61 per μm^2 and ~39 per μm^2 for samples with ALD films annealed at 600 °C and 800 °C, respectively.

SEM images of the samples with ZnO nanowires grown on an ALD ZnO thin film that was grown at 200 °C are presented in Figure 34(f-j). ALD films were used as grown (Figure 34(f)), annealed in Ar and O_2 at 600 °C (Figure 34(g) and Figure 34(i), respectively) and annealed at 800 °C in Ar and O_2 (Figure 34(h) and Figure 34(j), respectively). The surface density of ZnO nanowires on the as-grown ALD film was higher compared to ZnO nanowires grown on the ALD thin film grown at 150 °C and was ~255 per μm^2. ZnO nanowires grown on the annealed films had larger mean diameters and had a narrower size distribution compared to the samples grown on 150 °C ALD thin film. The surface densities of ZnO nanowires were ~115 per μm^2 and ~83 per μm^2 for samples grown on an ALD ZnO film annealed at 600 and 800 °C in Ar, respectively, and ~111 per μm^2 and ~88 per μm^2 for samples grown on films annealed at 600 and 800 °C in O_2, respectively. As shown in Figure 34(f-j), ZnO nanowires on all samples grown at this temperature had tapered tips.

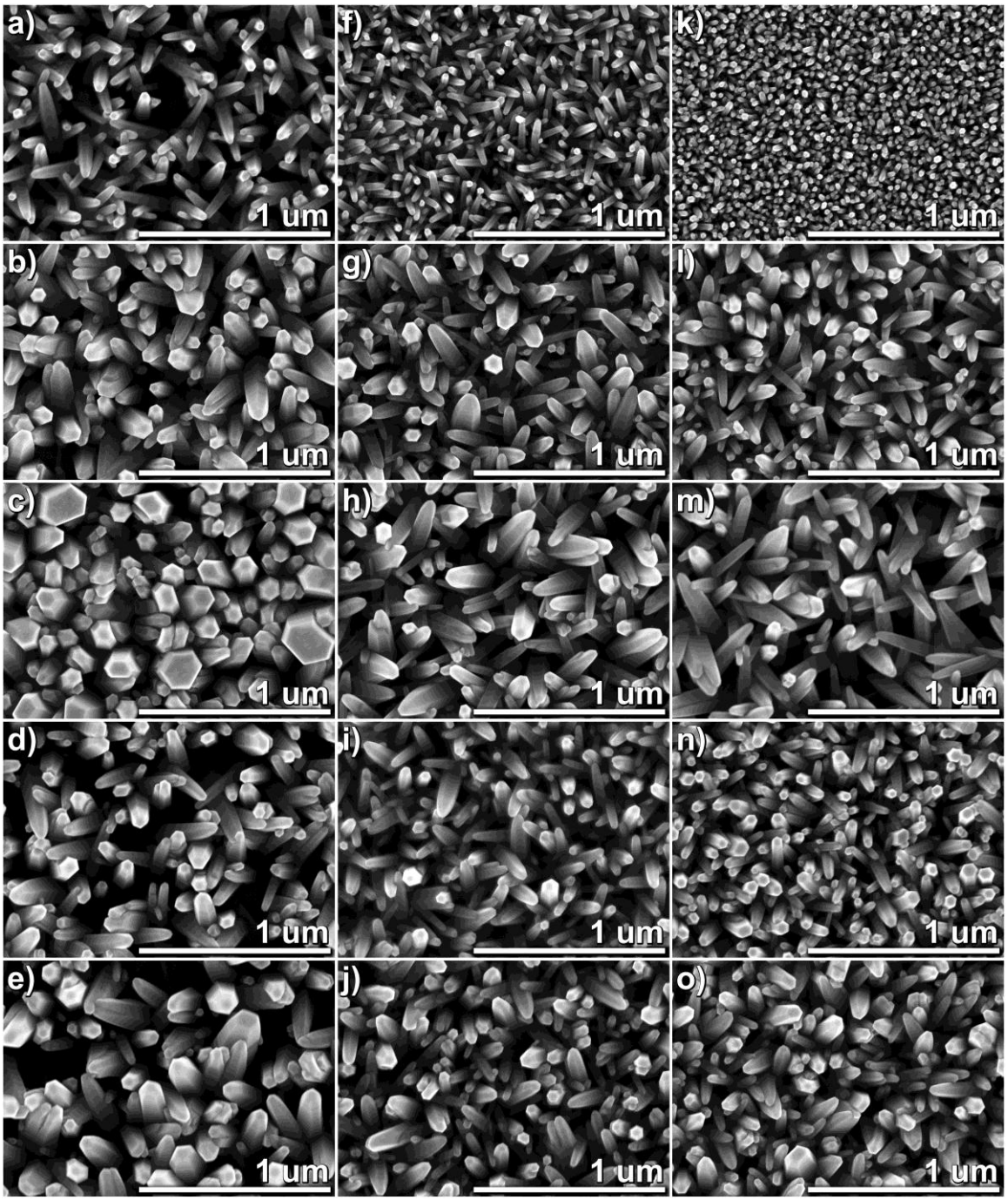

Figure 34. SEM images of samples with ZnO nanowires grown on ALD ZnO films that were grown at 150 °C (1st column, (a-e)), 200 °C (2nd column, (f-j)), and 250 °C (3rd column, (k-o)). These films acted as seeding layers, and were used as grown (1st row, (a), (f), (k)), Ar-annealed at 600 °C (2nd row, (b), (g), (l)), Ar-annealed at 800 °C (3rd row, (c), (h), (m)), O_2-annealed at 600 °C (4th row, (d), (i), (n)) or O_2-annealed at 800 °C (5th row, (e), (j), (o)).

SEM images of the samples with ZnO nanowires grown on an ALD ZnO thin film that was deposited at 250 °C are shown in Figure 34(k-o). ALD films were used as grown (Figure 34(k)), annealed in Ar and O_2 at 600 °C (Figure 34(l) and Figure 34(n), respectively) and annealed at 800 °C in Ar and O_2 (Figure 34(m) and Figure 34(o), respectively). The surface density of ZnO nanowires on as-grown ALD ZnO thin films was ~729 per μm^2, which was the highest among all the samples studied by this work. As shown in Figure 34(k), ZnO nanowires on this sample also had the highest degree of vertical alignment. Annealing of the seeding layer in both Ar and O_2 atmospheres leads, as in case of other samples, to smaller surface density of nanowires and larger mean size. For samples with ALD films annealed in Ar, the surface density of nanowires was ~118 per μm^2 for films annealed at 600 °C and ~60 per μm^2 for films annealed at 800 °C. For samples with ALD films annealed in O_2, the density of nanowires was ~156 per μm^2 for films annealed at 600 °C and ~110 per μm^2 for films annealed at 800 °C.

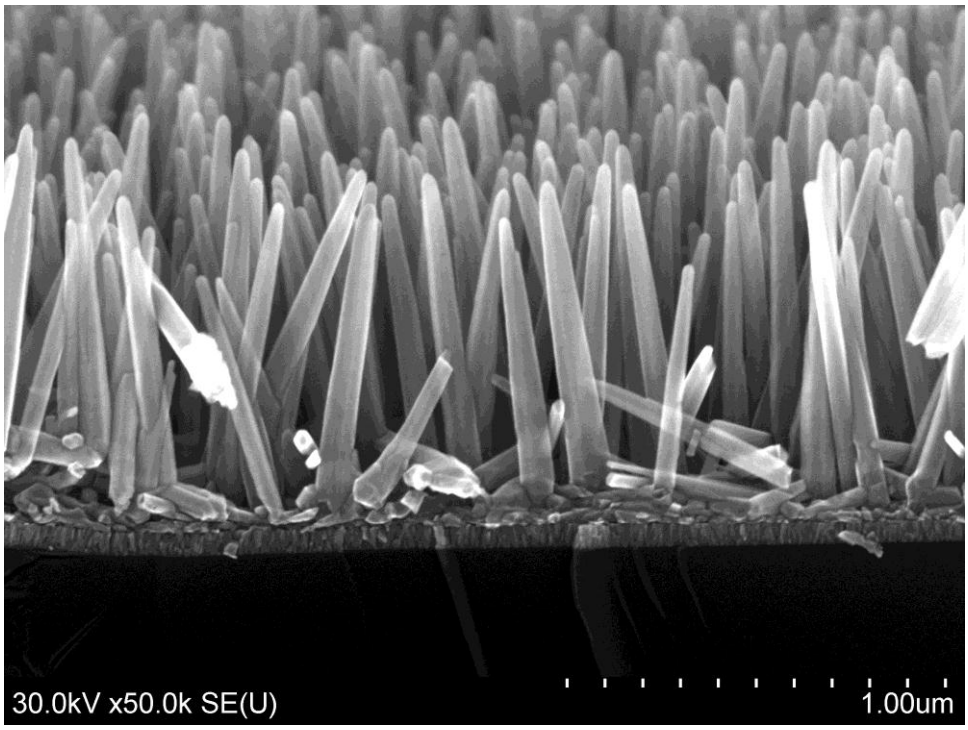

Figure 35. Cross sectional SEM of a sample with ZnO nanowires, grown on a thin film deposited at 150 °C and used as is.

Figure 35 presents an example of cross sectional view of ZnO nanowires, grown on a thin film deposited at 150 °C and used as is. The length of ZnO nanowires varies from 800 to 1200 nm. As can be seen from the image the degree of vertical alignment is high.

Table 3 summarizes the growth conditions for all the samples as well as measured properties of ZnO ALD thin films and density of ZnO nanowires grown on these films.

Table 3. Summary of all the growth conditions of the studied samples and their measured properties.

ALD process temperature, (°C)	Annealing atmosphere	Annealing temperature, (°C)	Film thickness, (nm)	Mean film roughness, (nm)	Density of ZnO nanowires, per μm^2
150		as is	69.50	0.585	100
	Ar	600	66.50	0.943	67
		800	56.20	4.270	57
	O_2	600	70.50	1.223	61
		800	83.50	11.596	39
200		as is	59.60	0.768	255
	Ar	600	60.20	1.491	115
		800	52.30	4.398	83
	O_2	600	60.50	1.034	111
		800	74.20	6.545	88
250		as is	53.70	0.971	729
	Ar	600	52.50	1.549	118
		800	39.70	2.067	60
	O_2	600	55.00	1.340	156
		800	65.90	10.670	110

Figure 36 presents XRD results for the sets of ZnO nanowire samples, synthesized on ALD films deposited at a) 150 °C, b) 200 °C and c) 250 °C, respectively. Special care was taken to standardize the XRD measurements to get consistent results from all the samples, so that the intensity of the XRD signal would reflect the thickness of the ZnO nanowires layer. On the left of each image, the full XRD spectra are shown. These spectra feature only one peak that could be assigned to ZnO, which is present at $2\theta = 34.4°$. This peak corresponds to a <002> crystallographic orientation and shows that ZnO nanowires were grown primarily with the *c*-axis perpendicular to the substrate.

Weak peaks around $2\theta = 33°$ can be assigned to the <200> orientation of the Si substrate. Peaks are shifted vertically for purpose of illustration. On the right side of the figures, the high resolution close-up of the <002> peak is shown. The peaks were normalized to have the same magnitude so that full width at half maximum could be estimated. The inset shows the non-normalized peaks. As can be seen from the normalized <002> peaks, FWHM is virtually the same for all the peaks, which indicates that differences in nanowire size was not large enough to cause changes in the shape or position of the peak. The only peak that is slightly shifted is that of a sample with ZnO nanowires that were grown on an as grown ALD thin film deposited at 250 °C. This sample had the densest ZnO nanowires with the smallest radius. Figure 37 shows the <002> peak intensities for all three sets of samples with ALD films grown at 150, 200 and 250 °C and annealed in Ar (left) and O_2 (right). For almost all ALD growth temperatures, the intensity of the peaks tended to increase with the seed layer annealing temperature. Samples grown on ALD ZnO films with no annealing had the lowest peak intensity, samples annealed at 600 °C were intermediate in peak intensity, and samples annealed at 800 °C were highest in peak intensity.

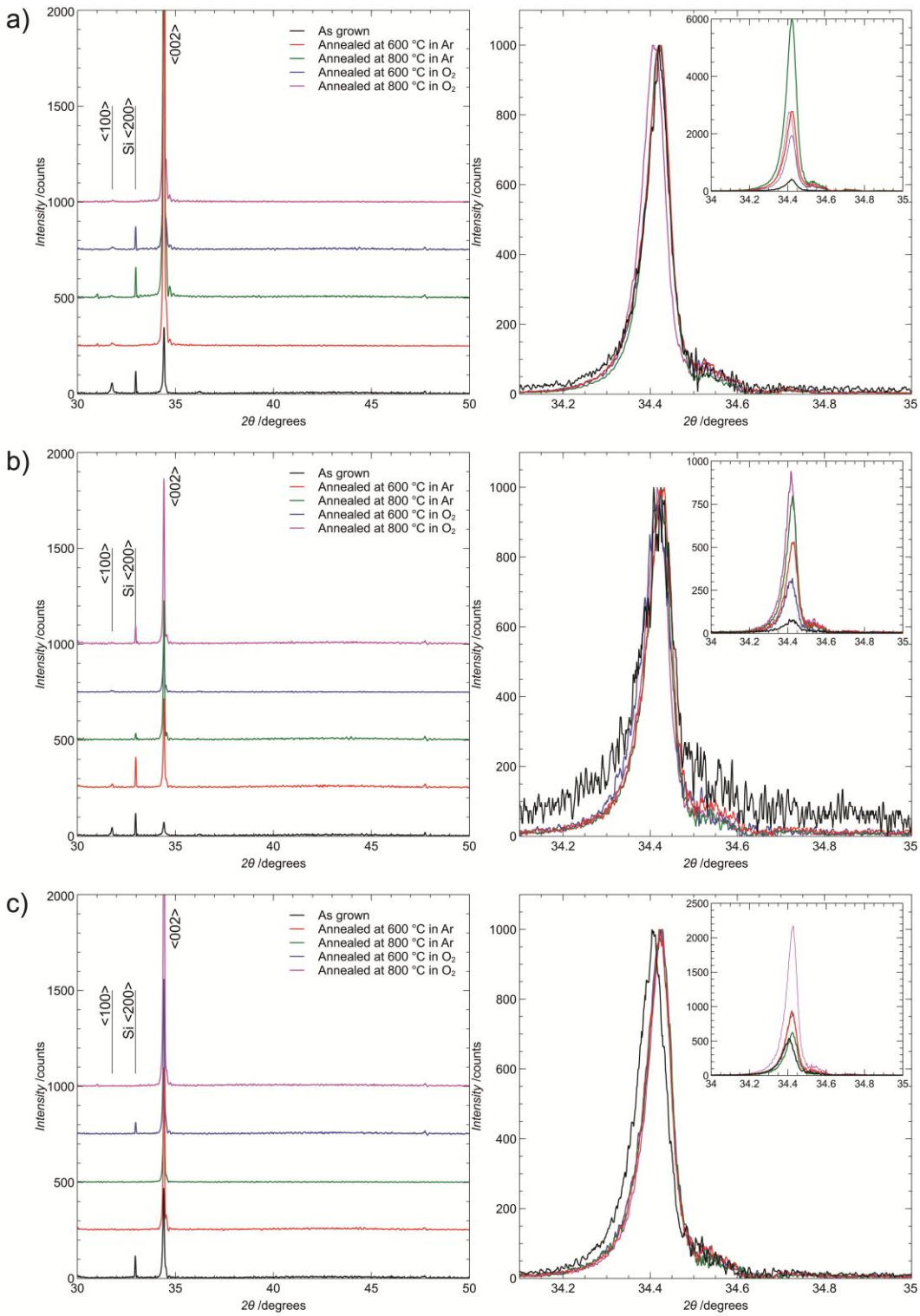

Figure 36. XRD of ZnO nanowires that were grown using identical recipes on ALD ZnO thin films grown at a) 150 °C; b) 200 °C; c) 250 °C. The complete XRD spectra are shown on the left with spectra shifted vertically for clarity, while normalized <002> peaks are shown on the right. Insets show relative intensities of <002> peaks of as-grown and annealed samples.

Moreover, samples with ZnO nanowires grown on ALD ZnO thin films deposited at 150 °C had the most intense peaks for the growth temperatures investigated. Samples grown on ALD films grown at 150 °C and annealed in Ar at 800 °C had the most intense <002> peak overall. As can be seen from Figure 34c, The ZnO nanowires grown on such samples also had a distinctive size and shape. This sample will be further discussed in supporting information. Interestingly, almost all samples that were grown on ALD films deposited at 200 °C have magnitude of <002> ZnO XRD peaks less than the magnitude of the same peaks for samples grown on ALD films deposited at both 150 °C and 250 °C. This might be accredited to differences in growth recipe for ALD films at different temperatures.

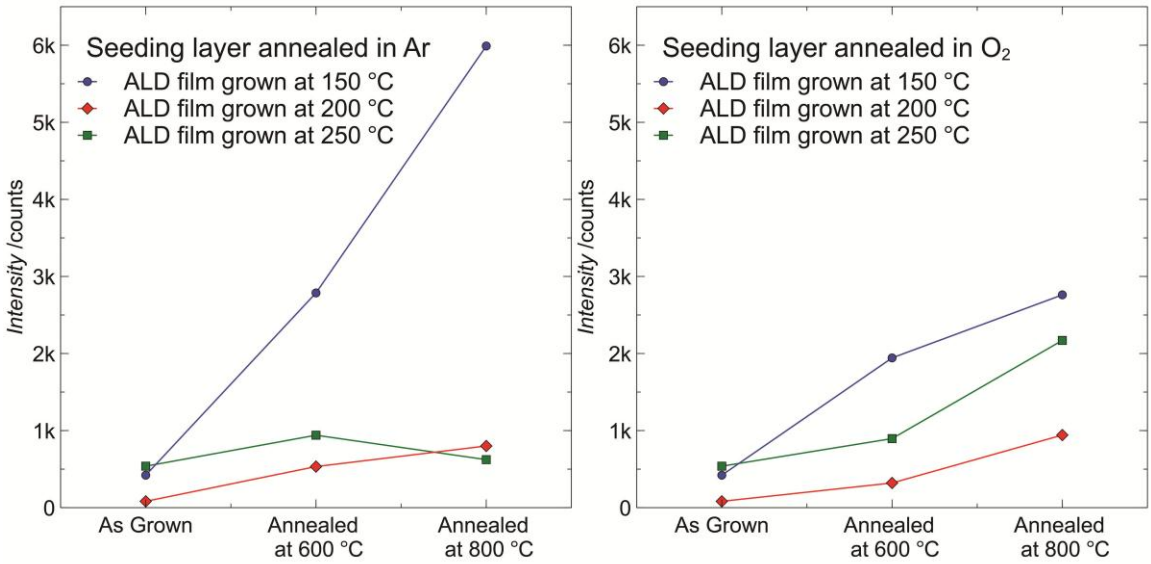

Figure 37. Intensity of <002> ZnO peak in measured XRD spectra.

Conclusions

In conclusion, the presented work addressed how different deposition processes and post-process treatments affect the properties of ZnO seeding layers and, in turn, how these seed layers affect the ZnO nanowires grown from them. We used an ALD technique to deposit ZnO thin films onto Si substrates at three different process temperatures, 150°C, 200°C and 250 °C. Thereafter, the substrates were diced, and some of them were used as grown, others after being annealed in Ar or O_2 at temperatures of either 600°C or 800 °C. Detailed characterization of the ALD grown thin-films was performed with a variety of metrology methods. ZnO nanowires then were grown using the hydrothermal process on these samples, using the ZnO thin film as a seeding layer.

Despite assuring that the growth parameters for the entire hydrothermal growth process remained unchanged, significant differences in the size and density of nanowires were observed. These differences can only be ascribed to the variation of the physical properties of the ALD ZnO seeding films. The smallest nanowire size combined with the highest density were obtained on samples that were grown at 250 °C and used without post-processing; the largest size of nanowires and the lowest density were obtained when using the

ZnO seed layer as synthesized at 150 °C and annealed at 800 °C in an Ar atmosphere.

The morphological properties of ZnO nanowires were found to be dependent not only on the preferred crystalline orientation of the seed layer but also on its roughness. In general, performing ALD at higher process temperatures produced seed layers that resulted in higher densities of ZnO nanowires. Moreover, the <002> ZnO peaks in the XRD spectra were more pronounced in samples with ALD films grown at higher temperatures, indicating that the crystalline orientation with *c*-axis perpendicular to the substrate was preferred when higher process temperatures were used. Substrates of this type resulted in smaller and more dense ZnO nanowires on "as grown" samples. On the other hand, while rapid thermal annealing generally (with exception of annealing in Ar at 800 °C) increased the crystalline quality of the thin films, as indicated by the <002> peak becoming more pronounced, annealing also greatly increased the roughness of the films. The increased roughness resulted in larger ZnO nanowires. The larger grains formed during the annealing process also reduced the vertical alignment of the nanowires. Combined, the results imply that the high degree of vertical alignment resulting from the "as grown" seeding layers was aided by the physical constraints introduced by the small grain size and tight packing of the smaller nanowires. It

was not clear whether rapid thermal annealing in Ar or O_2 is more favorable – while annealing in Ar should not be done at high temperatures (800 °C) as it greatly degraded the crystalline properties of the ZnO films and somewhat increased its roughness, annealing at 600 °C should be acceptable as it resulted in better crystalline quality with only a slight increase in roughness; alternatively, annealing in O_2 at both 600 °C and 800 °C increased the crystalline quality but also drastically increased the roughness of the films. As mentioned, the most favorable seed layer in this study was one grown at the highest ALD process temperature of 250 °C and used "as is".

Seeding layers produced using ALD would appear to be useful for the production of just such materials exhibiting densely packed nanowires with smaller diameters, while simultaneously enhancing their degree of vertical alignment.

ALD films may be used to further improve the potential performance of ZnO nanowires as an electrode material for supercapacitor applications: the resulting growth of high density, small mean size nanowires on surfaces with complex geometries would provide a means by which to further increase the electrode surface area per unit volume.

Acknowledgment

This research was partially supported by NSF Grant #0854023.

Chapter 7: Microfluidic Hydrothermal Growth of ZnO Nanowires Over High Aspect Ratio Microstructures

Abstract

A hydrothermal synthesis of densely-packed ZnO nanowires is realized in a confined space through forced circulation of the heated growth solution through microfluidic channels formed primarily by a set of high aspect ratio trenches in a Si substrate. An uniform and conformal seeding layer of ZnO was deposited to cover the entire surface of the trenches by means of atomic layer deposition (ALD). Densely-packed ZnO nanowires were formed inside the trenches on the sidewalls, where they would not grow through a conventional hydrothermal method. The strategy for controlled growth of ZnO nanowires over such high aspect ratio microstructures is deemed beneficial when this nanostructured ZnO nanowires are used as an electrode with high specific surface area for devices such as supercapacitors or any other electrochemical devices.

Introduction

ZnO nanostructures have been used in a wide variety of different electronic, optoelectronic and electrochemical devices such as

sensors,[7, 8, 63] solar cells,[16] lasers,[21, 37] transistors[7, 73, 76] and supercapacitors. Apart from their unique electronic and optical properties, their surface morphology is of great importance for aforementioned device applications. In general densely packed,[19] vertically aligned nanowires are desired for such devices as dye sensitized solar cells.[12] Aside from the great desire for smaller diameter, it is also advantageous to have longer length,[44] which results in a larger surface area for the process of charge separation. Individual ZnO nanowire often exhibits properties of a single crystal thus providing efficient transport of electron to the bottom contact. Performance of such devices as supercapacitor also depends on the surface area,[37] which determines the charge-storing capacity. The employment of vertically aligned and densely packed ZnO nanowires grown on a planar substrate already greatly increases the specific surface area of an electrode. One strategy to further increase the specific surface area of ZnO nanowires is to employ growth of hierarchical ZnO nanostructures,[15, 59, 68, 71] while another is a growth template with a complex three dimensional topography. The simplest topography with high area surface that could be used for the growth of ZnO nanowires is an array of deep trenches with high aspect ratio. Provided that ZnO nanowires would grow on the sidewalls and bottom surfaces of deep trenches, the quantity of ZnO nanowires, and

therefore the specific surface area of a resultant ZnO electrode would increase manyfold. To realize such growth by means of hydrothermal method one needs to satisfy two prerequisite conditions: conformal deposition of a seeding layer of thin film of ZnO and sufficient supply of fresh chemicals for hydrothermal growth. While the first requirement may be readily addressed by leveraging conformal deposition technique such as ALD, the replenishment of growth chemicals needs some discussion.

The growth rate of ZnO nanowires in hydrothermal process is determined, among other parameters, by the concentration of the ions in the vicinity of the growth location. In a conventional hydrothermal growth, where a flat substrate is immersed in bulk growth solution, concentration of ions depends on both depletion of ions due to crystallization of ZnO and replenishment of fresh ions due to diffusion, convection or mechanical stirring. When the growth site is located in a confined space such as a deep trench, the supply of fresh ions is only provided by diffusion, which might be insufficient for a sustained growth as ZnO crystallization occurs at faster rates to cause depletion of ions. A viable solution would be to allow a forced circulation of growth solution from a bulk volume through the deep trenches.

In this work, we have successfully demonstrated such a hydrothermal growth of ZnO nanowires in an array of parallel deep

trenches, which were formed in a silicon substrate by a deep reactive ion etching (DRIE) process along with inlet and outlet ports. Then an ALD process was used to deposit a conformal ZnO thin film inside all trenches that serves as a seeding layer for hydrothermal growth. Thereafter, these patterned trenches and ports were sealed with a PDMS top layer to effectively form microfluidic channels, which allow a heated growth solution to be pumped through. Hydrothermal growth was then performed through forced circulation of the growth solution. Finally, the PDMS top layer was removed and the growth of ZnO nanowire along the trench sidewalls was examined by cross-sectional and top view SEM images.

Experimental Details

Hydrothermal Growth

The solution for hydrothermal growth was prepared following a conventional recipe. The growth solution was composed of 25 mM of both zinc nitrate and hexamine in deionized water (DIW). Solution was used at 85 °C and at a room temperature for selected samples. 54 mg of PEI per 250 mL of growth solution was added as growth modifier. 5mL of 28% ammonium hydroxide per 250mL of solution was added for selected samples. This solution was used for microfluidic hydrothermal growth of ZnO nanowires.

ALD

A thin film of ZnO acting as a seeding layer is needed for a hydrothermal growth of ZnO nanowires. For the substrate geometry that is comprised of the deep trenches with high aspect ratio ALD is the obvious choice due to its superb conformity.

ZnO seeding layers were grown by a thermal ALD (Savannah 100, Cambridge Nanotechnology Inc.) at 250 °C using Diethyl zinc (DEZ) and H_2O as the reactant and oxidant, respectively. The growth sequence for atomic layer deposition consisted of: 1) a 0.015 sec water exposure; 2) 8 sec N_2 purge; 3) a 0.015 sec Diethyl Zinc (Et_2Zn) exposure; and 4) a 8 sec N_2 purge.

Array of High Aspect Ratio Trenches

In this work, an array of closely spaced parallel deep trenches was etched in Si wafer using DRIE method. The nominal length of the trenches was designed to be 1cm. On the opposite ends of these parallel trenches, an inlet and an outlet were formed for filling and draining of the growth solution. The patterned samples were covered with a PDMS top layer, which was impinged through by a pair of syringe needles to access inlet and outlet reservoirs. In order to seal the deep trench structure and ensure good contact between PDMS and the top surface of the silicon substrate, some pressure was uniformly applied to the PDMS layer normally to the surface. The sample was

then placed on the polished aluminum heat sink located on the hotplate.

Subsequently, the inlet and outlet needles were connected to the microfluidic peristaltic pump and the heated beaker filled with growth solution. A syringe filter with pore size of 0.2 μm was placed before the inlet to ensure that the nanocrystals formed in bulk solution of the beaker will not clog the deep trenches.

The growth solution was pumped through a set of sealed high aspect ratio trenches with nominal pumping speed of 0.55 ml/min and 0.91 ml/min. However, during the process, effective pumping speed was reduced due to the inevitable clogging of the microstructures and effectively narrowing of trenches due to the growth of ZnO nanowires. The forced circulation of growth solution was carried out until there was no measurable flow through the sample or up to 3 hrs of time. The microfluidics set up was in a pulling configuration with exception of one sample that grown in a pushing configuration. Moreover, the pumping direction was reversed from pushing to pulling for 15 seconds every 10 minutes.

Results and Discussion

Figure 38 shows SEM image of cross section of ZnO nanowires grown in a deep trench with width of about 35 μm. The growth was

performed using a conventional hydrothermal process by placing the substrate face down in the growth solution. The leftmost image was taken near the top edge of the trench, each consecutive image was taken approximately 10 μm deeper in the trench. As shown, the length of the nanowires decreases with the depth of the growth surface along the trench sidewall, which can be ascribed to depletion of Zn+ ions for the growth of ZnO due to insufficient diffusion or mechanical stirring deeper in the trench.

With pumping of the growth solution through the set of trenches, chemicals needed for the sustained growth of ZnO nanowires were effectively replenished, allowing growth of ZnO NW in a very confined space. Unlike the result by traditional bulk process, the length and the diameter of ZnO nanowires grown on the sidewalls were not dependent on how deep inside the trench the growth occurs.

Figure 39 shows a cross-sectional SEM image of a sample with

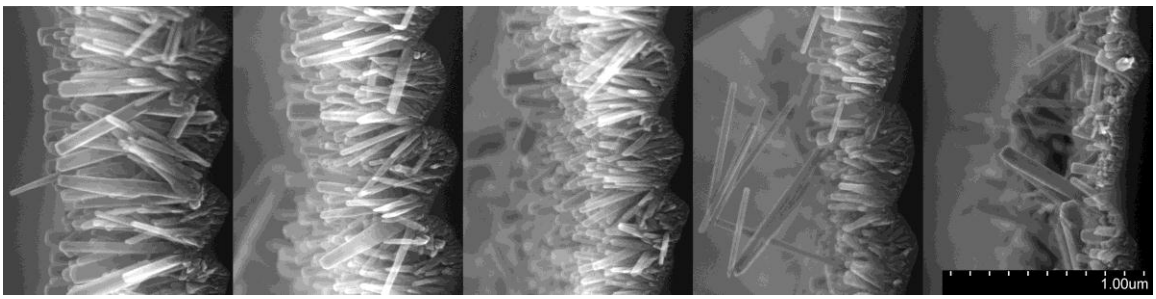

Figure 38. Cross-sectional SEM images of ZnO nanowires grown on a sidewall of a 30 μm-wide, 40μm-deep trench. Growth was performed using conventional hydrothermal route, where the substrate with etched trenches was places face down in the growth solution

ZnO nanowires grown along the sidewalls of deep trenches. As shown, unlike poorly controlled growth through conventional method, the length of the nanowires is fairly uniform over the whole depth of the each trench, with some variation at the regions close to the top and bottom of the trenches, which will be discussed later.

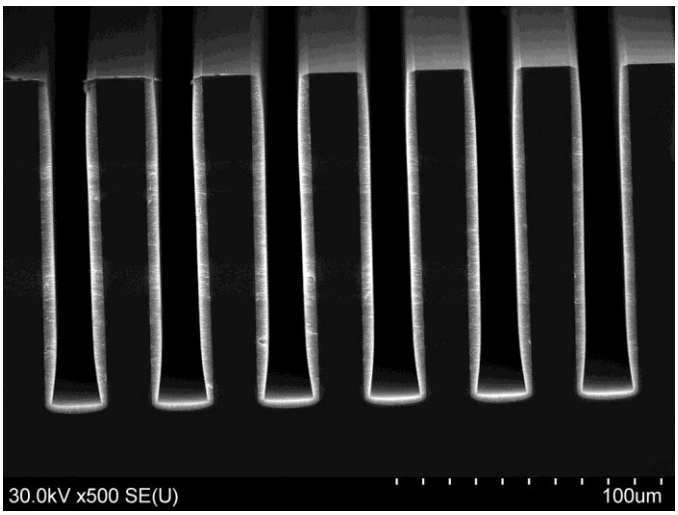

Figure 39. Cross-sectional SEM image of ZnO nanowires grown using forced growth solution circulation on sidewalls of an array of 20 μm-wide, approximately 120 μm-deep trenches.

As the growth in this manner is quite different from the conventional hydrothermal growth, several interesting effects should be discussed.

Figure 40 shows the SEM images of ZnO nanowires taken near the top edge of the trench after the PDMS sealing cover was taken off. As shown in Figure 40(a), the top surface of ZnO nanowires is flat with the nanowires merged together due to the contact with the PDMS cover, although the tips of nanowires are easily distinguished. Due to

the fact that the nanowires close to the top edge and bottom of the trench are shorter than the rest of the surface along the trench sidewalls, two lengths are given when describing the nanowires.

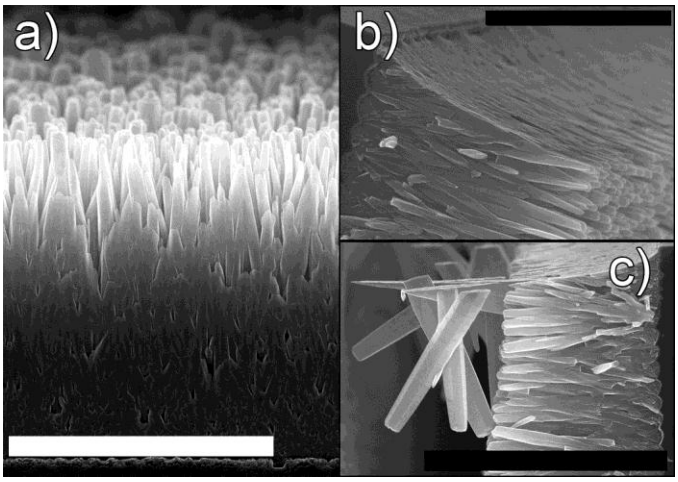

Figure 40. SEM images of a) a top view of ZnO nanowires grown along the side wall of a trench with PDMS top cover taken off. Nanowires exhibit flat structure where the growth was limited within the trench by PDMS top cover, b) a cross section view of a sample at location near the top of the trench, illustrating the effectiveness of PDMS for stopping the growth over the top surface of the substrate and a cleaved surface of densely packed ZnO nanowires grown perpendicular to the trench sidewall, c) a cross section view of a sample featuring large ZnO nanowires grown in bulk, the PDMS growth stop layer resulted in sharp needle-like structure. Scale bars are 5 μm, 4 μm and 10 μm for a), b) and c), respectively.

Even though we have obtained fairly uniform growth throughout the whole depth of a deep trench as shown in Figure 39, there was a significant amount of debris clogging the trenches at the region close to the entrance to the trenches that consisted of large nanowires that grew in the bulk of the growth solution as compared to the nanowires grown over the sidewalls, as shown on Figure 41(a). Moreover, often the space between walls and two layers of nanowires was clogged so much that some deposition of ZnO occurred on the PDMS layer,

reinforced by the large bulk-grown nanowires filling the trench, effectively forming uniform flat surface, as shown on Figure 41(b).

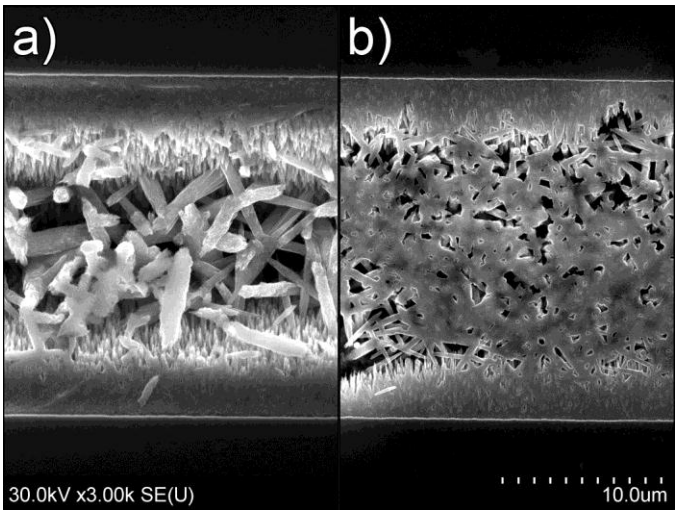

Figure 41. SEM image of a top view of clogged trenches with a) no deposition on PDMS top cover, b) with deposition on PDMS top cover.

It appears that the likelihood of a trench to be clogged was higher at location closer to the inlet. At the same time, the nanowires grown closer to the inlet could grow long enough to be very close to the nanowires on the opposite wall before clogging the trench.

Although a 0.2 um filter was used to filter the nanowires grown in the bulk in the beaker where solution was initially heated up, it appears that with the chosen nominal pumping speed of 0.55 ml/min there was enough time for these nanowires to form and grow to much bigger sizes on their way to the trenches.

To address this issue, a growth was performed with a higher nominal pumping speed of 0.91 ml/sec. Figure 42 presents a cross-sectional SEM image of a sample grown with higher pumping speed. With the pumping speed increased to 0.91 ml/min, it is less likely for a large enough crystal to form in the bulk of the growth solution during its travel from the syringe filter to the set of trenches. The amount of debris clogging the trenches was significantly decreased. As a consequence, flow is sustained up to 3 hours of growth time, even though the pumping speed is reduced. As a matter of fact, a large number of trenches were not clogged by debris at all until the end of the growth. This gives enough time for controlled growth of nanowires to reach up to 8 μm in the length. As shown in Figure 42, the nanowires grown in such trenches are almost long enough to touch the nanowires from the opposite wall. The maximum of this effect is

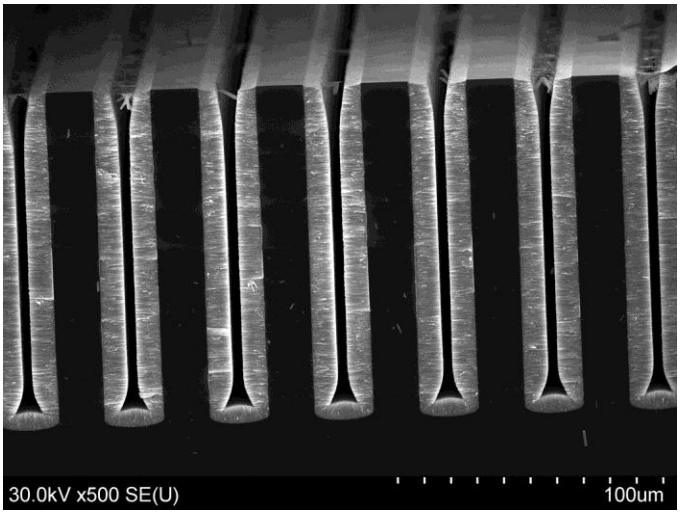

Figure 42. SEM image of a cross section of ZnO nanowires grown in trenches with width of 20 um at an increased pumping speed of 0.91 ml/min.

illustrated on Figure 43 (b).

However, as shown in Figure 43, the length of the nanowires was not quite uniform over the length of the trenches, since the growth solution flew through the set of trenches in pulsatile manner in the current microfluidics set up so that the exposure to the leaked air under negative pressure of any given part of the trench is more severe with increased distance from the inlet. Consequently, the length of nanowires on the walls of the trench closer to outlet was significantly shorter, than in the middle of the trench. The length of ZnO nanowires in the vicinity of the inlet was 7.7 μm at the top of the trench and 11.2 μm in the deeper regions (Figure 43 (b)). At the spot that is 1 mm away from the inlet, the length of ZnO nanowires at the top of the trench was 6.94 μm, while deeper in the trench it was 10.2 μm (Figure 43 (c)). At the spot that is 2 mm from the inlet, the length was 6.55 μm and 9.2 μm at the top of the trench and deeper in the trench, respectively (Figure 43 (d)). At 4 mm away from the inlet, the length was 5.75 μm and 7.4 um, respectively (Figure 43 (e)). Finally, in the vicinity of the outlet the length of ZnO nanowires was around 3μm (Figure 43 (e)).

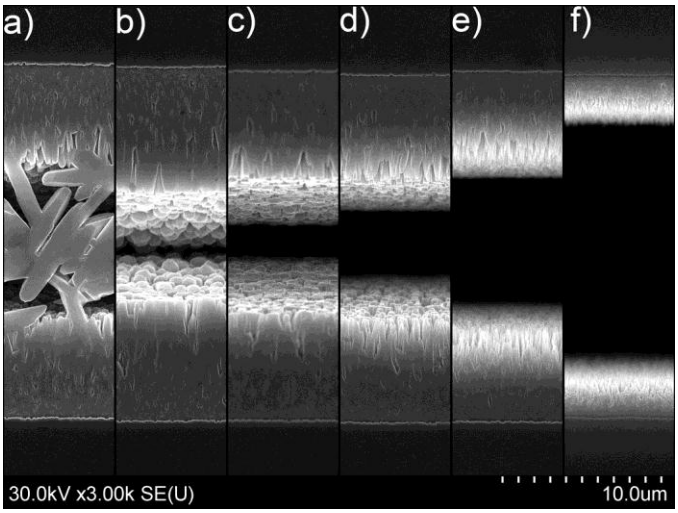

Figure 43. Top-view SEM images of ZnO nanowires grown in a set of trenches with width of 20 μm. Growth was performed at 0.91 ml/min in a pull configuration. Images were taken a) immediately at the entrance, where clogging occurred, b) immediately at the entrance with no clogging c) 1 mm, d) 2 mm, e) 4 mm away from the inlet and f) in the vicinity of the outlet

We have noticed that the variation of the length of ZnO nanowires due to pulsatile flow is much more severe for trenches with reduced width. Figure 44 shows top view SEM photos of ZnO nanowires grown in a deep silicon trench with the actual width of 6.9 um. Figure 44 (a) taken immediately at the inlet depicted that the length of nanowires at this region is 3 μm, while Figure 6 (b) and Figure 6 (c) taken at 500 μm and 1000 μm away from the inlet showed nanowires with lengths of 2.5 μm and 1.3 μm, respectively. It is observed that the effect of the length reduction in nanowires due to narrowed trench width is quite strong. On the Figure 44 (a) arrow points a trench which was clogged immediately after the start of the growth process, so that the whole trench was free from ZnO

nanowires. SEM of trenches on Figure 44 (b) and (c) were taken at a different region of set of trenches.

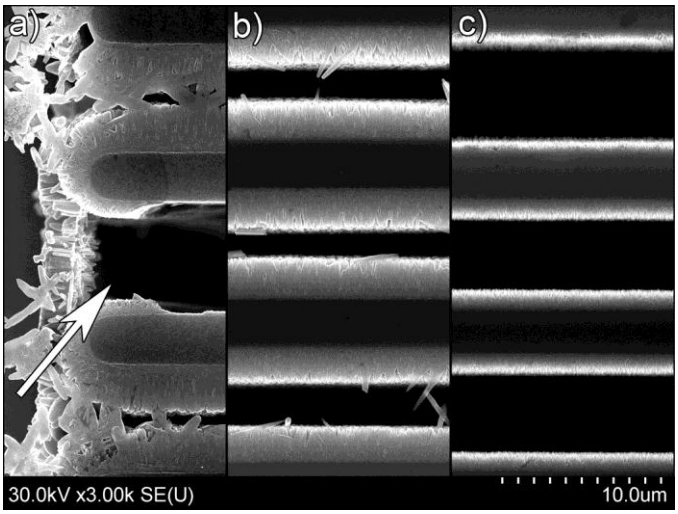

Figure 44. SEM image of a top view of ZnO nanowires grown in trenches with nominal width of 6.9 μm a) at the entrance; b) 500 μm away from the entrance; c) 1000 μm away from the entrance

One viable method to mitigate the aforementioned effect would be to grow ZnO nanowires in trenches with push scheme, rather than pull configuration discussed. It might be quite challenging since the PDMS top cover is not permanent bonded to the surface of the substrate, thus the slowest possible pumping speed of 0.55 ml/min was used. In addition to that, approximately every 10 minutes the pushing action was compensated with pulling for a short period of time (10-15 seconds). The growth was performed for a total of 2 hours. Figure 45 shows a set of SEM images, taken throughout the sample. The leftmost image (a) was taken at the left (inlet) end of trench, while each of the subsequent images, (b, c, d and so on) was taken at

spots 1 mm-distance further apart to the right, with the last one (j) being 1 mm away from the rightmost end of the trench.

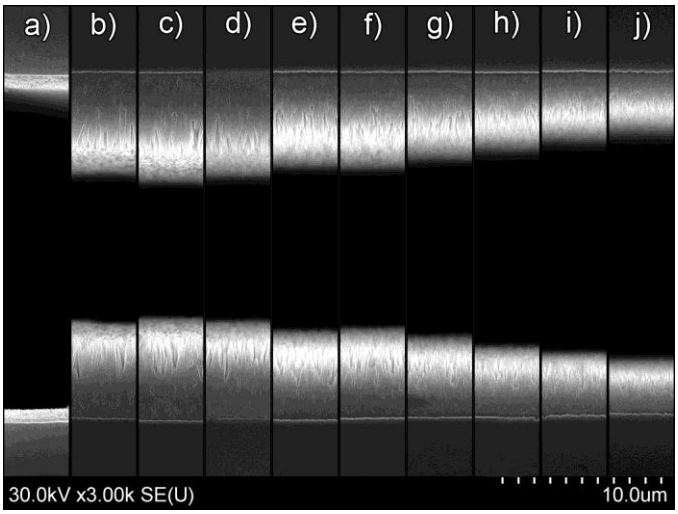

Figure 45. Top-view SEM images of ZnO nanowires grown in a set of trenches with width of 20 μm.Growth was performed at pumping speed of 0.55 ml/min, in a push configuration. Images were taken at a) entrance; b)-j) 1 mm further down the flow for each consecutive image.

As one can see the main difference is that in the vicinity of the entrance of trenches the length of nanowires is as small as ~1.2 μm (Figure 45 (a)). But as far as 1 mm into the trenches it increases greatly, reaching ~5 μm for the nanowires immediately on the top part of trenches, and reaching as much as ~6 μm for the deeper nanowires (Figure 45 (b)). The longest nanowires are at the mark of 3mm (Figure 45(c)), reaching ~5.65 μm at the top and ~6.75 μm deeper in the trench. Further (Figure 45 (d) through (j)) the length of the nanowires slowly decreases to approximately 2.25 μm at the rightmost end of trenches. The clogging of the trenches with nanowires formed in bulk was observed less frequently compared to samples with pull

configuration, with the most clogging appearing not less than 1 mm to the right from the entrance to the set of trenches. Virtually no clogging was observed immediately at the entrance. The length of the nanowires at the outlet was similar to the length of nanowires in Figure 43, under which scenario the sample was grown for 3 hours, and the nanowires closer to the inlet have much greater length as well as diameter (See Figure 43 (b)). Thus, one can conclude that the length variation of non-uniform ZnO nanowires alongside the length of the trenches can be controlled by using the above mentioned configuration.

Another method do decrease this effect is to improve sealing between the PDMS top cover and needle at the outlet port, as it is obvious that the primary reason for this effect is the leaking of air from outside due to negative pressure at the outlet end.

The sample that was grown for 3 hours with faster pumping speed of 0.91 ml/sec, which exhibited keyhole-like features in the top and bottom parts of the trenches. In Figure 46 one can see that the length of nanowires was decreased in the vicinity of the bottom of the trench and the top of the trench where it is covered by PDMS during the growth. Also, the top part of ZnO nanowires is somewhat bent. This is result of the pressure applied to PDMS, forcing it into the trench.

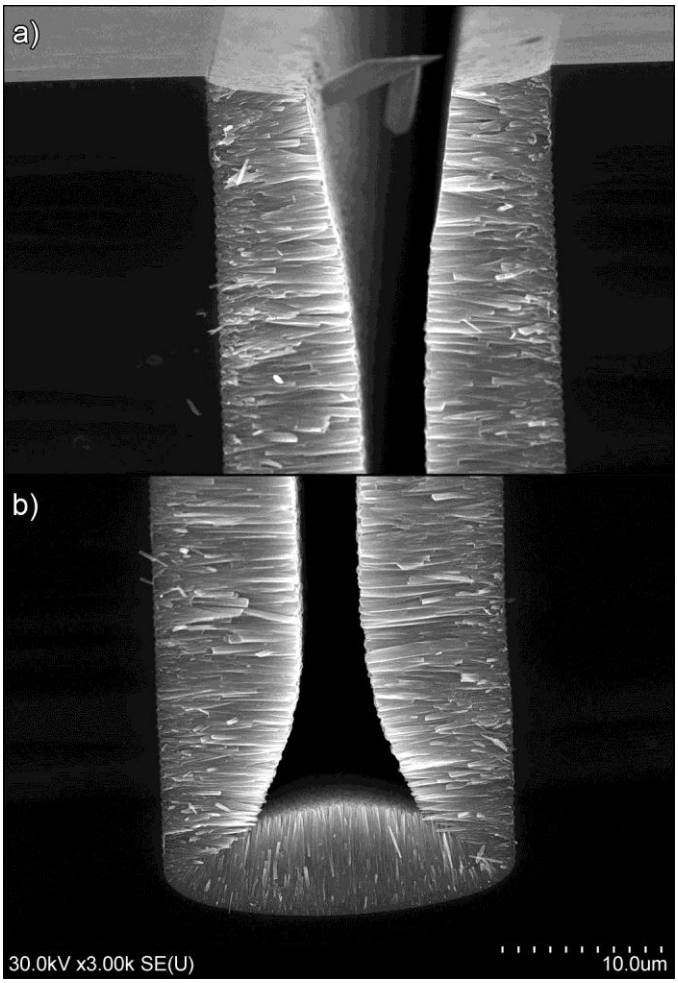

Figure 46. Cross-sectional SEM image of ZnO nanowires grown for 3 hours at pumping speed of 0.91 ml/sec, featuring the length profile of ZnO nanowires at a) the upper part of trench; b) the bottom of the trench.

For the sake of validating the growth mechanism, we have tried growth with cold growth solution. Growth solution with all the chemicals was prepared at room temperature and pumped into the deep trench microstructure, where it was heated through contact with the inlet reservoir and trenches to retain the temperature of 90-91 °C. It appeared that unusually large crystals formed in the growth solution immediately and effectively clogging trenches at their entrance at the very beginning of the growth process, thus effectively stopping flow

several minutes after beginning of the growth process. Figure 47 shows a tilted view of such a sample. ZnO crystals were formed before entering into the trenches, thus clogging them during initial stage of the growth. Inset of Figure 47 shows the top view of the same sample. As can be seen, clogging appeared at the very end of the trenches, which indicates that the ZnO crystals were formed either in the cold solution, or while being heated in the inlet reservoir.

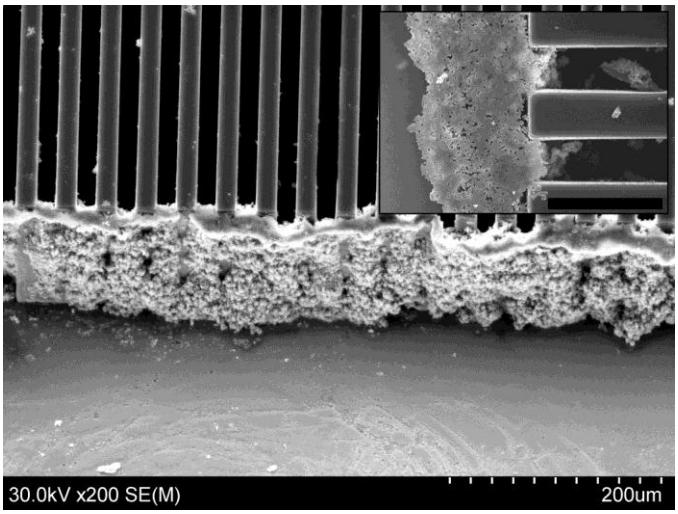

Figure 47. SEM image of a sample tilted at 40° with trenches clogged at the entrance where a growth with initially cold chemicals was attempted. Inset: top view of the same sample, showing absence of ZnO nanowires in the sidewalls of the trenches

It is worthwhile mentioning that in the sample with longer growth time, the nanowires are very densely packed, leaving virtually no space in between nanowires, which in turn reduces the porosity of the ZnO nanowires arrays. Obviously, this would not be desirable for implementation of porous electrode for devices such as supercapacitors and dye-sensitized solar cells.

Nanowires are separated from each other not only due to the variable growth speed on different crystal planes, but also to the lack of fresh chemicals in between nanowires in standard hydrothermal growth. As shown earlier, growth of ZnO nanowires is greatly dependent on the immediate vicinity of the growth site. So, we have observed significantly different nanowire morphology at the boundary of the nanowire forest.[63] When the hydrothermal growth is realized in confined space, the densely packed nanowires arrays might occupy the significant part of the volume of the channel. Then growth solution is forced to flow in between nanowires, effectively refreshing chemicals not only at the tip of the nanowire but in the immediate vicinity of the sidewalls of the nanowire. Consequently, the growth occurs not only in <002> direction, but also perpendicular to it. As shown in Figure 48, the nanowires are distinguishable from each other (crystal planes are

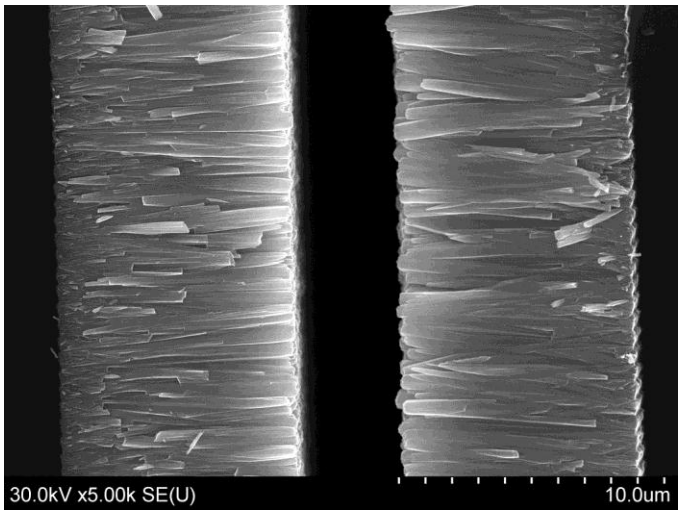

Figure 48. Cross-sectional SEM image of long ZnO nanowires effectively fused into a polycrystalline film.

visible) but are grown into each other, effectively fusing into one polycrystalline film.

Although we are using PEI as a growth modifier to inhibit growth of ZnO in the orientation perpendicular to <002> direction, one way to diminish this effect would be to further inhibit side growth by adding ammonium hydroxide. Figure 49 shows cross-sectional SEM image of sample with ZnO nanowires grown along the sidewall of trenches by using growth solution with addition of ammonium hydroxide as described in the experimental section. The inset of Figure 49 shows that the nanowires are separated from each other fairly well.

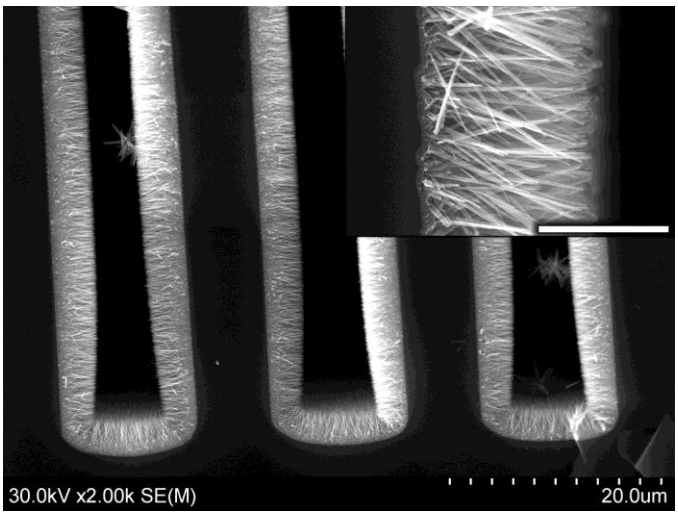

Figure 49. Cross-sectional SEM image of ZnO nanowires grown with addition of ammonium hydroxide. Inset shows closer view of high aspect ratio separated ZnO nanowires. Scale bar is 1μm.

Through strategic control of the growth time, it is possible to exploit nanowires packed with different density or porosity. By preventing ZnO nanowires from occupying the significant part of the

trench, one can direct the main flow of growth solution through the open space in between the two layers of nanowires. This will ensure slower liquid flow rate through the nanowires forest, which results in slower growth rate perpendicular to <002> direction.

Conclusion

We have successfully demonstrated a hydrothermal growth of ZnO nanowires within confined spaces such as deep trenches in Si by leveraging a microfluidic approach to the delivery of fresh chemicals to the confined space. The key advantage of this method can be traced back to the increased number of ZnO nanowires per unit area of the substrate, which can be desirable for applications where the grown ZnO nanowires forest acts as an electrode. As a result, the effectiveness of the ZnO nanowires largely depends upon the specific surface area of ZnO nanowires.

The proposed method allows for growth of ZnO nanowires in confined spaces (such as trench sidewalls) by forming three dimensional features with seeding layer conformally coated over the sidewall of the trenches. The sidewalls of the etched silicon trenches are employed to form the major portion of the sealed microfluidic channels and forced circulation of the growth solution through them to achieve fair uniform growth of ZnO nanowire forest along the sidewall.

This type of growth under forced circulation of growth solution is quite different from the conventional hydrothermal growth process, which leads to some unprecedented effects not commonly observed in bulk growth. There are several remaining challenges (e.g., non-uniformity in lateral direction, clogging, extremely densely-packed nanowires) that are distinctively different from a traditional hydrothermal growth. Obviously, the controlled growth of ZnO nanowires in confined spaces can be realized after mitigating aforementioned issues.

Chapter 8: Conclusions and Future Work

Controlled growth of ZnO nanowires is critical for repeatable production of devices with stable characteristics. Means to grow ZnO nanowires in predefined location with the most favorable morphology is of great interest for scientific community. While the most tight control and reproducibility can be achieved using gas phase growth, wet chemical methods are more suitable due to the lower costs, great potential for scalability and compatibility with IC processing. However, controlled growth of ZnO nanostructures is a more challenging task in this case. Several key aspects were addressed in the current work. Firstly, patterning of ZnO nanowires by means of microcontact printing was discussed. Repeatable method of resistless patterning was developed. Secondly, nucleation and growth of ZnO nanowires in bulk solution was studied. These nanostructures may be deemed useful for production of biocompatible polymers were these nanostructures may play the role as an enforcing agent. Thirdly, ZnO nanowires were studied as an electrode material for electrochemical and optoelectrochemical devices. Fourthly, effects of the physical properties of a seeding layer on the morphology of ZnO nanowires

were studied. Finally, growth of ZnO nanowires was realized in a confined microstructure, offering a new methodology of hydrothermal growth in confined spaces. This methodology exhibits particular effects which make hydrothermal growth quite different from the conventional method. For instance, it was shown, that the growth of ZnO nanowires is governed not only by the conventionally accepted mechanisms that ensure different growth rate on polar and non-polar planes of forming ZnO crystal, but also by a local environment in the vicinity of the growth site.

In order for successful implementation of ZnO nanowires in optoelectronical, sensing or other devices, thorough study of their optical and electrical properties is required. Such methods as steady state and time-resolved photoluminescence (PL), cathodoluminescence (CL) and optically detected magnetic resonance (ODMR) can be used for study of both intrinsic and extrinsic optical processes, as well as the nature of the defects in the ZnO nanocrystals. Raman spectroscopy in conjunction with Fourier transform infrared spectroscopy (FTIR) can provide valuable information on the vibrational spectra of ZnO nanowires, including quantum effects due to phonon confinement in nanoscale structures, thus leading to better understanding of thermal and electrical properties.

Although we have demonstrated the hydrothermal growth of ZnO nanowires in confined spaces, this methodology requires more work towards controlled growth of ZnO nanowires at optimized growth conditions to obtain suitable electrode material for the specific applications.

The next step would to build one or several device prototypes and test how the specially-tailored properties of ZnO nanowires would affect the overall performance of the devices. Several classes of devices are proposed including the following: photovoltaic devices and supercapacitors where ZnO nanowires serve as an electrode material.

List of References

1. Park, W. I.; Jun, Y. H.; Jung, S. W.; Yi, G.-C., Excitonic emissions observed in ZnO single crystal nanorods. *Appl. Phys. Lett.* **2003,** *82* (6), 964-966.

2. Djurišić, A. B.; Leung, Y. H., Optical Properties of ZnO Nanostructures. *Small* **2006,** *2* (8-9), 944-961.

3. Djurišić, A. B.; Ng, A. M. C.; Chen, X. Y., ZnO nanostructures for optoelectronics: Material properties and device applications. *Progress in Quantum Electronics* **2010,** *34* (4), 191-259.

4. Lu, M.-P.; Song, J.; Lu, M.-Y.; Chen, M.-T.; Gao, Y.; Chen, L.-J.; Wang, Z. L., Piezoelectric Nanogenerator Using p-Type ZnO Nanowire Arrays. *Nano Letters* **2009,** *9* (3), 1223-1227.

5. Wang, X.; Song, J.; Liu, J.; Wang, Z. L., Direct-Current Nanogenerator Driven by Ultrasonic Waves. *Science* **2007,** *316* (5821), 102-105.

6. Wang, Z. L.; Song, J., Piezoelectric Nanogenerators Based on Zinc Oxide Nanowire Arrays. *Science* **2006,** *312* (5771), 242-246.

7. Fan, Z.; Wang, D.; Chang, P.-C.; Tseng, W.-Y.; Lu, J. G., ZnO nanowire field-effect transistor and oxygen sensing property. *Appl. Phys. Lett.* **2004,** *85* (24), 5923-5923.

8. Wan, Q.; Li, Q. H.; Chen, Y. J.; Wang, T. H.; He, X. L.; Li, J. P.; Lin, C. L., Fabrication and ethanol sensing characteristics of ZnO nanowire gas sensors. *Appl. Phys. Lett.* **2004,** *84* (18), 3654-3654.

9. Li, S. Y.; Lee, C. Y.; Lin, P.; Tseng, T. Y., Gate-controlled ZnO nanowires for field-emission device application. *J. Vac. Sci. Technol. B* **2006,** *24* (1), 147-147.

10. Lee, C. J.; Lee, T. J.; Lyu, S. C.; Zhang, Y.; Ruh, H.; Lee, H. J., Field emission from well-aligned zinc oxide nanowires grown at low temperature. *Appl. Phys. Lett.* **2002,** *81* (19), 3648-3648.

11. Chiba, Y.; Islam, A.; Watanabe, Y.; Komiya, R.; Koide, N.; Han, L., Dye-Sensitized Solar Cells with Conversion Efficiency of 11.1%. *Japanese Journal of Applied Physics* **2006,** *45* (No. 25), L638-L640-L638-L640.

12. Gonzalez-Valls, I.; Lira-Cantu, M., Vertically-aligned nanostructures of ZnO for excitonic solar cells: a review. *Energy Environ. Sci.* **2008,** *2* (1), 19-34.

13. Haque, S. A.; Park, T.; Xu, C.; Koops, S.; Schulte, N.; Potter, R. J.; Holmes, A. B.; Durrant, J. R., Interface Engineering for Solid-State Dye-Sensitized Nanocrystalline Solar Cells: The Use of Ion-Solvating Hole-Transporting Polymers. *Adv. Funct. Mater.* **2004,** *14* (5), 435-440.

14. Ke, L.; Dolmanan, S. B.; Shen, L.; Pallathadk, P. K.; Zhang, Z.; Ying Lai, D. M.; Liu, H., Degradation mechanism of ZnO-based dye-sensitized solar cells. *Sol. Energy Mater. Sol. Cells* **2010,** *94* (2), 323-326.

15. Ko, S. H.; Lee, D.; Kang, H. W.; Nam, K. H.; Yeo, J. Y.; Hong, S. J.; Grigoropoulos, C. P.; Sung, H. J., Nanoforest of Hydrothermally Grown Hierarchical ZnO Nanowires for a High Efficiency Dye-Sensitized Solar Cell. *Nano Letters* **2011,** *11* (2), 666-671.

16. Law, M.; Greene, L. E.; Johnson, J. C.; Saykally, R.; Yang, P., Nanowire dye-sensitized solar cells. *Nat. Mater.* **2005,** *4* (6), 455-459.

17. Noh, J. H.; Lee, S. H. L. S.; Jung, H. S., Influence of ZnO Seed Layers on Charge Transport in ZnO Nanorod-based Dye-Sensitized Solar Cells. *Electron. Mater. Lett.* **2008,** *4* (2), 71-74.

18. Quintana, M.; Edvinsson, T.; Hagfeldt, A.; Boschloo, G., Comparison of Dye-Sensitized ZnO and TiO2 Solar Cells: Studies of Charge Transport and Carrier Lifetime. *J. Phys. Chem. C* **2006,** *111* (2), 1035-1041.

19. Liu, C. H.; Zapien, J. A.; Yao, Y.; Meng, X. M.; Lee, C. S.; Fan, S. S.; Lifshitz, Y.; Lee, S. T., High-Density, Ordered Ultraviolet Light-Emitting ZnO Nanowire Arrays. *Advanced Materials* **2003,** *15* (10), 838-841.

20. Huang, M. H.; Mao, S.; Feick, H.; Yan, H.; Wu, Y.; Kind, H.; Weber, E.; Russo, R.; Yang, P., Room-Temperature Ultraviolet Nanowire Nanolasers. *Science* **2001,** *292* (5523), 1897-1899.

21. Tang, Z. K.; Wong, G. K. L.; Yu, P.; Kawasaki, M.; Ohtomo, A.; Koinuma, H.; Segawa, Y., Room-temperature ultraviolet laser emission from self-assembled ZnO microcrystallite thin films. *Appl. Phys. Lett.* **1998,** *72* (25), 3270-3270.

22. Wang, Z. L., ZnO nanowire and nanobelt platform for nanotechnology. *Materials Science and Engineering: R: Reports* **2009,** *64* (3–4), 33-71.

23. Lee, J.; Kang, B. S.; Hicks, B.; Chancellor Jr, T. F.; Chu, B. H.; Wang, H.-T.; Keselowsky, B. G.; Ren, F.; Lele, T. P., The control of cell adhesion and viability by zinc oxide nanorods. *Biomaterials* **2008,** *29* (27), 3743-3749.

24. Pradhan, D.; Niroui, F.; Leung, K. T., High-Performance, Flexible Enzymatic Glucose Biosensor Based on ZnO Nanowires Supported on a Gold-Coated Polyester Substrate. *ACS Appl. Mater. Interfaces* **2010,** *2* (8), 2409-2412.

25. Ladanov, M.; Ram, M. K.; Matthews, G.; Kumar, A., Structure and Opto-electrochemical Properties of ZnO Nanowires Grown on n-Si Substrate. *Langmuir* **2011,** *27* (14), 9012-9017.

26. Chang, P.-C.; Fan, Z.; Wang, D.; Tseng, W.-Y.; Chiou, W.-A.; Hong, J.; Lu, J. G., ZnO Nanowires Synthesized by Vapor Trapping CVD Method. *Chem. Mater.* **2004,** *16* (24), 5133-5137.

27. Huang, M. H.; Wu, Y.; Feick, H.; Tran, N.; Weber, E.; Yang, P., Catalytic Growth of Zinc Oxide Nanowires by Vapor Transport. *Adv. Mater. (Weinheim, Ger.)* **2001,** *13* (2), 113-116.

28. Kirkham, M.; Wang, X.; Wang, Z. L.; Snyder, R. L., Solid Au nanoparticles as a catalyst for growing aligned ZnO nanowires: a new understanding of the vapour–liquid–solid process. *Nanotechnology* **2007,** *18* (36).

29. Amarilio-Burshtein, I.; Tamir, S.; Lifshitz, Y., Growth modes of ZnO nanostructures from laser ablation. *Appl. Phys. Lett.* **2010,** *96* (10), 103104-103104-3.

30. Rey; Madjidi, H.; Le Rouzic, M.; Bruyant, N.; Rapenne, L.; Jimenez, C.; Labeau, M.; Baxter, J. B.; Ternon, C.; Bellet, D., Comparison of CBD and MOCVD Method for ZnO Nanowires Growth Dedicated to Dye Sensitized Solar Cells. **2009**.

31. Lee, W.; Jeong, M.-C.; Myoung, J.-M., Catalyst-free growth of ZnO nanowires by metal-organic chemical vapour deposition (MOCVD) and thermal evaporation. *Acta Mater.* **2004,** *52* (13), 3949-3957.

32. Park, W. I.; Kim, D. H.; Jung, S. W.; Yi, G.-C., Metalorganic vapor-phase epitaxial growth of vertically well-aligned ZnO nanorods. *Appl. Phys. Lett.* **2002,** *80* (22), 4232-4232.

33. Heo, Y. W.; Varadarajan, V.; Kaufman, M.; Kim, K.; Norton, D. P.; Ren, F.; Fleming, P. H., Site-specific growth of Zno nanorods using catalysis-driven molecular-beam epitaxy. *Appl. Phys. Lett.* **2002,** *81* (16), 3046-3048.

34. Hartanto, A. B.; Ning, X.; Nakata, Y.; Okada, T., Growth mechanism of ZnO nanorods from nanoparticles formed in a laser ablation plume. *Appl. Phys. A: Mater. Sci. Process.* **2004,** *78* (3), 299-301.

35. Liu, W. Z.; Xu, H. Y.; Wang, L.; Li, X. H.; Liu, Y. C., Size-controlled growth of ZnO nanowires by catalyst-free high-pressure pulsed laser deposition and their optical properties. *AIP Advances* **2011,** *1* (2), 022145-022145-8.

36. Chiou, W.-T.; Wu, W.-Y.; Ting, J.-M., Growth of single crystal ZnO nanowires using sputter deposition. *Diamond Relat. Mater.* **2003,** *12* (10–11), 1841-1844.

37. Greene, L. E.; Law, M.; Goldberger, J.; Kim, F.; Johnson, J. C.; Zhang, Y.; Saykally, R. J.; Yang, P., Low-Temperature Wafer-Scale Production of ZnO Nanowire Arrays. *Angew. Chem. Int. Ed.* **2003,** *42* (26), 3031-3034.

38. Greene, L. E.; Law, M.; Tan, D. H.; Montano, M.; Goldberger, J.; Somorjai, G.; Yang, P., General Route to Vertical ZnO Nanowire Arrays Using Textured ZnO Seeds. *Nano Letters* **2005,** *5* (7), 1231-1236.

39. Hsu, Y. F.; Xi, Y. Y.; Tam, K. H.; Djurišić, A. B.; Luo, J.; Ling, C. C.; Cheung, C. K.; Ng, A. M. C.; Chan, W. K.; Deng, X., *et al.*, Undoped p-Type ZnO Nanorods Synthesized by a Hydrothermal Method. *Adv. Funct. Mater.* **2008,** *18* (7), 1020-1030.

40. Vayssieres, L., Growth of Arrayed Nanorods and Nanowires of ZnO from Aqueous Solutions. *Adv. Mater. (Weinheim, Ger.)* **2003,** *15* (5), 464-466.

41. Vayssieres, L.; Keis, K.; Lindquist, S.-E.; Hagfeldt, A., Purpose-Built Anisotropic Metal Oxide Material: 3D Highly Oriented Microrod Array of ZnO. *The Journal of Physical Chemistry B* **2001,** *105* (17), 3350-3352.

42. Fang, F.; Zhao, D. X.; Zhang, J. Y.; Shen, D. Z.; Lu, Y. M.; Fan, X. W.; Li, B. H.; Wang, X. H., The influence of growth temperature on ZnO nanowires. *Mater. Lett.* **2008,** *62* (6–7), 1092-1095.

43. Hu, H.; Huang, X.; Deng, C.; Chen, X.; Qian, Y., Hydrothermal synthesis of ZnO nanowires and nanobelts on a large scale. *Mater. Chem. Phys.* **2007,** *106* (1), 58-62.

44. Lu, C.; Qi, L.; Yang, J.; Tang, L.; Zhang, D.; Ma, J., Hydrothermal growth of large-scale micropatterned arrays of ultralong ZnO nanowires and nanobelts on zinc substrate. *Chem. Commun. (Cambridge, U. K.)* **2006,** (33).

45. Zhang, H.; Yang, D.; Ma, X.; Ji, Y.; Xu, J.; Que, D., Synthesis of flower-like ZnO nanostructures by an organic-free hydrothermal process. *Nanotechnology* **2004,** *15* (5), 622-626.

46. Cai, A.-J.; Wang, Y.-L.; Xing, S.-T.; Ma, Z.-C., Cavity of cyclodextrin, a useful tool for the morphological control of ZnO micro/nanostructures. *Ceram. Int.* **2012,** *38* (6), 5265-5270.

47. Cho, S.; Jang, J.-W.; Jung, S.-H.; Lee, B. R.; Oh, E.; Lee, K.-H., Precursor Effects of Citric Acid and Citrates on ZnO Crystal Formation. *Langmuir* **2009,** *25* (6), 3825-3831.

48. Mo, M.-S.; Wang, D.; Du, X.; Ma, J.; Qian, X.; Chen, D.; Qian, Y., Engineering of Nanotips in ZnO Submicrorods and Patterned Arrays. *Cryst. Growth Des.* **2009,** *9* (2), 797-802.

49. Kuo, C.-L.; Kuo, T.-J.; Huang, M. H., Hydrothermal Synthesis of ZnO Microspheres and Hexagonal Microrods with Sheetlike and Platelike Nanostructures. *The Journal of Physical Chemistry B* **2005,** *109* (43), 20115-20121.

50. Kozhummal, R.; Yang, Y.; Güder, F.; Hartel, A.; Lu, X.; Küçükbayrak, U. M.; Mateo-Alonso, A.; Elwenspoek, M.; Zacharias, M., Homoepitaxial Branching: An Unusual Polymorph of Zinc Oxide Derived from Seeded Solution Growth. *ACS Nano* **2012,** *6* (8), 7133-7141.

51. Liu, X. M.; Zhou, Y. C., Seed-mediated synthesis of uniform ZnO nanorods in the presence of polyethylene glycol. *J. Cryst. Growth* **2004,** *270* (3–4), 527-534.

52. Joo, J.; Chow, B. Y.; Prakash, M.; Boyden, E. S.; Jacobson, J. M., Face-selective electrostatic control of hydrothermal zinc oxide nanowire synthesis. *Nat. Mater.* **2011,** *10* (8), 596-601.

53. Xu, S.; Lao, C.; Weintraub, B.; Wang, Z. L., Density-controlled growth of aligned ZnO nanowire arrays by seedless chemical approach on smooth surfaces. *J. Mater. Res.* **2008,** *23* (08), 2072-2077.

54. Ma, T.; Guo, M.; Zhang, M.; Zhang, Y.; Wang, X., Density-controlled hydrothermal growth of well-aligned ZnO nanorod arrays. *Nanotechnology* **2007,** *18* (3).

55. Yang, L. L.; Zhao, Q. X.; Willander, M., Size-controlled growth of well-aligned ZnO nanorod arrays with two-step chemical bath deposition method. *J. Alloys Compd.* **2009,** *469* (1–2), 623-629.

56. Sugunan, A.; Warad, H.; Boman, M.; Dutta, J., Zinc oxide nanowires in chemical bath on seeded substrates: Role of hexamine. *J. Sol-Gel Sci. Technol.* **2006,** *39* (1), 49-56.

57. Willander, M.; Yang, L. L.; Wadeasa, A.; Ali, S. U.; Asif, M. H.; Zhao, Q. X.; Nur, O., Zinc oxide nanowires: controlled low temperature growth and some electrochemical and optical nano-devices. *J. Mater. Chem.* **2009,** *19* (7), 1006-1018.

58. Xu, C.; Shin, P.; Cao, L.; Gao, D., Preferential Growth of Long ZnO Nanowire Array and Its Application in Dye-Sensitized Solar Cells. *J. Phys. Chem. C* **2009,** *114* (1), 125-129.

59. Na, J.-S.; Gong, B.; Scarel, G.; Parsons, G. N., Surface Polarity Shielding and Hierarchical ZnO Nano-Architectures Produced Using Sequential Hydrothermal Crystal Synthesis and Thin Film Atomic Layer Deposition. *ACS Nano* **2009,** *3* (10), 3191-3199.

60. Kang, H. W.; Yeo, J.; Hwang, J. O.; Hong, S.; Lee, P.; Han, S. Y.; Lee, J. H.; Rho, Y. S.; Kim, S. O.; Ko, S. H.*, et al.*, Simple ZnO Nanowires Patterned Growth by Microcontact Printing for High Performance Field Emission Device. *The Journal of Physical Chemistry C* **2011,** *115* (23), 11435-11441.

61. Kind, H.; Bonard, J. M.; Emmenegger, C.; Nilsson, L. O.; Hernadi, K.; Maillard-Schaller, E.; Schlapbach, L.; Forró, L.; Kern, K., Patterned Films of Nanotubes Using Microcontact Printing of Catalysts. *Advanced Materials* **1999,** *11* (15), 1285-1289.

62. Hsu, J. W. P.; Tian, Z. R.; Simmons, N. C.; Matzke, C. M.; Voigt, J. A.; Liu, J., Directed Spatial Organization of Zinc Oxide Nanorods. *Nano Letters* **2005,** *5* (1), 83-86.

63. Ladanov, M.; Elineni, K. K.; Ram, M.; Gallant, N. D.; Kumar, A.; Matthews, G., A Resistless Process for the Production of Patterned, Vertically Aligned ZnO Nanowires. *MRS Online Proceedings Library* **2011,** *1302*, null-null.

64. Xu, S.; Wei, Y.; Kirkham, M.; Liu, J.; Mai, W.; Davidovic, D.; Snyder, R. L.; Wang, Z. L., Patterned Growth of Vertically Aligned ZnO Nanowire Arrays on Inorganic Substrates at Low Temperature without Catalyst. *J. Am. Chem. Soc.* **2008,** *130* (45), 14958-14959.

65. Yoon, S.-H.; Yang, H.; Kim, Y.-S., Ordered growth of ZnO nanorods for fabrication of a hybrid plasma display panel. *Nanotechnology* **2007,** *18* (20), 205608-205608.

66. Ladanov, M.; Ram, M.; Kumar, A.; Matthews, G., Novel Aster-Like ZnO Nanowire Clusters for Nanocomposites. *MRS Online Proceedings Library* **2011,** *1312*, null-null.

67. Sun, G.; Cao, M.; Wang, Y.; Hu, C.; Liu, Y.; Ren, L.; Pu, Z., Anionic surfactant-assisted hydrothermal synthesis of high-aspect-ratio ZnO nanowires and their photoluminescence property. *Mater. Lett.* **2006,** *60* (21–22), 2777-2782.

68. Lao, J. Y.; Wen, J. G.; Ren, Z. F., Hierarchical ZnO Nanostructures. *Nano Letters* **2002,** *2* (11), 1287-1291.

69. Peet, J.; Kim, J. Y.; Coates, N. E.; Ma, W. L.; Moses, D.; Heeger, A. J.; Bazan, G. C., Efficiency enhancement in low-bandgap polymer solar cells by processing with alkane dithiols. *Nat. Mater.* **2007,** *6* (7), 497-500.

70. Zhang, Y.; Russo, R. E.; Mao, S. S., Femtosecond laser assisted growth of ZnO nanowires. *Appl. Phys. Lett.* **2005,** *87* (13), 133115-133115.

71. Lyu, S. C.; Zhang, Y.; Lee, C. J.; Ruh, H.; Lee, H. J., Low-Temperature Growth of ZnO Nanowire Array by a Simple Physical Vapor-Deposition Method. *Chem. Mater.* **2003,** *15* (17), 3294-3299.

72. Sharp, K. G.; Blackman, G. S.; Glassmaker, N. J.; Jagota, A.; Hui, C.-Y., Effect of Stamp Deformation on the Quality of Microcontact Printing: Theory and Experiment. *Langmuir* **2004,** *20* (15), 6430-6438.

73. WangWang; Zhou, J.; Song; Liu, J.; Xu, N.; Wang, Z. L., Piezoelectric Field Effect Transistor and Nanoforce Sensor Based on a Single ZnO Nanowire. *Nano Letters* **2006,** *6* (12), 2768-2772.

74. Li, Z.; Yang, R.; Yu, M.; Bai, F.; Li, C.; Wang, Z. L., Cellular Level Biocompatibility and Biosafety of ZnO Nanowires. *The Journal of Physical Chemistry C* **2008,** *112* (51), 20114-20117.

75. Zhou, J.; Xu, N. S.; Wang, Z. L., Dissolving Behavior and Stability of ZnO Wires in Biofluids: A Study on Biodegradability and Biocompatibility of ZnO Nanostructures. *Adv. Mater. (Weinheim, Ger.)* **2006,** *18* (18), 2432-2435.

76. Arnold, M. S.; Avouris, P.; Pan, Z. W.; Wang, Z. L., Field-Effect Transistors Based on Single Semiconducting Oxide Nanobelts. *J. Phys. Chem. B* **2003,** *107* (3), 659-663.

77. Bae, J.; Song, M. K.; Park, Y. J.; Kim, J. M.; Liu, M.; Wang, Z. L., Fiber Supercapacitors Made of Nanowire-Fiber Hybrid Structures for Wearable/Flexible Energy Storage. *Angew. Chem. Int. Ed.* **2011,** *50* (7), 1683-1687.

78. Cross, R. B. M.; Souza, M. M. D.; Narayanan, E. M. S., A low temperature combination method for the production of ZnO nanowires. *Nanotechnology* **2005,** *16* (10), 2188-2192.

79. Li, Q.; Kumar, V.; Li, Y.; Zhang, H.; Marks, T. J.; Chang, R. P. H., Fabrication of ZnO Nanorods and Nanotubes in Aqueous Solutions. *Chem. Mater.* **2005,** *17* (5), 1001-1006.

80. Pung, S.-Y.; Choy, K.-L.; Hou, X.; Shan, C., Preferential growth of ZnO thin films by the atomic layer deposition technique. *Nanotechnology* **2008,** *19* (43), 435609-435609.

81. Solís-Pomar, F.; Martínez, E.; Meléndrez, M. F.; Pérez-Tijerina, E., Growth of vertically aligned ZnO nanorods using textured ZnO films. *Nanoscale Research Letters* **2011,** *6* (1), 524-524.

82. Knez, M.; Nielsch, K.; Niinistö, L., Synthesis and Surface Engineering of Complex Nanostructures by Atomic Layer Deposition. *Advanced Materials* **2007,** *19* (21), 3425-3438.

Appendix A: A Resistless Process for the Production of Patterned, Vertically Aligned ZnO Nanowires

In this appendix, we present the final version of manuscript titled "A Resistless Process for the Production of Patterned, Vertically Aligned ZnO Nanowires" published in Mater. Res. Soc. Symp. Proc. Vol. 1302 by Materials Research Society. All the co-authors have authorized the inclusion of this document in the dissertation. The license to use this document was obtained from the publisher and is included in Appendix D: Copyright Permissions.

Appendix A (continued)

Mater. Res. Soc. Symp. Proc. Vol. 1302 © 2011 Materials Research Society
DOI: 10.1557/opl.2011.82

A Resistless Process for the Production of Patterned, Vertically Aligned ZnO Nanowires.

Mikhail Ladanov[1, 2, 3], Kranthi Kumar Elineni[2], Manoj Ram[2, 3], Nathan D. Gallant[2], Ashok Kumar[2, 3], Garrett Matthews[4]

[1]Department of Electrical Engineering, University of South Florida, Tampa, FL, United States.
[2]Department of Mechanical Engineering, University of South Florida, Tampa, FL, United States.
[3]Nanotechnology Research and Education Center, University of South Florida, Tampa, FL, United States.
[4]Department of Physics, University of South Florida, Tampa, FL, United States.

ABSTRACT

ZnO nanostructures have attracted a great deal of interest because of their biocompatibility and outstanding optical and piezoelectric properties. Their uses are widely varying, including as the active element in sensors, solar cells, and nanogenerators. One of the major complications in device development is how to grow ZnO nanowires in well aligned and patterned films with predefined geometrical shape and aspect ratio. Controlled growth is required to achieve the optimal density of nanowires and to produce a defined geometric structure for incorporation in the device. In this work, we have presented a method by which vertically aligned ZnO nanowires could be grown in defined patterns on surfaces without the use of resists. We used a hydrothermal method to grow ZnO nanowires on a substrate through growth modifiers that was pre-patterned with a seeding solution by means of microcontact printing. This method produced vertically aligned ZnO nanowires of predefined size and shape with pattern resolution high enough for the production of rows of single nanowires. The nanowires were characterized by using scanning electron microscopy (SEM) and X-ray diffraction spectroscopy (XRD) techniques.

INTRODUCTION

Recently, ZnO nanostructures have attracted great attention. ZnO is a II-VI semiconductor with a wide direct band gap of 3.37 eV and large exciton binding energy of 60 meV making it suitable for application in UV lasers[1], light emitting diodes[2], sensors[3], nanogenerators[4-6] and solar cells[7].

Many methods have been used to prepare ZnO nanowires, including using chemical vapor deposition[3, 8], metal–organic chemical deposition[8, 9], pulsed laser deposition[10], physical vapor deposition[11, 12], vapor-liquid-solid methods[6, 13] as well as the hydrothermal method[1, 14, 15] used in this work. The latter is one of the most simple and cost effective methods, making it straightforward to scale up production[1, 14, 16].

Patterned growth of ZnO nanowires using hydrothermal methods have been studied extensively[17, 18] as it is a simple way to produce spatially distributed nanowires for device fabrication. The use of microcontact printing (μCP)[19] has become common for the modification of surfaces with monolayer domains, though its use as a method for patterning nanowire growth has not been well explored.

In this paper we have demonstrated vertically aligned and patterned ZnO nanowires on silicon substrates. These structures were produced using μCP to control the regions where a seeding layer is deposited on a surface. In turn, the patterned seeding layer controls the regions where the nanowires are grown from the surface using a hydrothermal growth technique. Additionally, the effects of spatial distribution on the size and morphology of ZnO nanowires are discussed in this paper.

EXPERIMENTAL

Microcontact printing

For μCP, two types of stamps were made from polydimethylsiloxane (PDMS). Type I was made by molding PDMS on a silicon calibration grating, producing stamps with parallel features of 1500 nm wide platforms having a height of 500 nm. The spacing between the platforms was maintained to be 1500 nm. This stamp would be expected to transfer material onto the surface in a pattern of 1.5 μm wide parallel lines with 1.5 μm wide separation. Type II was made by molding PDMS on wafer template consisting of recessed 10 μm circles or annular rings with a lateral thickness of 1μm obtained by photolithography using using Shipley 1813 as photoresist. The height of the stamp features was 2 μm and the spacing between features was 75 μm.

The stamping inks were solutions of zinc acetate in ethanol. These solutions were prepared at four different concentrations: 0.1, 0.2, 2, 10 mM/L. For transferring the zinc acetate onto the silicon substrate, the selected stamp was soaked in the zinc acetate solution for 30 to 60 seconds. The 'inked' stamps were then blown dry with a stream of nitrogen, brought in contact with the silicon substrates for 10 seconds, and then quickly separated. Consistent force was applied from sample to sample by ensuring conformal contact due to work of adhesion. After this printing procedure, the samples were baked on a hotplate for 30 min at 350°C. This heat causes the zinc acetate to decompose, reacting with atmospheric oxygen and forming ZnO nanocrystals. These nanocrystals, now patterned on the on Si substrate, acted as a nucleation layer for the growth of nanowires growth.

Hydrothermal growth

ZnO nanowires were grown using the conventional hydrothermal method. 25 mM L^{-1} of both zinc nitrate and hexamine solutions were prepared in deionized water (DIW) and heated to 80°C. This solution was used as the growth solution. 10 μL of a 10mM L^{-1} stock solution of sodium citrate were added per 250 mL of growth solution. The Si substrate was placed face down in the growth solution, and held for 2 hours while the solution was stirred vigorously. Afterward, the silicon was removed from the growth solution, and rinsed with DI water and, optionally, sonicated in DIW for 3-5 seconds to remove ZnO debris – ZnO nanowires grown not on the substrate, but rather in the solution and deposited on the substrate afterwards. This debris has been observed in some of the scanning electron microscopy (SEM) images. It typically appears much brighter than nanowires grown on the substrate as they have an open contact with the substrate, therefore experiencing a stronger charging effect. Finally, samples were dried using dry N_2.

RESULTS AND DISCUSSION

Figure 1a shows an SEM image of ZnO nanowires grown with the hydrothermal method on patterned substrates. Patterning was done with the use of microcontact printing with a parallel grating (type I) stamp. The width and spacing of printed lines is approximately 1.5 μm.

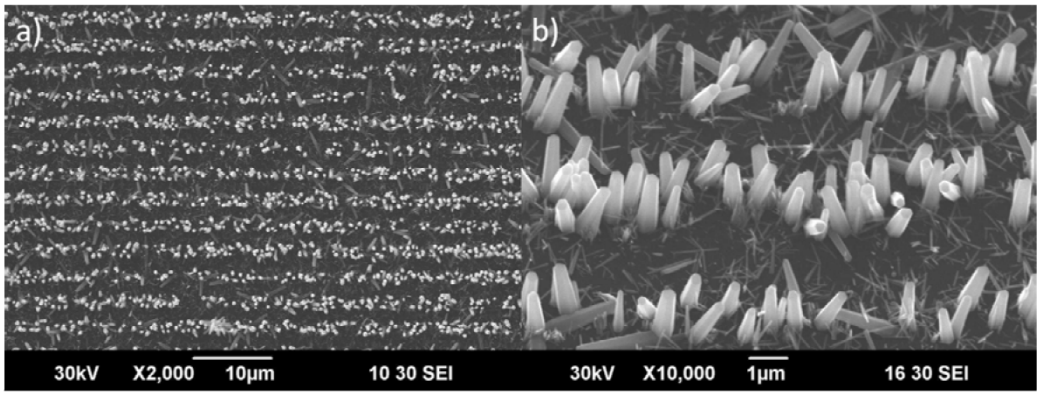

Figure 1. a) SEM image of ZnO nanowires patterned using microcontact printing with type I stamp. b) Zoomed in and tilted 60° SEM image of the same nanowires, revealing their shape and length.

As seen in Figure 1b, the nanowires have a conical shape with a base diameter of approximately 500 nm and an apical diameter of approximately 200-400 nm. These sizes are considerably larger than the sizes observed for nanowires grown under the same conditions on uniformly seeded, rather than patterned, substrates. The reasons for the different sizes observed are unclear. However, a potential explanation may lie in a difference in seeding between the two techniques – even though the same seeding solution was used both for patterned and uniformly seeded samples, the different seeding techniques may introduce a variation in the density of zinc acetate molecules on surface. After baking, different sizes of ZnO nanocrystals would result. Since these nanocrystals serve as growth sites for nanowires, the nanowires produced would have different dimensions. Another potential explanation would be a difference in the growth environment – the patterned nanowires are confined to regions defined by the patterned seeding solution. The patterned surface produces fewer growth sites per area, providing more free space around the wires during the growing stage. This reduced crowding may lead to more free and rapid access to the zinc ions during the growth. Although a more likely explanation is a combination of these two effects.

Comparable results were observed in work presented below and support the explanations given above. Samples were produced which had relatively large areas patterned with the seeding solution separated by large bare surface. These samples exhibited variations in the size of the nanorods grown within a single sample. Moving from the bare region further into the area of uniform seeding, the nanowires have been found to decrease in size. This decrease is quite dramatic, on the order of a ten-fold change. Also varying is the lateral spacing of the nanowires, with the densest coverage being at the center of the uniformly coated region.

The image in Figure 2 is representative of the ZnO nanowires as patterned by contact printing the seeding solution with an annular type II stamp. Again, the mean diameter of the resulting nanowires is greater than the mean diameter of the nanowires grown under the same conditions but on surfaces continuously covered by the seeding solution. The nanowires lying

around the annular ring are most likely nanowires grown simultaneously in the solution without seeding crystals and deposited on the surface after growth. Alternatively, they may have been grown on the substrate, but they detached and were redeposited. They have a weaker contact with the substrate than the nanowires grown from the seeded ring; therefore, they often have more charging by the SEM and appear much brighter on the SEM images (lower part of the image).

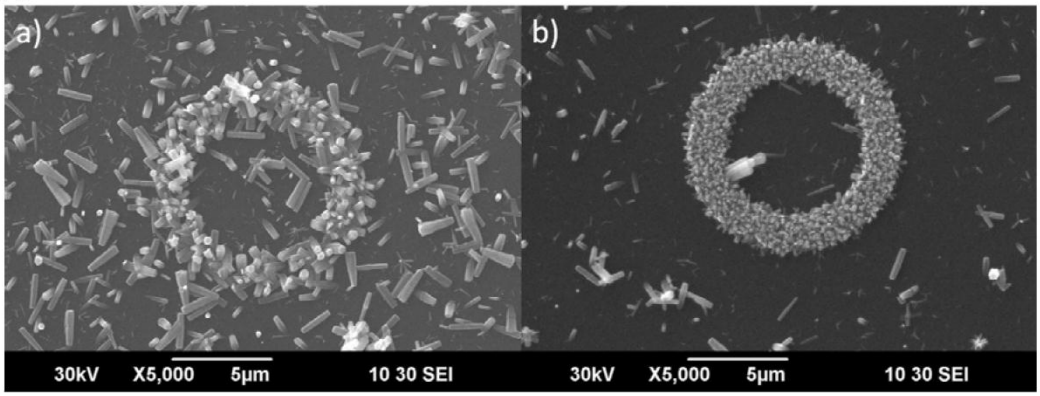

Figure 2. SEM images of ZnO nanowires patterned as annular rings with 10 μm outer diameter and lateral thickness of 1 μm before (a) and after (b) sonication.

Figure 2b is an SEM image of the same patterned ZnO nanowire sample at a different location after light (~3 sec) sonication in DI water. As can be seen, most of the debris is gone. The patterned nanowires predominantly are still attached to the surface, as are some fraction of the nanowires that were grown in the non-seeded areas. The observed in Figure 2a and Figure 2b difference in the density and size of the nanowires across patterned regions on the same sample may be due to the nature of conformal contact in μCP.

Figure 3a is representative of the SEM images of ZnO nanowires patterned with another Type II stamp that had 10 μm solid circles, rather than rings. Interesting to note is that the nanowires on the outside of the circle are of larger diameter than those inside the circle, and the growth is mostly horizontal. Results of this type support the assertion that the larger diameter nanowires has resulted from greater diffusion of the ionic zinc to the growing wires at the edge of the pattern.

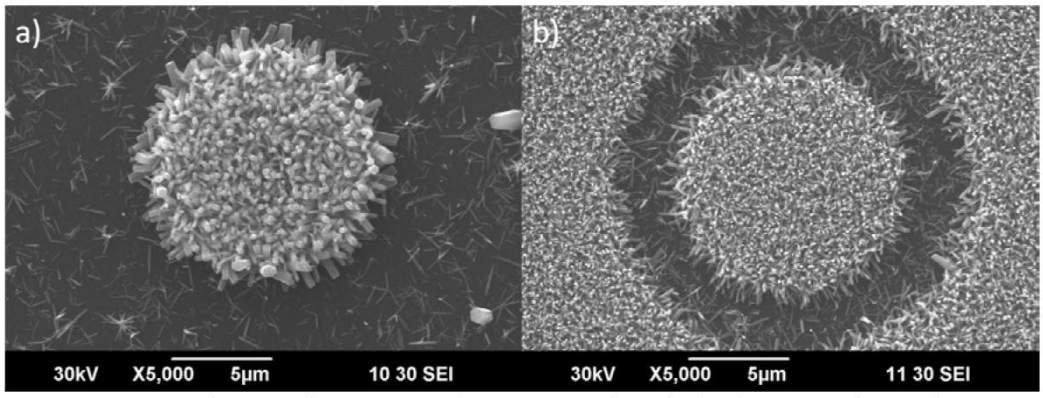

Figure 3. SEM image of ZnO nanowires patterned as circles in areas where microcontact printing was performed (a) normally, (b) with intentionally collapsed roof.

Figure 3b shows an SEM image of ZnO nanowires grown on the same patterned surface that produced the image shown in Figure 3a, but in a region where the roof of the stamp was intentionally collapsed. The collapsed part of the stamp printed the seeding solution everywhere except for the region immediately around the feature (residual moat of unsealed area)[20]. Here the restoring forces within the stamp balanced the forces of adhesion between the stamp and the substrate, preventing collapse close to the feature. The variation in nanowire sizes has not occurred in this case. Two reasons likely explain this behavior – 1. the modified distribution of forces in this geometry has changed the deposition density of the seeding solution, resulting in a more uniform distribution of the zinc acetate, and/or 2. the growth of the nanowires around the feature prevented effective refreshing of the chemicals so that the nanowires could not grow at the same conditions as shown in the previous figure. The latter explanation can also be confirmed by the fact that samples with lines printed with stamps of Type I have nanowires of larger sizes as compared with the samples with uniform seeding grown under the same conditions.

Figure 4 shows the typical X-ray diffraction (XRD) patterns of the ZnO nanowire coated substrate.

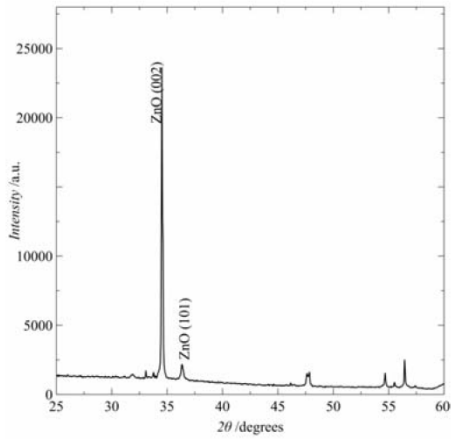

Figure 4. Typical XRD of samples grown with technique described. Pronounced (002) peaks is an indication of predominantly vertically aligned nanowires.

Two peaks are pronounced for the ZnO diffraction pattern: (002) and (101) which appear at 2θ=34.4°, 36.3°, respectively. The ZnO nanowires in the samples under investigation have shown a dominate diffraction peak for (002), which indicates a high degree of orientation with the *c*-axis vertical to the substrate surface. The XRD results suggest that our sample is highly crystallized wurtzite type.

CONCLUSION

A simple and cost effective technique for the hydrothermal growth of patterned ZnO nanowires is shown in this paper. The microcontact printing technique is employed for growing spatially distributed ZnO nanowires for device applications. Our study has also shown that both the seeding and the local growth environment are critical for the sizes and shapes of the produced nanowires.

ACKNOWLEDGMENTS

This research was partially supported by NSF Grant#0854023.

REFERENCES

1. L. E. Greene, M. Law, J. Goldberger, F. Kim, J. C. Johnson, Y. Zhang, R. J. Saykally and P. Yang, Angew. Chem. Int. Ed. **42** (26), 3031-3034 (2003).
2. C. H. Liu, J. A. Zapien, Y. Yao, X. M. Meng, C. S. Lee, S. S. Fan, Y. Lifshitz and S. T. Lee, Adv. Mater. (Weinheim, Ger.) **15** (10), 838-841 (2003).
3. Z. Fan, D. Wang, P.-C. Chang, W.-Y. Tseng and J. G. Lu, Appl. Phys. Lett. **85** (24), 5923-5923 (2004).
4. M.-P. Lu, J. Song, M.-Y. Lu, M.-T. Chen, Y. Gao, L.-J. Chen and Z. L. Wang, Nano Lett. **9** (3), 1223-1227 (2009).
5. X. Wang, J. Song, J. Liu and Z. L. Wang, Science **316** (5821), 102-105 (2007).
6. Z. L. Wang and J. Song, Science **312** (5771), 242-246 (2006).
7. M. Law, L. E. Greene, J. C. Johnson, R. Saykally and P. Yang, Nat. Mater. **4** (6), 455-459 (2005).
8. P.-C. Chang, Z. Fan, D. Wang, W.-Y. Tseng, W.-A. Chiou, J. Hong and J. G. Lu, Chem. Mater. **16** (24), 5133-5137 (2004).
9. W. I. Park, D. H. Kim, S. W. Jung and G.-C. Yi, Appl. Phys. Lett. **80** (22), 4232-4232 (2002).
10. Y. Zhang, R. E. Russo and S. S. Mao, Appl. Phys. Lett. **87** (13), 133115-133115 (2005).
11. W. Lee, M.-C. Jeong and J.-M. Myoung, Acta Mater. **52** (13), 3949-3957 (2004).
12. S. C. Lyu, Y. Zhang, C. J. Lee, H. Ruh and H. J. Lee, Chem. Mater. **15** (17), 3294-3299 (2003).
13. M. H. Huang, Y. Wu, H. Feick, N. Tran, E. Weber and P. Yang, Adv. Mater. (Weinheim, Ger.) **13** (2), 113-116 (2001).
14. L. E. Greene, M. Law, D. H. Tan, M. Montano, J. Goldberger, G. Somorjai and P. Yang, Nano Lett. **5** (7), 1231-1236 (2005).
15. Y. F. Hsu, Y. Y. Xi, K. H. Tam, A. B. Djurišić, J. Luo, C. C. Ling, C. K. Cheung, A. M. C. Ng, W. K. Chan, X. Deng, C. D. Beling, S. Fung, K. W. Cheah, P. W. K. Fong and C. C. Surya, Adv. Funct. Mater. **18** (7), 1020-1030 (2008).
16. L. Vayssieres, Adv. Mater. (Weinheim, Ger.) **15** (5), 464-466 (2003).
17. S. Xu, Y. Wei, M. Kirkham, J. Liu, W. Mai, D. Davidovic, R. L. Snyder and Z. L. Wang, J. Am. Chem. Soc. **130** (45), 14958-14959 (2008).
18. S.-H. Yoon, H. Yang and Y.-S. Kim, Nanotechnology **18** (20), 205608-205608 (2007).
19. J. W. P. Hsu, Z. R. Tian, N. C. Simmons, C. M. Matzke, J. A. Voigt and J. Liu, Nano Lett. **5** (1), 83-86 (2005).
20. K. G. Sharp, G. S. Blackman, N. J. Glassmaker, A. Jagota and C.-Y. Hui, Langmuir **20** (15), 6430-6438 (2004).

Appendix B: Novel Aster-like ZnO Nanowire Clusters for Nanocomposites

In this appendix, we present the final version of manuscript titled "Novel Aster-like ZnO Nanowire Clusters for Nanocomposites" published in Mater. Res. Soc. Symp. Proc. Vol. 1312 by Materials Research Society. All the co-authors have authorized the inclusion of this document in the dissertation. The license to use this document was obtained from the publisher and is included in Appendix D: Copyright Permissions.

Appendix B (Continued)

Mater. Res. Soc. Symp. Proc. Vol. 1312 © 2011 Materials Research Society
DOI: 10.1557/opl.2011.264

Novel Aster-like ZnO Nanowire Clusters for Nanocomposites

Mikhail Ladanov[1, 2, 3], Manoj Ram[2, 3], Ashok Kumar[2, 3], Garrett Matthews[4]

[1]Department of Electrical Engineering, University of South Florida, Tampa, FL, United States.
[2]Department of Mechanical Engineering, University of South Florida, Tampa, FL, United States.
[3]Nanotechnology Research and Education Center, University of South Florida, Tampa, FL, United States.
[4]Department of Physics, University of South Florida, Tampa, FL, United States.

ABSTRACT

ZnO nanostructures have attracted a great deal of interest because of their biocompatibility and outstanding optical and piezoelectric properties. Their uses are widely varying, including incorporation in sensors, solar cells, and nanogenerators. Biological systems are yet another area of application of ZnO nanowires. Apart from their electrical and optical properties, ZnO nanostructures can be used for the mechanical reinforcement of existing biomimetic scaffolds such as collagen and/or other biodegradable polymers (poly(lactic acid), polyglycolide, poly(alkyene succinate)s or polyhydroxylalkanoates). In this work, we have demonstrated a cheap and comparatively facile hydrothermal growth method for the bulk production of ZnO nanostructures exhibiting an aster-like geometry. The novel nanostructures of ZnO can be used as reinforced material to biopolymers. The aster shape has presented an increased surface area, providing a means for enhancing the stabilization of the gels and\or polymers. With controllable growth of ZnO nanostructures this method allows the geometry which could be tuned for maximal coupling between the two phases of composite and increased mechanical strength.

INTRODUCTION

ZnO is a biocompatible piezoelectric II-VI semiconductor with a wide direct band gap of 3.37 eV and large exiton binding energy of 60 meV. Recently, ZnO nanostructures have attracted great attention as a promising functional material due to its suitability for application in UV lasers[1, 2], light emitting diodes[3], sensors[4-6], nanogenerators[7-9] and solar cells. Due to biocompatibility[10, 11], ZnO can be used as a functional material in implantable devices or even as a reinforcing material for different biopolymers. In this case bulk growth of structures with large surface area to volume ratios while keeping the effective volume large enough for successful incorporation into biopolymers is desired.

Many methods have been used to prepare ZnO nanowires, including using chemical vapor deposition[4, 12], metal–organic chemical deposition[13, 14], pulsed laser deposition[15], physical vapor deposition[13, 16], vapor-liquid-solid methods[9, 17] and hydrothermal methods[1, 18, 19]. The hydrothermal method is one of the most simple and cost effective methods, making the scaling up of production straightforward.

Growth of ZnO nanostructures using the hydrothermal method has been studied extensively as it is a simple way to produce various shapes and geometries of nanostructures. The use of modifying agents, various substrates, wide spectra of seeding techniques and electric field assistance has become common for the modification of resultant properties, such as shape, size

and morphology of ZnO nanostructures. However, mostly these techniques are suitable for the growth of ZnO nanostructures on various substrates.

In this paper, we demonstrate the growth of ZnO nanostructures in a bulk solution, where different sizes of ZnO nanoparticles were used as nucleation sites for the hydrothermal growth. During conventional hydrothermal growth ZnO nanowires grow not only on the surface of the substrate, but in the solution as well. This method often leaves debris on the resultant samples, but has the advantage that adding ZnO nanoparticles as growth sites changes the bulk-grown nanostructures greatly. We demonstrate these nanostructures, and discuss possibilities for large scale repeatable growth of such structures.

EXPERIMENTAL

Chemicals and reagents

The zinc nitrate hexahydrate ($Zn(NO_3)_2 \cdot 6H_2O$) and hexamethylenetetramine (HMTA), trisodium citrate ($C_6H_5Na_3O_7$), were all ACS grade and purchased from Sigma-Aldrich (USA). Zinc Oxide Nanoparticles with a nominal size of 10-30 nm were purchased from SkySpring Nanomaterials, Inc. and Zinc Oxide Nanopowder of nominal sizes <50 nm and <100 nm were purchased from Sigma Aldrich. All solvents and materials were employed as purchased without any further purification unless specified.

TEM of the nanoparticles was performed. The method followed was: a small amount of nanoparticles as purchased were mixed with ethanol and actively sonicated to separate bundled particles. A TEM copper mesh was dipped in the solution and dried. TEM was performed on this grid.

ZnO nanostructures growth

ZnO nanostructures were grown using the conventional hydrothermal method. 25 mM L^{-1} of zinc nitrate and hexamine solutions in deionized water (DIW) at 80°C were used as the growth solution. Different amounts of sodium citrate solution in DIW were added into selected samples, as specified.

ZnO nanoparticles in amount of 20-30 mg were vigorously sonicated in 1 mL of DIW to effectively separate and unclog them and were added to the growth solution. They acted as nucleation sites for nanostructure growth.

The solution was kept at 80°C with vigorous stirring for 4 hours and then washed with DIW and ethanol and finally filtered. Samples obtained were studied using SEM technique.

RESULTS AND DISCUSSION

Figure 1a shows a TEM image of as purchased ZnO nanoparticles with nominal size <30 nm. The TEM picture reveals less distribution in size than other samples with nanoparticles size of nearly 200 nm in comparison with the nominal 10-30. Figure 1b shows a TEM image of as purchased ZnO nanoparticles with nominal size <50 nm. ZnO nanoparticles have a large distribution in size and generally are of size much less than 50 nm. Figure 1c shows a TEM image of as purchased ZnO nanoparticles with nominal size <100 nm. ZnO nanoparticles have a

large distribution in size and generally are of size ~100 nm. Insets in Figure 1 show atomic planes of the corresponding particles; the scale bar is 2 nm.

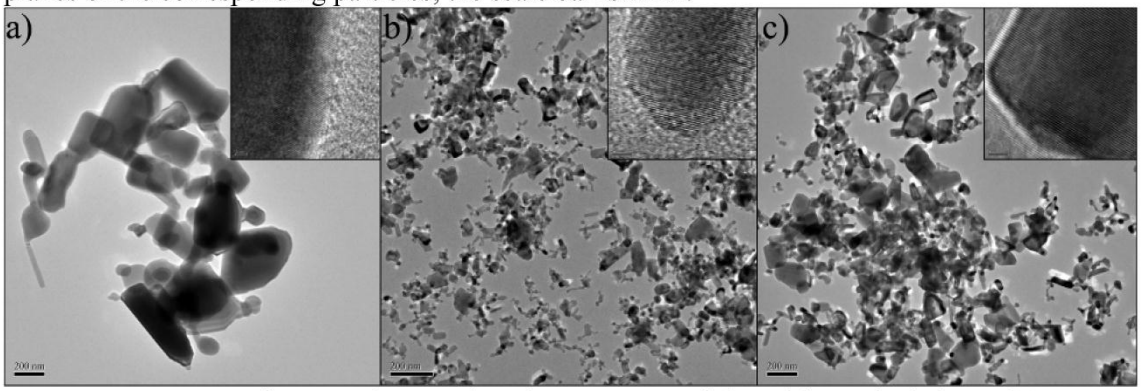

Figure 1. TEM images of as purchased ZnO nanoparticles with nominal sizes of a) 10-30 nm, b) <50 nm, c) <100 nm. Scale bar on the images is 200 nm. Insets: high resolution TEM of atomic planes of the nanoparticles. Scale bar is 2 nm.

Figure 2a shows a TEM image of ZnO nanostructures grown in bulk solution as described before with addition of 2μL of 0.1 mM/L of sodium citrate. Approximately 24 mg of ZnO nanoparticles with nominal size 10-30 nm were added as nucleation seeds. Aster-like shape of resultant ZnO nanostructure has been observed in the image, showing ZnO nanowires growing out of common nucleation site.

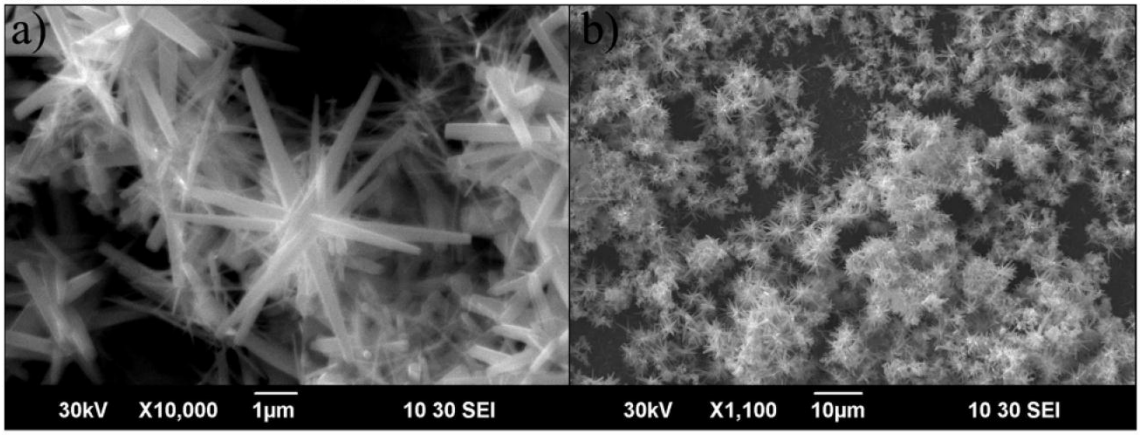

Figure 2. a) SEM image of as grown ZnO aster-like nanostructures with ZnO nanparticles of the nominal size of 10-30 nm acting as nucleation sites, b) Zoomed out SEM image of as grown ZnO aster-like nanostructures with ZnO nanparticles of the nominal size of 10-30 nm acting as nucleation sites. The aster-like structures are the preferable resultant structure with these growth conditions.

A lower magnification image of the same sample is presented in Figure 2b and shows the abundance of aster-like structures in the samples. This indicates that this growth mode is preferable under the present growth conditions.

An SEM image of ZnO aster-like structures grown with ZnO nanoparticles of nominal size of <50 nm are shown in Figure 3a. The nanostructures growth was performed following the

general recipe with no sodium citrate added. 25 mg of ZnO nanoparticles of nominal size <50 nm were used as nucleation sites. Aster-like nanostructures are not as pronounced as structures with 30 nm ZnO nanoparticles nucleation, but are in abundance as shown in Figure 3a.

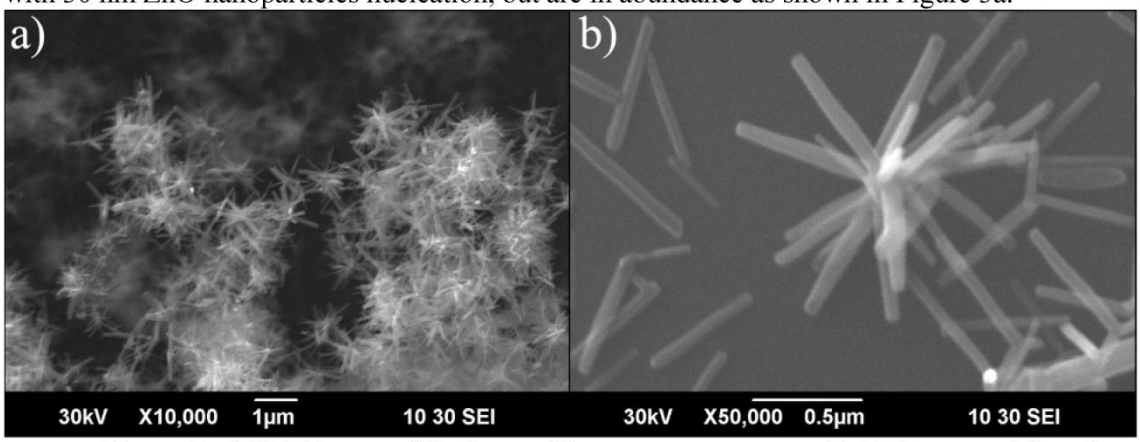

Figure 3. a) SEM image of ZnO aster-like structures grown with ZnO nanparticles of nominal size of <50 nm, b) SEM image of ZnO aster-like structures grown with ZnO nanoparticles of nominal size of <100 nm.

Figure 3b shows ZnO nanostructures grown with the same general recipe, with no sodium citrate added. 27 mg ZnO nanoparticles of <100 nm nominal size were added as nucleation sites in this growth. Although aster-like nanostructures have been observed, the resultant nanostructures are in mass plain ZnO nanowires.

Also performed was a series of experiments in which higher concentrations of sodium citrate, which acts as surfactant agent, were used. Here aster-like structures were not observed in any sample, as can be seen in Figure 4. Instead, rod-like nanowires of increased size (with addition of 20 μL of 10 mM/L sodium citrate) were obtained. The use of even larger concentrations of the surfactant (addition of 2 mL of 10 mM/L of sodium citrate) somewhat cubic-like structures resulted (Figure 4b).

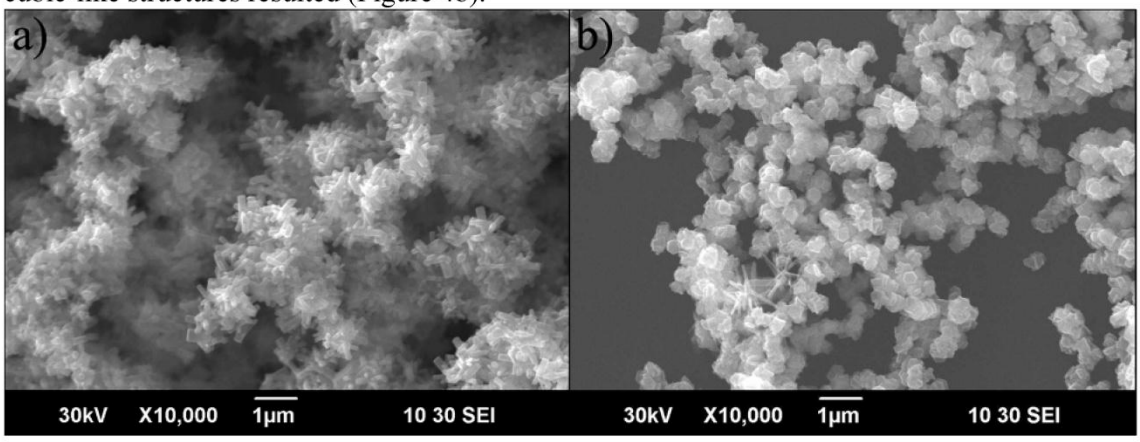

Figure 4. SEM image of ZnO nanostructures grown following general recipe with addition of a) 20 μL of 10 mM/L of sodium citrate per 250 mL of growth solution and b) 2 mL of 10 mM/L of sodium citrate per 250 mL of growth solution.

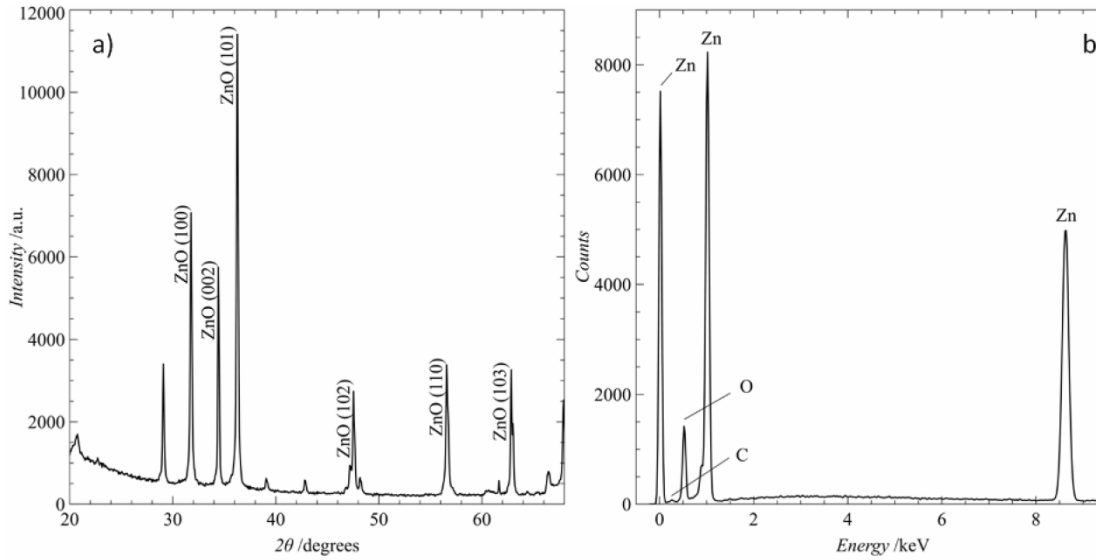

Figure 5. Typical a) XRD spectra and b) EDS spectra of ZnO nanostructures grown following general recipe. Nanostructures were diluted in ethanol, dropcasted on Si substrate and dried for XRD and EDS measurements.

X-ray diffraction (XRD) and Energy-dispersive X-ray spectroscopy (EDS) measurements were also performed to characterize obtained ZnO nanostructures. Figures 5a and 5b show typical XRD and EDS spectra, respectively. In XRD measurements obtained peaks at 31.77°, 34.43°, 36.26°, 47.55°, 56.61° and 62.87° correspond to hexagonal ZnO structure with crystallographic (100), (002), (101), (102), (110) and (103) directions, respectively. EDS measurements reveal that sample generally contains the atomic ratio 35.7% and 53.76% of zinc and oxygen, respectively. Higher atomic percent of oxygen is not uncommon for metal oxides. Meanwhile, EDS measurements support the proper identification of peaks in XRD spectra of ZnO nanostructures.

CONCLUSION

Conventional hydrothermal growth with addition of ZnO nanoparticles as nucleation sites could be used for growth of aster-like nanostructures. Care should be taken regarding the size and quality of nanoparticles. Uniformly sized seeding particles with lateral dimensions of ~200 nm should be used as nucleation sites. In this study the best results were obtained using nanoparticles with nominal size of 10-30 nm.

REFERENCES

1. L. E. Greene, M. Law, J. Goldberger, F. Kim, J. C. Johnson, Y. Zhang, R. J. Saykally and P. Yang, Angew. Chem. Int. Ed. **42** (26), 3031-3034 (2003).
2. Z. K. Tang, G. K. L. Wong, P. Yu, M. Kawasaki, A. Ohtomo, H. Koinuma and Y. Segawa, Appl. Phys. Lett. **72** (25), 3270-3270 (1998).
3. C. H. Liu, J. A. Zapien, Y. Yao, X. M. Meng, C. S. Lee, S. S. Fan, Y. Lifshitz and S. T. Lee, Adv. Mater. (Weinheim, Ger.) **15** (10), 838-841 (2003).

Appendix B (Continued)

4. Z. Fan, D. Wang, P.-C. Chang, W.-Y. Tseng and J. G. Lu, Appl. Phys. Lett. **85** (24), 5923-5923 (2004).
5. Q. Wan, Q. H. Li, Y. J. Chen, T. H. Wang, X. L. He, J. P. Li and C. L. Lin, Appl. Phys. Lett. **84** (18), 3654-3654 (2004).
6. WangWang, J. Zhou, Song, J. Liu, N. Xu and Z. L. Wang, Nano Lett. **6** (12), 2768-2772 (2006).
7. M.-P. Lu, J. Song, M.-Y. Lu, M.-T. Chen, Y. Gao, L.-J. Chen and Z. L. Wang, Nano Lett. **9** (3), 1223-1227 (2009).
8. X. Wang, J. Song, J. Liu and Z. L. Wang, Science **316** (5821), 102-105 (2007).
9. Z. L. Wang and J. Song, Science **312** (5771), 242-246 (2006).
10. Z. Li, R. Yang, M. Yu, F. Bai, C. Li and Z. L. Wang, The Journal of Physical Chemistry C **112** (51), 20114-20117 (2008).
11. J. Zhou, N. S. Xu and Z. L. Wang, Adv. Mater. (Weinheim, Ger.) **18** (18), 2432-2435 (2006).
12. P.-C. Chang, Z. Fan, D. Wang, W.-Y. Tseng, W.-A. Chiou, J. Hong and J. G. Lu, Chem. Mater. **16** (24), 5133-5137 (2004).
13. W. Lee, M.-C. Jeong and J.-M. Myoung, Acta Mater. **52** (13), 3949-3957 (2004).
14. W. I. Park, D. H. Kim, S. W. Jung and G.-C. Yi, Appl. Phys. Lett. **80** (22), 4232-4232 (2002).
15. Y. Zhang, R. E. Russo and S. S. Mao, Appl. Phys. Lett. **87** (13), 133115-133115 (2005).
16. S. C. Lyu, Y. Zhang, C. J. Lee, H. Ruh and H. J. Lee, Chem. Mater. **15** (17), 3294-3299 (2003).
17. M. H. Huang, Y. Wu, H. Feick, N. Tran, E. Weber and P. Yang, Adv. Mater. (Weinheim, Ger.) **13** (2), 113-116 (2001).
18. L. E. Greene, M. Law, D. H. Tan, M. Montano, J. Goldberger, G. Somorjai and P. Yang, Nano Lett. **5** (7), 1231-1236 (2005).
19. Y. F. Hsu, Y. Y. Xi, K. H. Tam, A. B. Djurišić, J. Luo, C. C. Ling, C. K. Cheung, A. M. C. Ng, W. K. Chan, X. Deng, C. D. Beling, S. Fung, K. W. Cheah, P. W. K. Fong and C. C. Surya, Adv. Funct. Mater. **18** (7), 1020-1030 (2008).

Appendix C: Structure and Opto-electrochemical Properties of ZnO Nanowires Grown on *n*-Si Substrate

In this appendix, we present the final version of manuscript titled "Structure and Opto-electrochemical Properties of ZnO Nanowires Grown on *n*-Si Substrate" published in Langmuir by ACS Publications. All the co-authors have authorized the inclusion of this document in the dissertation. Reprinted (adapted) with permission from M. Ladanov, M. K. Ram, G. Matthews, and A. Kumar, Langmuir, **27**, 9012 (2011). Copyright (2011) American Chemical Society. The license to use this document is included in Appendix D: Copyright Permissions.

Langmuir

ARTICLE

pubs.acs.org/Langmuir

Structure and Opto-electrochemical Properties of ZnO Nanowires Grown on *n*-Si Substrate

Mikhail Ladanov,[†,‡,∥] Manoj K. Ram,[*,‡] Garrett Matthews,[§] and Ashok Kumar[‡,∥]

[†]Department of Electrical Engineering, University of South Florida, Tampa, Florida 33620, United States

[‡]Nanotechnology Research and Education Center, University of South Florida, Tampa, Florida 33620, United States

[§]Department of Physics, University of South Florida, Tampa, Florida 33620, United States

[∥]Department of Mechanical Engineering, University of South Florida, Tampa, Florida 33620, United States

ABSTRACT: Zinc oxide (ZnO) nanostructures have attracted great attention as a promising functional material with unique properties suitable for applications in UV lasers, light emitting diodes, field emission devices, sensors, field effect transistors, and solar cells. In the present work, ZnO nanowires have been synthesized on an *n*-type Si substrate using a hydrothermal method where surfactant acted as a modifying and protecting agent. The surface morphology, electrochemical properties, and opto-electrochemical properties of ZnO nanowires are investigated by using scanning electron microscopy (SEM), energy dispersive X-ray spectroscopy (EDS), cyclic voltammetry, and impedance spectroscopy techniques. The cycling characteristics and rate capability of the ZnO nanowires are explored through electrochemical studies performed under varying electrolytes. The photo response is observed using UV radiation. It is demonstrated that crystallinity, particle size, and morphology all play significant roles in the electrochemical performance of the ZnO electrodes.

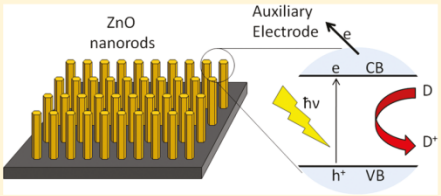

1. INTRODUCTION

Zinc oxide (ZnO) is a II−VI semiconductor with a wide direct band gap of 3.37 eV at 300 K and large exciton binding energy (60 meV). Its nanostructures have attracted great attention as a promising functional material. The unique properties of nanostructured ZnO make it suitable for applications in UV lasers,[1,2] light emitting diodes,[3] electrochromic and field emission devices,[4] sensors,[5−7] field effect transistors,[6−8] nanogenerators actuated by atomic force microscopy (AFM) tips[9,10] or driven by ultrasonic waves,[11] and solar cells.[12]

Among the various ZnO nanostructures, well-aligned nanowire arrays are one of the most promising, and consequently they have been extensively studied.[13,14] Many methods have been used to prepare ZnO nanowire arrays, including chemical vapor deposition (CVD),[6,15] metal−organic chemical vapor deposition (MOCVD),[14,16] pulsed laser deposition (PLD),[17] physical vapor deposition,[16,18] vapor−liquid−solid (VLS) methods[9,19] and the hydrothermal method.[2,20,21] These techniques are well developed and show efficiency and accurate control of the processes as well as the resulting morphology of ZnO nanostructures. Moreover, they are generally inexpensive. However, for practical reasons, fabrication of devices based on ZnO should be relatively simple and straightforward, as well as cost-effective. Therefore, a solution phase approach recently has attracted great attention due to its simplicity compared to other methods, and due to its ability to produce large-scale, low-cost, and controllable growth of one-dimensional ZnO nanocrystals.[2,21,22]

It is known that crystallinity, particle size, and morphology play significant roles in the electrochemical performance of ZnO anode materials. Also, previously it has been demonstrated that controlling the morphologies of transition metal oxides could improve their electrochemical performance such as cycling characteristics and rate capability. However, detailed studies of the structure, the electrochemical and opto-electrochemical properties of ZnO nanowires will improve greatly their applicability in photocell devices. From this point of view, we utilized a conventional hydrothermal method to synthesize ZnO nanowires directly on a conducting Si surface. We used a surfactant as the modifying and protecting agent in this process. As the seeding of ZnO nanocrystals plays an important role in the resulting morphology of ZnO nanostructures,[20] special attention was paid to developing a repeatable and tunable seeding recipe combined with utilization of surfactant agents. This approach led to broad control over the morphology of the ZnO nanostructures produced. The synthesis process did not require high temperature or preformed templates. Thus the advantages of this method for the preparation of ZnO nanowires include its simplicity and mild reaction conditions, as well as its suitability for large-scale preparation of samples with controlled morphologies.

Received: February 15, 2011
Revised: May 23, 2011
Published: June 20, 2011

Appendix C (Continued)

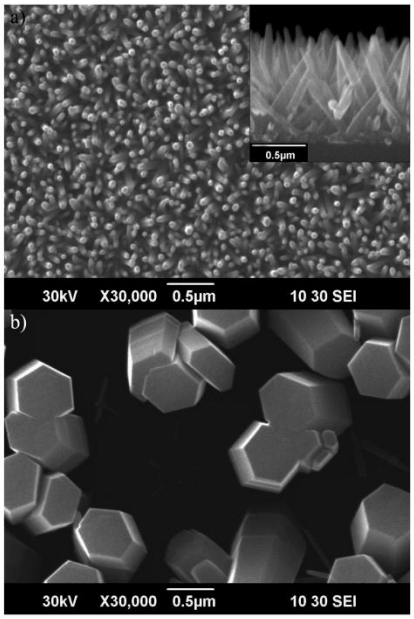

Figure 1. (a) SEM image of the as grown nanowires. Inset: cross section of the sample with nanowires. (b) SEM image of nanowires on the same sample in the transition area between seeded and nonseeded regions. With the same growth conditions, the density of ZnO nanocrystals combined with the surfactant agent plays a significant role in the formation of nanowires.

2. EXPERIMENTAL SECTION

2.1. Reagents and Materials. The nitrate hexahydrate ($Zn(NO_3)_2 \cdot 6H_2O$), hexamethylenetetramine (HMTA), and diethylenetriamine sodium citrate were all ACS grade and purchased from Sigma-Aldrich (U.S.A.). All solvents and materials were employed as purchased without further purification unless specified.

2.2. ZnO Nanowire Growth and Characterization. ZnO nanowires were grown using the conventional hydrothermal method. Twenty-five millimolar zinc nitrate and hexamine solutions in deionized water (DIW) at 80 °C were used as the growth solution. Ten microliters of a 10 mM solution of sodium citrate per 250 mL of growth solution were added.

ZnO nanocrystals on Si substrate acted as a nucleation layer for nanowire growth and were created by the following recipe: 2 mL of 0.5 mM of zinc acetate in ethanol were spun on 2 in. Si substrate at 1000−1200 rpm for 40−50 s. Immediately after ethanol visibly evaporated from the substrate, the substrate was dried by a flow of dry N_2 while spinning to ensure removal of water remnants and achieve uniform seeding. After that, the Si wafer was baked at 350 °C on a hot plate for 30 min.

ZnO nanowires were grown by submerging the seeded *n*-type Si substrates inverted in the growth solution at 80 °C for 2 h. Temperature was controlled by a water circulation system, and the growth solution was constantly stirred.

The average turnover time to refresh the chemical solution in the reactor was 3 to 5 h in order to enhance the growth rate and aspect ratio of the nanowires for a specific growth time. Finally, substrates were removed from the growth solution, rinsed with DIW, and dried under nitrogen flow.

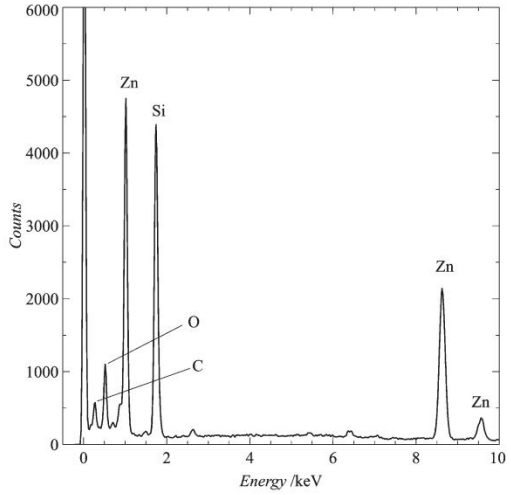

Figure 2. EDS data of the as-grown sample with ZnO nanowires. Zn, O, Si, and C peaks are present.

The basic reaction responsible for the growth of nanowires from solution is described as follows:

Decomposition reaction:

$$(CH_2)_6N_4 + 6H_2O \rightarrow 6HCHO + 4NH_3$$

Hydroxyl supply reaction:

$$NH_3 + H_2O \leftrightarrow NH_4^+ + OH^-$$

Supersaturation reaction:

$$2OH^- + Zn^{+2} \rightarrow Zn(OH)_2$$

ZnO nanowires growth reaction:

$$Zn(OH)_2 \rightarrow ZnO + H_2O$$

2.3. Surface/Structure Characterization. The surface morphology of ZnO nanowires was investigated by scanning electron microscopy (SEM) to determine their size, shape, and density. X-ray diffraction (XRD) of the samples was used to demonstrate the crystallinity of the nanowires and preferred crystal orientation. Energy dispersive X-ray spectroscopy (EDS) was used to determine the chemical composition of the obtained structures.

2.4. Electrochemical Measurements/Photo-electrochemical Response Setup. The electrochemical and photochemical measurements were carried out using a Potentiostat/Galvanostat (Voltalab). A standard three electrode configuration was employed, where the *n*-Si/ZnO nanowires acted as the working electrode, a platinum wire acted as the counter electrode, and Ag/AgCl acted as the reference electrode. The electrochemical studies were performed in 0.05 mM HCl, 0.01 M NaOH in DIW and 0.1 M $LiClO_4$ in acetonitrile electrolytes. UV light with maximum intensity at 366 nm was used to illuminate the sample from 2 to 3 cm away from the working electrode. The power supplied to the UV light were controlled manually.

3. RESULTS AND DISCUSSION

3.1. Structural Studies. The SEM studies indicated that the morphology of the ZnO nanowires produced by this method was not homogeneous across the surface of the silicon substrate.

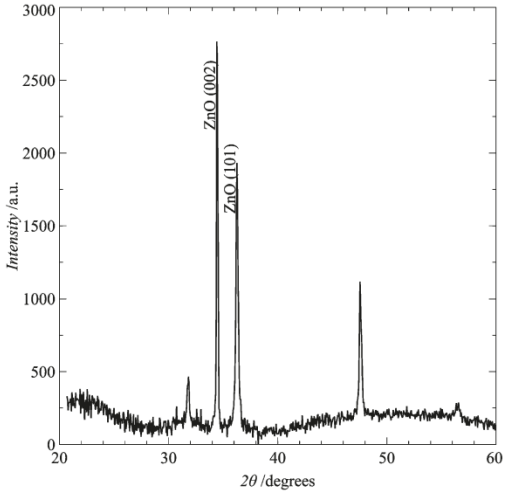

Figure 3. XRD data of the as-grown sample, revealing the crystalline structure of ZnO nanowires. Pronounced (002) peak suggests dominating vertical alignment of nanowires.

One can clearly distinguish areas with the same seeding as the developed recipe as well as areas with no seeding at all (no ZnO NW observed). Figure 1a shows a top-down image of the ZnO nanowires grown in a densely seeded region. The diameter of the nanowires in this region was ~50−100 nm, with clear hexagonal structure. Also shown in Figure 1a is an SEM image of the cross-section (see inset), revealing that the orientation of the nanowires was predominately vertical. The length of these nanowires was approximately 1 μm for a 2 h growth period, as described in the Experimental Section. In the region transitioning from dense seeding to minimal seeding, the morphology of the nanowires changes. Figure 1b shows an SEM image taken from the same sample, but near the edge of the seeded area. The ZnO nanowires grown in this region had several times larger diameters and again showed clear hexagonal structure. Moreover, the density of the nanowires was much lower. Apparently, the density of ZnO microcrystals that served as the seeding layer was diminished. This change in density resulted in ZnO nanowires being grown under different conditions from those shown in Figure 1a, even though the growth solution, temperature, and time were identical. It has been shown previously that, even with the same growth conditions, the morphology of nanowires is dependent upon the seeding method.[20] Thus, we have shown that ZnO growth primarily was controlled by the density and the quality (i.e., grain size, thickness of film and\or crystallographic orientation) of seeded ZnO nanocrystals.

EDS of ZnO nanowires grown on *n*-Si was performed, and the resulting spectrographic data is shown in Figure 2. EDS determines the composition of the synthesized ZnO nanostructures, and the results reveal that the nanostructure was composed of Zn, O, C, and Si. Quantitative EDS analysis showed that the element weight ratio of Zn to O was about 1:1. The presence of C can be understood as the residue left from the organic solvent used in preparation of the ZnO nanowires. The presence of the Si peak in the EDS pattern can be assigned to the Si substrate.

Figure 3 shows the XRD patterns of the substrate coated with ZnO nanowires. Four peaks were pronounced for the ZnO

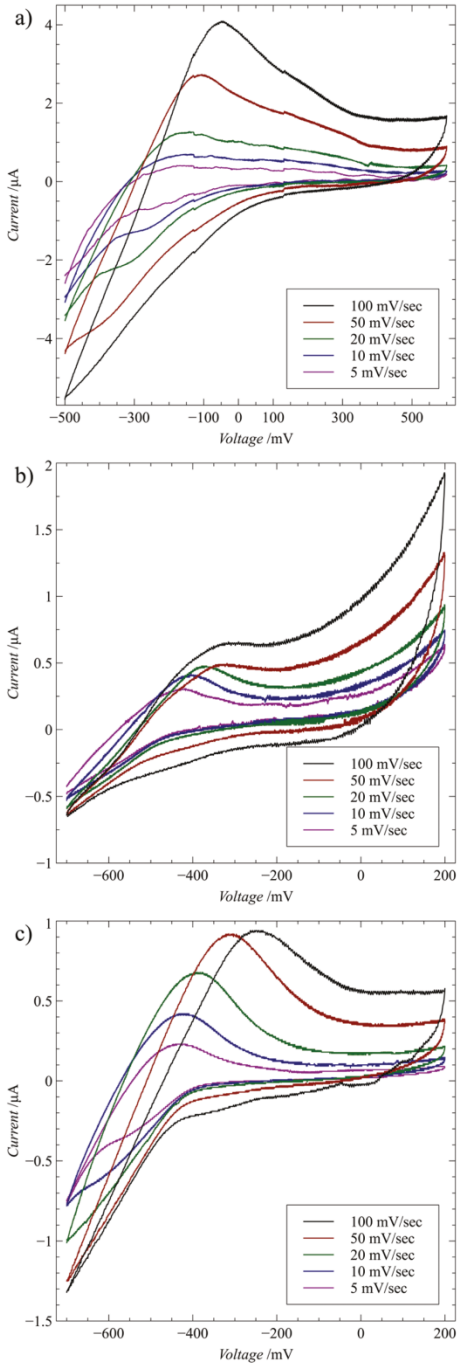

Figure 4. CVs at different scanning speeds for (a) $LiClO_4$, (b) NaOH, and (c) HCl electrolytes.

diffraction pattern: (100), (002), (001) and (102) appear at $2\theta = 31.7°$, 34.4°, 36.3° and 47.5°, respectively. As expected, the

dx.doi.org/10.1021/la200584j |*Langmuir* 2011, 27, 9012–9017

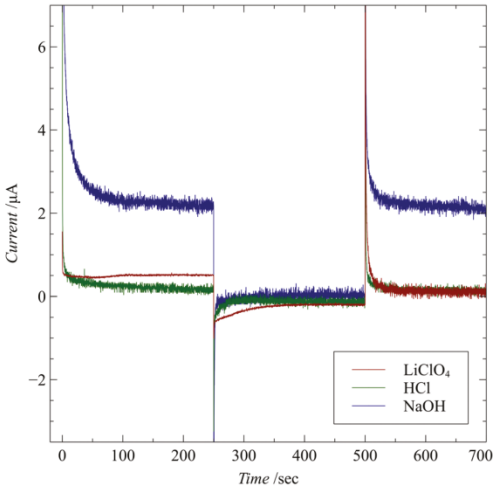

Figure 5. Chronoamperometry for $LiClO_4$, NaOH, and HCl electrolytes.

ZnO nanowires in the sample showed a dominate diffraction peak for (002), indicating a high degree of orientation with the *c*-axis vertical to the substrate surface. The XRD results suggest that our sample was highly crystallized wurtzite type.

3.2. Electrochemical Study. In order to explore their possible application, the electrocatalytic performance of the as-prepared ZnO nanowires on doped silicon substrate was characterized. An *n*-Si substrate covered with ZnO nanowires was used as a working electrode, platinum was used as a counter electrode, and Ag/AgCl was used as a reference electrode in the presence of different electrolytic solutions. Figure 4a shows cyclic voltammograms (CVs) of the ZnO array electrode in 0.1 M $LiClO_4$ solution as a function of the scan rate. The CV showed a pair of well-defined redox peaks for ZnO nanowires. The oxidation of the ZnO nanowires was around 0.2 V, whereas the reduction peak was observed at around −0.4 V vs Ag/AgCl. These results imply that the ZnO arrays demonstrate electrocatalytic activity to oxidation in the presence of the $LiClO_4$ electrolyte. The cathodic reduction peak at −0.4 V can be assigned to the reduction of ZnO into Zn. ZnO showed the classical reduction−oxidation behavior of metallic Zinc in ZnO nanorods. There is an increase in the current density due to reduction of Zn^{2+} to Zn, which was accomplished with a hysteresis effect, followed by an anodic peak close to 0.2 V during the reverse scan. Figure 4b shows the CVs of the ZnO array electrode in 0.01 M NaOH solution as a function of the scan rate. The CVs of ZnO in 0.01 M NaOH generally were used to understand the charge capacity of ZnO. The results revealed interesting CV properties in the oxidation potential at around −0.33 V, and the peak decreased as the scan rate decreased. The reduction potential was not as sharp as was observed for the oxidation potential. Figure 4c shows CVs of the ZnO array electrode in 0.5 mM HCl solution as a function of the scan rate. This figure shows the oxidation peak at around −200 mV at 100 mV/s. Interestingly, the oxidation peak was found to shift toward more negative potential as a function of scan rate. The observed shift in redox potential was negative due to the slow kinetics of ZnO reduction. The kinetics of ZnO decreased as a function of scan rate. In the reduction of ZnO electrode, the diffusion coefficient also changed in different solutions. The CVs

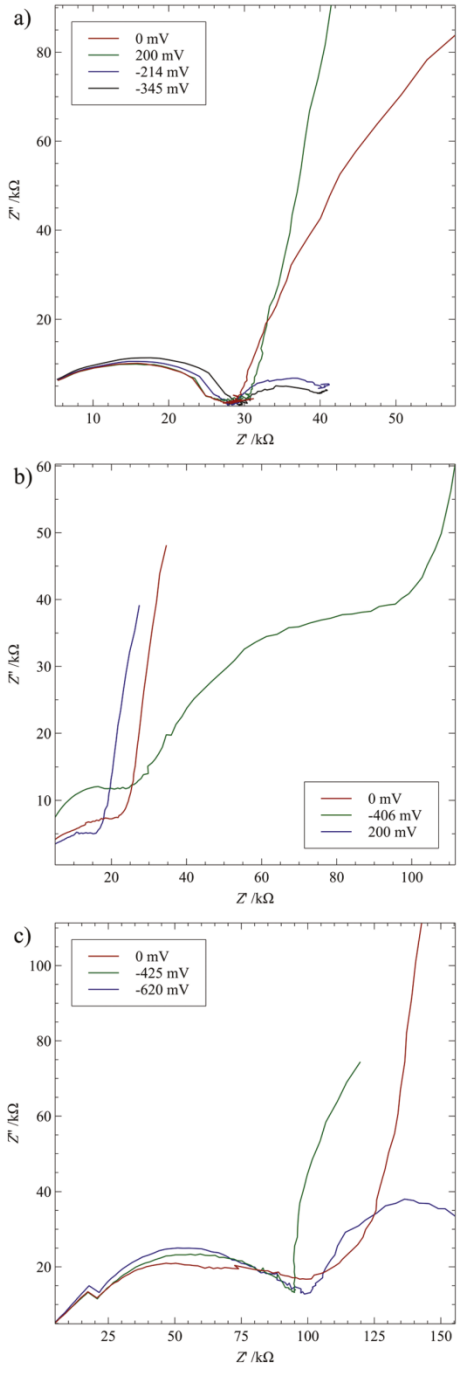

Figure 6. Nyquist plot of samples with ZnO nanowires in (a) $LiClO_4$, (b) NaOH, and (c) HCl electrolytes.

of ZnO nanowires in different electrolytes show the hysteretic characteristics of electron accumulation and discharge in ZnO

dx.doi.org/10.1021/la200584j |*Langmuir* 2011, 27, 9012–9017

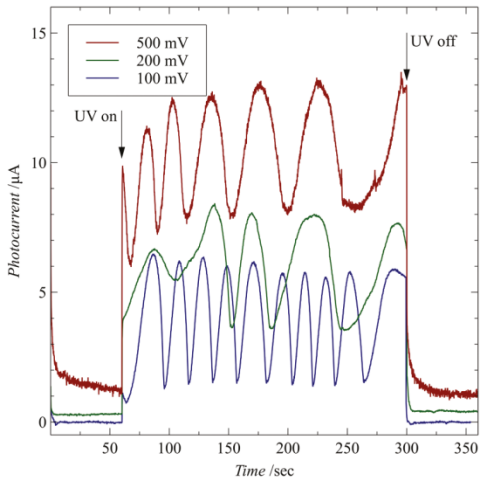

Figure 7. Photocurrent response to UV light at different DC biases.

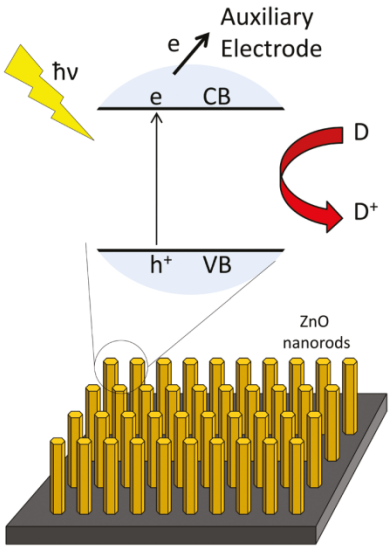

Figure 8. Schematics of electrochemical processes on the surface of the sample.

nanowires superimposed upon the Faradic current due to the electrolytes. The voltammogram is also completely dependent upon the scan rate. A similar effect was observed for the reduction peak shifting toward more negative potential as a function of scan rate. The reverse scan gives the corresponding cathodic peak, and the anodic peak was well-defined for the repeated scans. The CV measurements shown in Figure 4a,b,c are indicative of an electrochemical diffusion controlled system. Thus, the observed oxidation was totally reversible.

Figure 5 represents chronoamperometric studies, where the potential was varied from −0.2 to 0.5 V vs Ag/AgCl in three different electrolytic systems. The current transient was recorded for the oxidation and reduction potentials. The chronoamperometry study serves as an alternative probe of electron occupancy in ZnO NWs film. The oxidation shows higher current and faster response than the reduction system. A similar effect was observed in Figure 4 for the CV studies. The reduction and oxidation showed a sharp transition as shown in Figure 5. The transient current exhibited a "fast" phase in ZnO NWs, which was complete within 1 s at the applied negative potential.

Electrochemical impedance spectroscopy (EIS), which provides information regarding the resistance and capacitance of the electrode materials, is an effective approach for investigating electron transfer across the electrolyte and the surface of the electrode. Figure 6a shows the typical impedance spectra of the ZnO nanowire electrode in 0.1 M LiClO4 solution at an AC frequency varying from 100 kHz to 0.1 Hz. The ZnO electrode displayed semicircles at the high-frequency region and a straight line at the low-frequency region, indicating that the electrochemical reaction at the ZnO electrode was controlled by a mixed process of charge transfer and diffusion limitation. A similar effect was demonstrated in Figure 6b,c in 0.01 M NaOH and 0.5 mM HCl electrolytes, respectively.

3.3. Photoelectrochemical Current. Figure 7 shows the response of photopotential of the ZnO nanowire electrode under UV irradiation. When the UV-light was switched on, an electron−hole pair was generated showing the photocurrent. The initial charge separation competes with recombination, so both processes have to take place on the same time scale. The net transport through the electrode was divided into two subsequent processes: one process was charge transport through the nonilluminated part of the ZnO, and the other process was transport through the *n*-Si substrate to the back contact. The UV irradiation changed the current abruptly with little variation, and returns to the initial value after the light is switched off. In addition, it also was noticed that the photopotential sharply reverted when the light was switched off. Although recombination of photogenerated carriers occurred in the ZnO under dark conditions, it was restrained effectively by the internal electrostatic field in the junction region. The separated electrons migrated easily to the external circuit. However, it is well established that liquid electrolytes create Schottky junctions when brought into contact with ZnO. We have tried to understand the junction between the liquid electrolyte and ZnO rather than *n*-silicon and *n*-type ZnO.

The electron transfer process in the ZnO electrochemical set up is similar to that in a semiconductor−metal composite. The electrons in the valence band of ZnO were excited to its conduction band, giving rise to the formation of an electron−hole pair, as shown in the schematic in Figure 8. The UV irradiation caused a rise in the transient photocurrent followed by an exponential decay after the UV light was switched off.

4. CONCLUSION

The growth of ZnO was primarily controlled by the density of seeded ZnO nanocrystals. The electrochemical studies at various electrolytes showed the cycling characteristics and the rate capability of ZnO nanowires. It was established that crystallinity, particle size, and morphology play significant roles in the electrochemical performance of the ZnO nanowire electrode. The electrochemical study also indicated that ZnO nanowires were able to be doped with ions, and the process was reversible. The photoelectrochemical current was observed by illumination with UV-light in an electrochemical cell where ZnO acted as the

working electrode in electrolytic media. The detailed structure, electrochemical, and opto-electrochemical studies on ZnO nanowires could provide for their application in photocells and photosensors.

AUTHOR INFORMATION

Corresponding Author
*E-mail: mkram@usf.edu.

ACKNOWLEDGMENT

This research was partially supported by NSF Grant #0854023.

REFERENCES

(1) Tang, Z. K.; Wong, G. K. L.; Yu, P.; Kawasaki, M.; Ohtomo, A.; Koinuma, H.; Segawa, Y. Room-temperature ultraviolet laser emission from self-assembled ZnO microcrystallite thin films. *Appl. Phys. Lett.* **1998**, *72* (25), 3270–3270.

(2) Greene, L. E.; Law, M.; Goldberger, J.; Kim, F.; Johnson, J. C.; Zhang, Y.; Saykally, R. J.; Yang, P. Low-temperature wafer-scale production of ZnO nanowire arrays. *Angew. Chem., Int. Ed.* **2003**, *42* (26), 3031–3034.

(3) Liu, C. H.; Zapien, J. A.; Yao, Y.; Meng, X. M.; Lee, C. S.; Fan, S. S.; Lifshitz, Y.; Lee, S. T. High-density, ordered ultraviolet light-emitting ZnO nanowire arrays. *Adv. Mater. (Weinheim, Ger.)* **2003**, *15* (10), 838–841.

(4) Li, S. Y.; Lee, C. Y.; Lin, P.; Tseng, T. Y. Gate-controlled ZnO nanowires for field-emission device application. *J. Vac. Sci. Technol. B* **2006**, *24* (1), 147–147.

(5) Wan, Q.; Li, Q. H.; Chen, Y. J.; Wang, T. H.; He, X. L.; Li, J. P.; Lin, C. L. Fabrication and ethanol sensing characteristics of ZnO nanowire gas sensors. *Appl. Phys. Lett.* **2004**, *84* (18), 3654–3654.

(6) Fan, Z.; Wang, D.; Chang, P.-C.; Tseng, W.-Y.; Lu, J. G. ZnO nanowire field-effect transistor and oxygen sensing property. *Appl. Phys. Lett.* **2004**, *85* (24), 5923–5923.

(7) Wang, Wang; Zhou, J.; Song; Liu, J.; Xu, N.; Wang, Z. L. Piezoelectric Field Effect Transistor and Nanoforce Sensor Based on a Single ZnO Nanowire. *Nano Lett.* **2006**, *6* (12), 2768–2772.

(8) Arnold, M. S.; Avouris, P.; Pan, Z. W.; Wang, Z. L. Field-Effect Transistors Based on Single Semiconducting Oxide Nanobelts. *J. Phys. Chem. B* **2003**, *107* (3), 659–663.

(9) Wang, Z. L.; Song, J. Piezoelectric Nanogenerators Based on Zinc Oxide Nanowire Arrays. *Science* **2006**, *312* (5771), 242–246.

(10) Lu, M.-P.; Song, J.; Lu, M.-Y.; Chen, M.-T.; Gao, Y.; Chen, L.-J.; Wang, Z. L. Piezoelectric Nanogenerator Using p-Type ZnO Nanowire Arrays. *Nano Lett.* **2009**, *9* (3), 1223–1227.

(11) Wang, X.; Song, J.; Liu, J.; Wang, Z. L. Direct-current nanogenerator driven by ultrasonic waves. *Science* **2007**, *316* (5821), 102–105.

(12) Law, M.; Greene, L. E.; Johnson, J. C.; Saykally, R.; Yang, P. Nanowire dye-sensitized solar cells. *Nat. Mater.* **2005**, *4* (6), 455–459.

(13) Lee, C. J.; Lee, T. J.; Lyu, S. C.; Zhang, Y.; Ruh, H.; Lee, H. J. Field emission from well-aligned zinc oxide nanowires grown at low temperature. *Appl. Phys. Lett.* **2002**, *81* (19), 3648–3648.

(14) Park, W. I.; Kim, D. H.; Jung, S. W.; Yi, G.-C. Metalorganic vapor-phase epitaxial growth of vertically well-aligned ZnO nanorods. *Appl. Phys. Lett.* **2002**, *80* (22), 4232–4232.

(15) Chang, P.-C.; Fan, Z.; Wang, D.; Tseng, W.-Y.; Chiou, W.-A.; Hong, J.; Lu, J. G. ZnO nanowires synthesized by vapor trapping CVD method. *Chem. Mater.* **2004**, *16* (24), 5133–5137.

(16) Lee, W.; Jeong, M.-C.; Myoung, J.-M. Catalyst-free growth of ZnO nanowires by metal−organic chemical vapour deposition (MOCVD) and thermal evaporation. *Acta Mater.* **2004**, *52* (13), 3949–3957.

(17) Zhang, Y.; Russo, R. E.; Mao, S. S. Femtosecond laser assisted growth of ZnO nanowires. *Appl. Phys. Lett.* **2005**, *87* (13), 133115–133115.

(18) Lyu, S. C.; Zhang, Y.; Lee, C. J.; Ruh, H.; Lee, H. J. Low-temperature growth of ZnO nanowire array by a simple physical vapor-deposition method. *Chem. Mater.* **2003**, *15* (17), 3294–3299.

(19) Huang, M. H.; Wu, Y.; Feick, H.; Tran, N.; Weber, E.; Yang, P. Catalytic growth of zinc oxide nanowires by vapor transport. *Adv. Mater. (Weinheim, Ger.)* **2001**, *13* (2), 113–116.

(20) Hsu, Y. F.; Xi, Y. Y.; Tam, K. H.; Djurišić, A. B.; Luo, J.; Ling, C. C.; Cheung, C. K.; Ng, A. M. C.; Chan, W. K.; Deng, X.; Beling, C. D.; Fung, S.; Cheah, K. W.; Fong, P. W. K.; Surya, C. C. Undoped p-type ZnO nanorods synthesized by a hydrothermal method. *Adv. Funct. Mater.* **2008**, *18* (7), 1020–1030.

(21) Greene, L. E.; Law, M.; Tan, D. H.; Montano, M.; Goldberger, J.; Somorjai, G.; Yang, P. General route to vertical ZnO nanowire arrays using textured ZnO seeds. *Nano Lett.* **2005**, *5* (7), 1231–1236.

(22) Vayssieres, L. Growth of arrayed nanorods and nanowires of ZnO from aqueous solutions. *Adv. Mater. (Weinheim, Ger.)* **2003**, *15* (5), 464–466.

Appendix D: Copyright Permissions

Appendix D (Continued)

Copyright Permission for "A Resistless Process for the Production of Patterned, Vertically Aligned ZnO Nanowires"

CAMBRIDGE UNIVERSITY PRESS LICENSE TERMS AND CONDITIONS

Jul 20, 2012

This is a License Agreement between Mikhail Ladanov ("You") and Cambridge University Press ("Cambridge University Press") provided by Copyright Clearance Center ("CCC"). The license consists of your order details, the terms and conditions provided by Cambridge University Press, and the payment terms and conditions.

All payments must be made in full to CCC. For payment instructions, please see information listed at the bottom of this form.

License Number	2953180771670
License date	Jul 20, 2012
Licensed content publisher	Cambridge University Press
Licensed content publication	MRS Online Proceedings Library
Licensed content title	A Resistless Process for the Production of Patterned, Vertically Aligned ZnO Nanowires.
Licensed content author	Mikhail Ladanov, Kranthi Kumar Elineni, Manoj Ram, Nathan D. Gallant, Ashok Kumar and Garrett Matthews
Licensed content date	Jan 1, 2012
Volume number	1302
Issue number	-1
Start page	0
End page	0
Type of Use	Dissertation/Thesis
Requestor type	Author
Portion	Full article
Author of this Cambridge University Press article	Yes
Author / editor of the new work	Yes
Order reference number	
Territory for reuse	North America Only
Title of your thesis / dissertation	ZnO nanostructures for multifunctional application: growth, characterization and device fabrication
Expected completion date	Nov 2012
Estimated size(pages)	150
Billing Type	Invoice
Billing address	[redacted]

Appendix D (Continued)

United States

Customer reference info

Total 0.00 USD

Terms and Conditions

TERMS & CONDITIONS

Cambridge University Press grants the Licensee permission on a non-exclusive non-transferable basis to reproduce, make available or otherwise use the Licensed content 'Content' in the named territory 'Territory' for the purpose listed 'the Use' on Page 1 of this Agreement subject to the following terms and conditions.

1. The License is limited to the permission granted and the Content detailed herein and does not extend to any other permission or content.
2. Cambridge gives no warranty or indemnity in respect of any third-party copyright material included in the Content, for which the Licensee should seek separate permission clearance.
3. The integrity of the Content must be ensured.
4. The License does extend to any edition published specifically for the use of handicapped or reading-impaired individuals.
5. The Licensee shall provide a prominent acknowledgement in the following format: author/s, title of article, name of journal, volume number, issue number, page references, , reproduced with permission.

Other terms and conditions: None

v1.0

If you would like to pay for this license now, please remit this license along with your payment made payable to "COPYRIGHT CLEARANCE CENTER" otherwise you will be invoiced within 48 hours of the license date. Payment should be in the form of a check or money order referencing your account number and this invoice number RLNK500822651.
Once you receive your invoice for this order, you may pay your invoice by credit card. Please follow instructions provided at that time.

Make Payment To:
Copyright Clearance Center
Dept 001
P.O. Box 843006
Boston, MA 02284-3006

For suggestions or comments regarding this order, contact RightsLink Customer Support: customercare@copyright.com or +1-877-622-5543 (toll free in the US) or +1-978-646-2777.

Gratis licenses (referencing $0 in the Total field) are free. Please retain this printable license for your reference. No payment is required.

Appendix D (Continued)

Copyright Permission for "Novel Aster-like ZnO Nanowire Clusters for Nanocomposites"

CAMBRIDGE UNIVERSITY PRESS LICENSE TERMS AND CONDITIONS

Jul 20, 2012

This is a License Agreement between Mikhail Ladanov ("You") and Cambridge University Press ("Cambridge University Press") provided by Copyright Clearance Center ("CCC"). The license consists of your order details, the terms and conditions provided by Cambridge University Press, and the payment terms and conditions.

All payments must be made in full to CCC. For payment instructions, please see information listed at the bottom of this form.

License Number	2953180513397
License date	Jul 20, 2012
Licensed content publisher	Cambridge University Press
Licensed content publication	MRS Online Proceedings Library
Licensed content title	Novel Aster-like ZnO Nanowire Clusters for Nanocomposites
Licensed content author	Mikhail Ladanov, Manoj Ram, Ashok Kumar and Garrett Matthews
Licensed content date	Jan 1, 2011
Volume number	1312
Issue number	-1
Start page	0
End page	0
Type of Use	Dissertation/Thesis
Requestor type	Author
Portion	Full article
Author of this Cambridge University Press article	Yes
Author / editor of the new work	Yes
Order reference number	
Territory for reuse	North America Only
Title of your thesis / dissertation	ZnO nanostructures for multifunctional application: growth, characterization and device fabrication
Expected completion date	Nov 2012
Estimated size(pages)	150
Billing Type	Invoice
Billing address	[redacted]

Customer reference info

Total 0.00 USD

Terms and Conditions

TERMS & CONDITIONS

Cambridge University Press grants the Licensee permission on a non-exclusive non-transferable basis to reproduce, make available or otherwise use the Licensed content 'Content' in the named territory 'Territory' for the purpose listed 'the Use' on Page 1 of this Agreement subject to the following terms and conditions.

1. The License is limited to the permission granted and the Content detailed herein and does not extend to any other permission or content.
2. Cambridge gives no warranty or indemnity in respect of any third-party copyright material included in the Content, for which the Licensee should seek separate permission clearance.
3. The integrity of the Content must be ensured.
4. The License does extend to any edition published specifically for the use of handicapped or reading-impaired individuals.
5. The Licensee shall provide a prominent acknowledgement in the following format: author/s, title of article, name of journal, volume number, issue number, page references, , reproduced with permission.

Other terms and conditions: None

v1.0

If you would like to pay for this license now, please remit this license along with your payment made payable to "COPYRIGHT CLEARANCE CENTER" otherwise you will be invoiced within 48 hours of the license date. Payment should be in the form of a check or money order referencing your account number and this invoice number RLNK500822647.
Once you receive your invoice for this order, you may pay your invoice by credit card. Please follow instructions provided at that time.

Make Payment To:
Copyright Clearance Center
Dept 001
P.O. Box 843006
Boston, MA 02284-3006

For suggestions or comments regarding this order, contact RightsLink Customer Support: customercare@copyright.com or +1-877-622-5543 (toll free in the US) or +1-978-646-2777.

Gratis licenses (referencing $0 in the Total field) are free. Please retain this printable license for your reference. No payment is required.

Appendix D (Continued)

Copyright Permission for "Structure and Opto-electrochemical Properties of ZnO Nanowires Grown on *n*-Si Substrate"

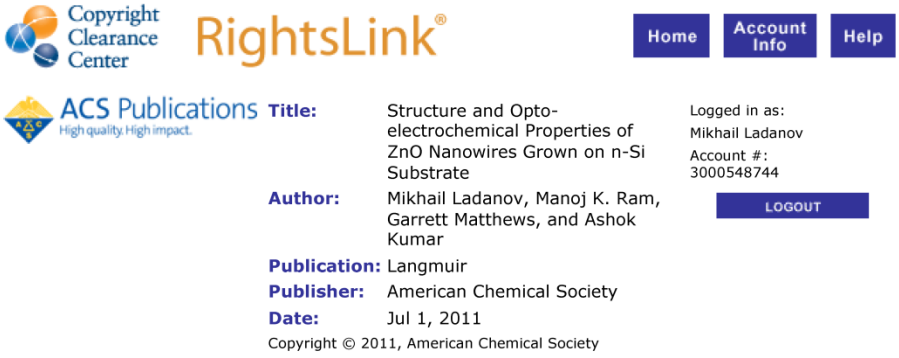

PERMISSION/LICENSE IS GRANTED FOR YOUR ORDER AT NO CHARGE

This type of permission/license, instead of the standard Terms & Conditions, is sent to you because no fee is being charged for your order. Please note the following:

- Permission is granted for your request in both print and electronic formats, and translations.
- If figures and/or tables were requested, they may be adapted or used in part.
- Please print this page for your records and send a copy of it to your publisher/graduate school.
- Appropriate credit for the requested material should be given as follows: "Reprinted (adapted) with permission from (COMPLETE REFERENCE CITATION). Copyright (YEAR) American Chemical Society." Insert appropriate information in place of the capitalized words.
- One-time permission is granted only for the use specified in your request. No additional uses are granted (such as derivative works or other editions). For any other uses, please submit a new request.

BACK CLOSE WINDOW

Appendix D (Continued)

Other Copyright Permissions

ELSEVIER LICENSE
TERMS AND CONDITIONS

Oct 09, 2012

This is a License Agreement between Mikhail Ladanov ("You") and Elsevier ("Elsevier") provided by Copyright Clearance Center ("CCC"). The license consists of your order details, the terms and conditions provided by Elsevier, and the payment terms and conditions.

All payments must be made in full to CCC. For payment instructions, please see information listed at the bottom of this form.

Supplier	Elsevier Limited The Boulevard,Langford Lane Kidlington,Oxford,OX5 1GB,UK
Registered Company Number	1982084
Customer name	Mikhail Ladanov
Customer address	[redacted]
License number	3004990377783
License date	Oct 09, 2012
Licensed content publisher	Elsevier
Licensed content publication	Materials Today
Licensed content title	Nanostructures of zinc oxide
Licensed content author	Zhong Lin Wang
Licensed content date	June 2004
Licensed content volume number	7
Licensed content issue number	6
Number of pages	8
Start Page	26
End Page	33
Type of Use	reuse in a thesis/dissertation
Intended publisher of new work	other
Portion	figures/tables/illustrations
Number of figures/tables/illustrations	1
Format	both print and electronic
Are you the author of this Elsevier article?	No

Will you be translating?	No
Order reference number	
Title of your thesis/dissertation	ZnO nanostructures for multifunctional application: growth, characterization and device fabrication
Expected completion date	Nov 2012
Estimated size (number of pages)	150
Elsevier VAT number	GB 494 6272 12
Permissions price	0.00 USD
VAT/Local Sales Tax	0.0 USD / 0.0 GBP
Total	0.00 USD
Terms and Conditions	

INTRODUCTION

1. The publisher for this copyrighted material is Elsevier. By clicking "accept" in connection with completing this licensing transaction, you agree that the following terms and conditions apply to this transaction (along with the Billing and Payment terms and conditions established by Copyright Clearance Center, Inc. ("CCC"), at the time that you opened your Rightslink account and that are available at any time at http://myaccount.copyright.com).

GENERAL TERMS

2. Elsevier hereby grants you permission to reproduce the aforementioned material subject to the terms and conditions indicated.

3. Acknowledgement: If any part of the material to be used (for example, figures) has appeared in our publication with credit or acknowledgement to another source, permission must also be sought from that source. If such permission is not obtained then that material may not be included in your publication/copies. Suitable acknowledgement to the source must be made, either as a footnote or in a reference list at the end of your publication, as follows:

"Reprinted from Publication title, Vol /edition number, Author(s), Title of article / title of chapter, Pages No., Copyright (Year), with permission from Elsevier [OR APPLICABLE SOCIETY COPYRIGHT OWNER]." Also Lancet special credit - "Reprinted from The Lancet, Vol. number, Author(s), Title of article, Pages No., Copyright (Year), with permission from Elsevier."

4. Reproduction of this material is confined to the purpose and/or media for which permission is hereby given.

5. Altering/Modifying Material: Not Permitted. However figures and illustrations may be altered/adapted minimally to serve your work. Any other abbreviations, additions, deletions and/or any other alterations shall be made only with prior written authorization of Elsevier Ltd. (Please contact Elsevier at permissions@elsevier.com)

6. If the permission fee for the requested use of our material is waived in this instance, please be advised that your future requests for Elsevier materials may attract a fee.

7. Reservation of Rights: Publisher reserves all rights not specifically granted in the combination of (i) the license details provided by you and accepted in the course of this licensing transaction, (ii) these terms and conditions and (iii) CCC's Billing and Payment terms and conditions.

8. License Contingent Upon Payment: While you may exercise the rights licensed immediately upon issuance of the license at the end of the licensing process for the transaction, provided that you have disclosed complete and accurate details of your proposed use, no license is finally effective unless and until full payment is received from you (either by publisher or by CCC) as provided in CCC's Billing and Payment terms and conditions. If full payment is not received on a timely basis, then any license preliminarily granted shall be deemed automatically revoked and shall be void as if never granted. Further, in the event that you breach any of these terms and conditions or any of CCC's Billing and Payment terms and conditions, the license is automatically revoked and shall be void as if never granted. Use of materials as described in a revoked license, as well as any use of the materials beyond the scope of an unrevoked license, may constitute copyright infringement and publisher reserves the right to take any and all action to protect its copyright in the materials.

9. Warranties: Publisher makes no representations or warranties with respect to the licensed material.

10. Indemnity: You hereby indemnify and agree to hold harmless publisher and CCC, and their respective officers, directors, employees and agents, from and against any and all claims arising out of your use of the licensed material other than as specifically authorized pursuant to this license.

11. No Transfer of License: This license is personal to you and may not be sublicensed, assigned, or transferred by you to any other person without publisher's written permission.

12. No Amendment Except in Writing: This license may not be amended except in a writing signed by both parties (or, in the case of publisher, by CCC on publisher's behalf).

13. Objection to Contrary Terms: Publisher hereby objects to any terms contained in any purchase order, acknowledgment, check endorsement or other writing prepared by you, which terms are inconsistent with these terms and conditions or CCC's Billing and Payment terms and conditions. These terms and conditions, together with CCC's Billing and Payment terms and conditions (which are incorporated herein), comprise the entire agreement between you and publisher (and CCC) concerning this licensing transaction. In the event of any conflict between your obligations established by these terms and conditions and those established by CCC's Billing and Payment terms and conditions, these terms and conditions shall control.

14. Revocation: Elsevier or Copyright Clearance Center may deny the permissions described in this License at their sole discretion, for any reason or no reason, with a full refund payable to you. Notice of such denial will be made using the contact information provided by you. Failure to receive such notice will not alter or invalidate the denial. In no event will Elsevier

or Copyright Clearance Center be responsible or liable for any costs, expenses or damage incurred by you as a result of a denial of your permission request, other than a refund of the amount(s) paid by you to Elsevier and/or Copyright Clearance Center for denied permissions.

LIMITED LICENSE

The following terms and conditions apply only to specific license types:

15. **Translation**: This permission is granted for non-exclusive world **English** rights only unless your license was granted for translation rights. If you licensed translation rights you may only translate this content into the languages you requested. A professional translator must perform all translations and reproduce the content word for word preserving the integrity of the article. If this license is to re-use 1 or 2 figures then permission is granted for non-exclusive world rights in all languages.

16. **Website**: The following terms and conditions apply to electronic reserve and author websites:
Electronic reserve: If licensed material is to be posted to website, the web site is to be password-protected and made available only to bona fide students registered on a relevant course if:
This license was made in connection with a course,
This permission is granted for 1 year only. You may obtain a license for future website posting,
All content posted to the web site must maintain the copyright information line on the bottom of each image,
A hyper-text must be included to the Homepage of the journal from which you are licensing at http://www.sciencedirect.com/science/journal/xxxxx or the Elsevier homepage for books at http://www.elsevier.com , and
Central Storage: This license does not include permission for a scanned version of the material to be stored in a central repository such as that provided by Heron/XanEdu.

17. **Author website** for journals with the following additional clauses:

All content posted to the web site must maintain the copyright information line on the bottom of each image, and the permission granted is limited to the personal version of your paper. You are not allowed to download and post the published electronic version of your article (whether PDF or HTML, proof or final version), nor may you scan the printed edition to create an electronic version. A hyper-text must be included to the Homepage of the journal from which you are licensing at http://www.sciencedirect.com/science/journal/xxxxx . As part of our normal production process, you will receive an e-mail notice when your article appears on Elsevier's online service ScienceDirect (www.sciencedirect.com). That e-mail will include the article's Digital Object Identifier (DOI). This number provides the electronic link to the published article and should be included in the posting of your personal version. We ask that you wait until you receive this e-mail and have the DOI to do any posting.

Central Storage: This license does not include permission for a scanned version of the material to be stored in a central repository such as that provided by Heron/XanEdu.

18. **Author website** for books with the following additional clauses:
Authors are permitted to place a brief summary of their work online only.
A hyper-text must be included to the Elsevier homepage at http://www.elsevier.com . All content posted to the web site must maintain the copyright information line on the bottom of each image. You are not allowed to download and post the published electronic version of your chapter, nor may you scan the printed edition to create an electronic version.

Central Storage: This license does not include permission for a scanned version of the material to be stored in a central repository such as that provided by Heron/XanEdu.

19. **Website** (regular and for author): A hyper-text must be included to the Homepage of the journal from which you are licensing at http://www.sciencedirect.com/science/journal/xxxxx. or for books to the Elsevier homepage at http://www.elsevier.com

20. **Thesis/Dissertation**: If your license is for use in a thesis/dissertation your thesis may be submitted to your institution in either print or electronic form. Should your thesis be published commercially, please reapply for permission. These requirements include permission for the Library and Archives of Canada to supply single copies, on demand, of the complete thesis and include permission for UMI to supply single copies, on demand, of the complete thesis. Should your thesis be published commercially, please reapply for permission.

21. **Other Conditions**:

v1.6

If you would like to pay for this license now, please remit this license along with your payment made payable to "COPYRIGHT CLEARANCE CENTER" otherwise you will be invoiced within 48 hours of the license date. Payment should be in the form of a check or money order referencing your account number and this invoice number RLNK500873766.
Once you receive your invoice for this order, you may pay your invoice by credit card. Please follow instructions provided at that time.

Make Payment To:
Copyright Clearance Center
Dept 001
P.O. Box 843006
Boston, MA 02284-3006

For suggestions or comments regarding this order, contact RightsLink Customer Support: customercare@copyright.com or +1-877-622-5543 (toll free in the US) or +1-978-646-2777.

Gratis licenses (referencing $0 in the Total field) are free. Please retain this printable license for your reference. No payment is required.

Appendix D (Continued)

ELSEVIER LICENSE
TERMS AND CONDITIONS

Oct 16, 2012

This is a License Agreement between Mikhail Ladanov ("You") and Elsevier ("Elsevier") provided by Copyright Clearance Center ("CCC"). The license consists of your order details, the terms and conditions provided by Elsevier, and the payment terms and conditions.

All payments must be made in full to CCC. For payment instructions, please see information listed at the bottom of this form.

Supplier	Elsevier Limited The Boulevard,Langford Lane Kidlington,Oxford,OX5 1GB,UK
Registered Company Number	1982084
Customer name	Mikhail Ladanov
Customer address	[redacted]
License number	3011040272064
License date	Oct 16, 2012
Licensed content publisher	Elsevier
Licensed content publication	Materials Science and Engineering: R: Reports
Licensed content title	ZnO nanowire and nanobelt platform for nanotechnology
Licensed content author	Zhong Lin Wang
Licensed content date	3 April 2009
Licensed content volume number	64
Licensed content issue number	3–4
Number of pages	39
Start Page	33
End Page	71
Type of Use	reuse in a thesis/dissertation
Intended publisher of new work	other
Portion	figures/tables/illustrations
Number of figures/tables /illustrations	3
Format	both print and electronic
Are you the author of this Elsevier article?	No
Will you be translating?	No
Order reference number	

Appendix D (Continued)

Title of your thesis/dissertation	ZnO nanostructures for multifunctional application: growth, characterization and device fabrication
Expected completion date	Nov 2012
Estimated size (number of pages)	150
Elsevier VAT number	GB 494 6272 12
Permissions price	0.00 USD
VAT/Local Sales Tax	0.0 USD / 0.0 GBP
Total	0.00 USD
Terms and Conditions	

INTRODUCTION

1. The publisher for this copyrighted material is Elsevier. By clicking "accept" in connection with completing this licensing transaction, you agree that the following terms and conditions apply to this transaction (along with the Billing and Payment terms and conditions established by Copyright Clearance Center, Inc. ("CCC"), at the time that you opened your Rightslink account and that are available at any time at http://myaccount.copyright.com).

GENERAL TERMS

2. Elsevier hereby grants you permission to reproduce the aforementioned material subject to the terms and conditions indicated.

3. Acknowledgement: If any part of the material to be used (for example, figures) has appeared in our publication with credit or acknowledgement to another source, permission must also be sought from that source. If such permission is not obtained then that material may not be included in your publication/copies. Suitable acknowledgement to the source must be made, either as a footnote or in a reference list at the end of your publication, as follows:

"Reprinted from Publication title, Vol /edition number, Author(s), Title of article / title of chapter, Pages No., Copyright (Year), with permission from Elsevier [OR APPLICABLE SOCIETY COPYRIGHT OWNER]." Also Lancet special credit - "Reprinted from The Lancet, Vol. number, Author(s), Title of article, Pages No., Copyright (Year), with permission from Elsevier."

4. Reproduction of this material is confined to the purpose and/or media for which permission is hereby given.

5. Altering/Modifying Material: Not Permitted. However figures and illustrations may be altered/adapted minimally to serve your work. Any other abbreviations, additions, deletions and/or any other alterations shall be made only with prior written authorization of Elsevier Ltd. (Please contact Elsevier at permissions@elsevier.com)

6. If the permission fee for the requested use of our material is waived in this instance, please be advised that your future requests for Elsevier materials may attract a fee.

7. Reservation of Rights: Publisher reserves all rights not specifically granted in the combination of (i) the license details provided by you and accepted in the course of this

licensing transaction, (ii) these terms and conditions and (iii) CCC's Billing and Payment terms and conditions.

8. License Contingent Upon Payment: While you may exercise the rights licensed immediately upon issuance of the license at the end of the licensing process for the transaction, provided that you have disclosed complete and accurate details of your proposed use, no license is finally effective unless and until full payment is received from you (either by publisher or by CCC) as provided in CCC's Billing and Payment terms and conditions. If full payment is not received on a timely basis, then any license preliminarily granted shall be deemed automatically revoked and shall be void as if never granted. Further, in the event that you breach any of these terms and conditions or any of CCC's Billing and Payment terms and conditions, the license is automatically revoked and shall be void as if never granted. Use of materials as described in a revoked license, as well as any use of the materials beyond the scope of an unrevoked license, may constitute copyright infringement and publisher reserves the right to take any and all action to protect its copyright in the materials.

9. Warranties: Publisher makes no representations or warranties with respect to the licensed material.

10. Indemnity: You hereby indemnify and agree to hold harmless publisher and CCC, and their respective officers, directors, employees and agents, from and against any and all claims arising out of your use of the licensed material other than as specifically authorized pursuant to this license.

11. No Transfer of License: This license is personal to you and may not be sublicensed, assigned, or transferred by you to any other person without publisher's written permission.

12. No Amendment Except in Writing: This license may not be amended except in a writing signed by both parties (or, in the case of publisher, by CCC on publisher's behalf).

13. Objection to Contrary Terms: Publisher hereby objects to any terms contained in any purchase order, acknowledgment, check endorsement or other writing prepared by you, which terms are inconsistent with these terms and conditions or CCC's Billing and Payment terms and conditions. These terms and conditions, together with CCC's Billing and Payment terms and conditions (which are incorporated herein), comprise the entire agreement between you and publisher (and CCC) concerning this licensing transaction. In the event of any conflict between your obligations established by these terms and conditions and those established by CCC's Billing and Payment terms and conditions, these terms and conditions shall control.

14. Revocation: Elsevier or Copyright Clearance Center may deny the permissions described in this License at their sole discretion, for any reason or no reason, with a full refund payable to you. Notice of such denial will be made using the contact information provided by you. Failure to receive such notice will not alter or invalidate the denial. In no event will Elsevier or Copyright Clearance Center be responsible or liable for any costs, expenses or damage incurred by you as a result of a denial of your permission request, other than a refund of the amount(s) paid by you to Elsevier and/or Copyright Clearance Center for denied permissions.

LIMITED LICENSE

The following terms and conditions apply only to specific license types:

15. **Translation**: This permission is granted for non-exclusive world **English** rights only unless your license was granted for translation rights. If you licensed translation rights you may only translate this content into the languages you requested. A professional translator must perform all translations and reproduce the content word for word preserving the integrity of the article. If this license is to re-use 1 or 2 figures then permission is granted for non-exclusive world rights in all languages.

16. **Website**: The following terms and conditions apply to electronic reserve and author websites:
Electronic reserve: If licensed material is to be posted to website, the web site is to be password-protected and made available only to bona fide students registered on a relevant course if:
This license was made in connection with a course,
This permission is granted for 1 year only. You may obtain a license for future website posting,
All content posted to the web site must maintain the copyright information line on the bottom of each image,
A hyper-text must be included to the Homepage of the journal from which you are licensing at http://www.sciencedirect.com/science/journal/xxxxx or the Elsevier homepage for books at http://www.elsevier.com , and
Central Storage: This license does not include permission for a scanned version of the material to be stored in a central repository such as that provided by Heron/XanEdu.

17. **Author website** for journals with the following additional clauses:

All content posted to the web site must maintain the copyright information line on the bottom of each image, and the permission granted is limited to the personal version of your paper. You are not allowed to download and post the published electronic version of your article (whether PDF or HTML, proof or final version), nor may you scan the printed edition to create an electronic version. A hyper-text must be included to the Homepage of the journal from which you are licensing at http://www.sciencedirect.com/science/journal/xxxxx . As part of our normal production process, you will receive an e-mail notice when your article appears on Elsevier's online service ScienceDirect (www.sciencedirect.com). That e-mail will include the article's Digital Object Identifier (DOI). This number provides the electronic link to the published article and should be included in the posting of your personal version. We ask that you wait until you receive this e-mail and have the DOI to do any posting.

Central Storage: This license does not include permission for a scanned version of the material to be stored in a central repository such as that provided by Heron/XanEdu.

18. **Author website** for books with the following additional clauses:
Authors are permitted to place a brief summary of their work online only.
A hyper-text must be included to the Elsevier homepage at http://www.elsevier.com . All content posted to the web site must maintain the copyright information line on the bottom of each image. You are not allowed to download and post the published electronic version of your chapter, nor may you scan the printed edition to create an electronic version.

Central Storage: This license does not include permission for a scanned version of the

material to be stored in a central repository such as that provided by Heron/XanEdu.

19. **Website** (regular and for author): A hyper-text must be included to the Homepage of the journal from which you are licensing at http://www.sciencedirect.com/science/journal/xxxxx. or for books to the Elsevier homepage at http://www.elsevier.com

20. **Thesis/Dissertation**: If your license is for use in a thesis/dissertation your thesis may be submitted to your institution in either print or electronic form. Should your thesis be published commercially, please reapply for permission. These requirements include permission for the Library and Archives of Canada to supply single copies, on demand, of the complete thesis and include permission for UMI to supply single copies, on demand, of the complete thesis. Should your thesis be published commercially, please reapply for permission.

21. **Other Conditions**:

v1.6

If you would like to pay for this license now, please remit this license along with your payment made payable to "COPYRIGHT CLEARANCE CENTER" otherwise you will be invoiced within 48 hours of the license date. Payment should be in the form of a check or money order referencing your account number and this invoice number RLNK500878405.
Once you receive your invoice for this order, you may pay your invoice by credit card. Please follow instructions provided at that time.

Make Payment To:
Copyright Clearance Center
Dept 001
P.O. Box 843006
Boston, MA 02284-3006

For suggestions or comments regarding this order, contact RightsLink Customer Support: customercare@copyright.com or +1-877-622-5543 (toll free in the US) or +1-978-646-2777.

Gratis licenses (referencing $0 in the Total field) are free. Please retain this printable license for your reference. No payment is required.

Appendix D (Continued)

AMERICAN INSTITUTE OF PHYSICS LICENSE TERMS AND CONDITIONS

Oct 10, 2012

All payments must be made in full to CCC. For payment instructions, please see information listed at the bottom of this form.

License Number	3005470777477
Order Date	Oct 10, 2012
Publisher	American Institute of Physics
Publication	Applied Physics Letters
Article Title	Growth modes of ZnO nanostructures from laser ablation
Author	I. Amarilio-Burshtein, S. Tamir, Y. Lifshitz
Online Publication Date	Mar 8, 2010
Volume number	96
Issue number	10
Type of Use	Thesis/Dissertation
Requestor type	Student
Format	Print and electronic
Portion	Figure/Table
Number of figures/tables	2
Title of your thesis / dissertation	ZnO nanostructures for multifunctional application: growth, characterization and device fabrication
Expected completion date	Nov 2012
Estimated size (number of pages)	150
Total	0.00 USD
Terms and Conditions	

American Institute of Physics -- Terms and Conditions: Permissions Uses

American Institute of Physics ("AIP") hereby grants to you the non-exclusive right and license to use and/or distribute the Material according to the use specified in your order, on a one-time basis, for the specified term, with a maximum distribution equal to the number that you have ordered. Any links or other content accompanying the Material are not the subject of this license.

1. You agree to include the following copyright and permission notice with the reproduction of the Material: "Reprinted with permission from [FULL CITATION]. Copyright [PUBLICATION YEAR], American Institute of Physics." For an article, the copyright and permission notice must be printed on the first page of the article or book chapter. For photographs, covers, or tables, the copyright and permission notice may appear with the Material, in a footnote, or in the reference list.
2. If you have licensed reuse of a figure, photograph, cover, or table, it is your responsibility to ensure that the material is original to AIP and does not contain the copyright of another entity, and that the copyright notice of the figure, photograph, cover, or table does not indicate that it was reprinted by AIP, with permission, from another source. Under no circumstances does AIP, purport or intend to grant permission to reuse material to which it does not hold copyright.

3. You may not alter or modify the Material in any manner. You may translate the Material into another language only if you have licensed translation rights. You may not use the Material for promotional purposes. AIP reserves all rights not specifically granted herein.
4. The foregoing license shall not take effect unless and until AIP or its agent, Copyright Clearance Center, receives the Payment in accordance with Copyright Clearance Center Billing and Payment Terms and Conditions, which are incorporated herein by reference.
5. AIP or the Copyright Clearance Center may, within two business days of granting this license, revoke the license for any reason whatsoever, with a full refund payable to you. Should you violate the terms of this license at any time, AIP, American Institute of Physics, or Copyright Clearance Center may revoke the license with no refund to you. Notice of such revocation will be made using the contact information provided by you. Failure to receive such notice will not nullify the revocation.
6. AIP makes no representations or warranties with respect to the Material. You agree to indemnify and hold harmless AIP, American Institute of Physics, and their officers, directors, employees or agents from and against any and all claims arising out of your use of the Material other than as specifically authorized herein.
7. The permission granted herein is personal to you and is not transferable or assignable without the prior written permission of AIP. This license may not be amended except in a writing signed by the party to be charged.
8. If purchase orders, acknowledgments or check endorsements are issued on any forms containing terms and conditions which are inconsistent with these provisions, such inconsistent terms and conditions shall be of no force and effect. This document, including the CCC Billing and Payment Terms and Conditions, shall be the entire agreement between the parties relating to the subject matter hereof.

This Agreement shall be governed by and construed in accordance with the laws of the State of New York. Both parties hereby submit to the jurisdiction of the courts of New York County for purposes of resolving any disputes that may arise hereunder.

If you would like to pay for this license now, please remit this license along with your payment made payable to "COPYRIGHT CLEARANCE CENTER" otherwise you will be invoiced within 48 hours of the license date. Payment should be in the form of a check or money order referencing your account number and this invoice number RLNK500874446.
Once you receive your invoice for this order, you may pay your invoice by credit card. Please follow instructions provided at that time.

Make Payment To:
Copyright Clearance Center
Dept 001
P.O. Box 843006
Boston, MA 02284-3006

For suggestions or comments regarding this order, contact RightsLink Customer Support: customercare@copyright.com or +1-877-622-5543 (toll free in the US) or +1-978-646-2777.

Gratis licenses (referencing $0 in the Total field) are free. Please retain this printable license for your reference. No payment is required.